STUDIES OF MOLECULAR COMPLEXES

By

TZE CHI JAO

A DISSERTATION PRESENTED TO THE GRADUATE COUNCIL OF THE UNIVERSITY OF FLORIDA IN PARTIAL FULFILLMENT OF THE REQUIREMENTS FOR THE DEGREE OF DOCTOR OF PHILOSOPHY

UNIVERSITY OF FLORIDA
1974

To my parents

and

my wife Carmen

ACKNOWLEDGEMENTS

Special thanks are for Dr. Willis B. Person for his wise counsel, constant enthusiasm, and encouragement throughout the entire project. I should also like to express thanks for their help to Dr. Keith E. Gubbins, Dr. Yngue Öhrn, Dr. Thomas M. Reed and Dr. John R. Sabin.

I am grateful to the University of Puerto Rico (Mayagüez Campus) for financial support of my graduate studies at the University of Florida and also for support from the National Science Foundation (Research Grant No. GP 17818).

Support of computing expenses by the College of Arts and Sciences of the University of Florida is gratefully acknowledged.

I should like to express my sincere thanks to Dr. Shigeo Kondo, Mr. Robert Levine, Mr. James H. Newton, Mr. Gary Peyton and Miss Barbara Zilles for their friendship and assistance.

Finally, I express my appreciation to Mrs. James H. Newton for her patience in typing this manuscript.

TABLE OF CONTENTS

Chapter Page

LIST OF TABLES

Table | Page

LIST OF FIGURES

Figure

Page

Abstract of Dissertation Presented to the
Graduate Council of the University of Florida in Partial
Fulfillment of the Requirements for the Degree of Doctor of Philosophy

STUDIES OF MOLECULAR COMPLEXES

By

Tze Chi Jao

March, 1974

Chairman: Willis B. Person
Major Department: Chemistry

Molecular complexes of chlorine in benzene solutions were studied by ultraviolet, Raman and infrared spectroscopic techniques. Ultraviolet spectroscopic studies verify the order of magnitude of the previously reported equilibrium constant for the assumed benzene-chlorine 1:1 complex. Its value, $K = 0.025 \pm 0.015$ liter $mole^{-1}$, agrees quite well with values obtained from Raman and infrared spectroscopic data.

Careful experimental measurements were made of the absolute Raman and infrared intensities of the Cl-Cl stretching vibration of chlorine in solutions of benzene in carbon tetrachloride. Specially designed infrared long path liquid cells, inert to chlorine, were constructed and used to obtain the absorption spectra of chlorine in the mixtures of benzene and carbon tetrachloride. The resulting infrared studies

were more acurate than previous work, and the collision-induced infrared absorption spectrum of Cl_2 in CCl_4 could also be observed.

The wavenumber of the Raman band of Cl_2 shifts uniformly from 530 cm^{-1} in benzene solution to 543 cm^{-1} in carbon tetrachloride solution, although the half band width clearly broadens at a 1:1 ratio of benzene to carbon tetrachloride. The infrared absorption by chlorine shifts slightly from 527 cm^{-1} in pure benzene to 532 cm^{-1} in 2.26 M benzene in CCl_4; with a big jump to 545 cm^{-1} for chlorine in pure carbon tetrachloride. This difference between the Raman and infrared spectra for chlorine in benzene solutions suggests that the infrared absorption is from only the complexed chlorine, while the Raman band is a composite of two unresolved bands, one for the complexed chlorine and the other from free chlorine. The absolute infrared intensity and the relative Raman intensity for the Cl-Cl vibration of chlorine both increase approximately by a factor of five from those for the Cl_2 solution in carbon tetrachloride to the solution in benzene.

In order to interpret these observed Raman and infrared spectra, theoretical calculations were made of the effect on the Raman and infrared intensities from direct electrostatic interactions. The basic theory of collision-induced infrared absorption intensity by Van Kranendonk and Fahrenfort and of the Raman intensity enhancement by Bernstein was applied, using statistical mechanics of liquid structures with angularly dependent pair-correlation functions of chlorine in benzene solutions. The isotropic and anisotropic effects were taken into consideration for the calculations of both Raman and infrared intensities. The calculated intensities were then compared with the

experimentally measured values.

The electrostatic effect predicts a maximum Raman intensity enhancement of 100% for chlorine from gas phase to solution in CCl_4, and 134% for solution in benzene, compared with an observed enhancement of more than 400% from solution in carbon tetrachloride to solution in benzene. The contribution of the electrostatic effect to the infrared intensity of chlorine in benzene was predicted to be, at most, 50% of the total measured intensity of 333 cm mmole^{-1}. The vibronic charge-transfer effect may be responsible for the intensification of infrared absorption while a pre-resonance Raman effect involving the charge-transfer absorption band may explain the enhancement of the Raman band.

CHAPTER I

INTRODUCTION

Complexes of halogens with benzene have been studied quite intensively in the last two decades by both experimental and theoretical methods (1-34). The general subject of molecular complexes has been reviewed by several authors (35-40). The experimental studies include those by ultraviolet, visible, Raman and infrared spectroscopic techniques, while the theoretical studies are concerned with the mechanism of the interaction and the theory of the associated experimental phenomena, and particularly the relative importance of the electrostatic and charge-transfer effects. The complexes of iodine with aromatic donors have been studied quite thoroughly by these methods. Less attention has been paid to the complexes of bromine and chlorine with benzene or other aromatic donors, because the latter are more reactive.

In the first careful study by Andrews and Keefer (6) the complex of chlorine with benzene was found to exhibit an additional strong ultraviolet adsorption band near 278 nm, which is absent in the spectrum of each individual constituent solution. From their ultraviolet data, they found by the Benesi-Hildebrand method (2) that the equilibrium constant of the complex is about 0.033 liter $mole^{-1}$ with a maximum absorptivity ε_{max} for the complex at 280nm of 9090 liter $mole^{-1}$ cm^{-1}.

The equilibrium constant for the complex of iodine with benzene

was found (2) to be about 0.17 liter mole^{-1}, with ε_{max} of about 15000 liter mole^{-1}cm^{-1}, so that the complex of chlorine with benzene is weaker than that for iodine with benzene, in agreement with the expected Lewis acid strengths of chlorine and iodine.

In an attempt to explain the results of these ultraviolet spectroscopic studies (1, 2) of iodine with benzene, Mulliken (11) introduced the "charge-transfer" resonance structure theory. This theory described the ground state electronic wavefunction Ψ_N of a donor-acceptor complex approximately by a combination of two resonance structure functions Ψ_0 and Ψ_1:

$$\Psi_N(D\cdot A) \simeq a\Psi_0(D,A) + b\Psi_1(D^+ - A^-) \quad . \qquad (1\text{-}1)$$
$$\text{(no-bond)} \quad \text{(dative)}$$

Here a and b are the coefficients of the no-bond and dative structures, respectively. In the ground state of a weak complex, a is expected to be approximately 1.0 and b expected to be less than about 0.1. The stability of the complex depends on the extent of the mixing between the wavefunctions of the no-bond and dative structures.

If the ground state structure of a complex is given by Ψ_N, then according to the "charge-transfer" theory, there is an excited state Ψ_V which is called a charge-transfer state, given by

$$\Psi_V = - b^*\Psi_0(D,A) + a^*\Psi_1(D^+ - A^-) \quad . \qquad (1\text{-}2)$$

The coefficients b^* and a^* are determined by the quantum theory requirement that the excited state wavefunction be orthogonal to the ground state function:

$$\int \Psi_N^* \Psi_V \, d\tau = 0.$$

The electronic absorption frequency of the new band formed in the complex corresponds to the energy difference between the ground state (N) and this charge-transfer excited state (V) of the complex. The charge-transfer theory also explains the characteristically high intensity of the electronic absorption band of the complex (for further discussion see Ref. 37).

The first infrared study of the complex of chlorine with benzene was made by Collin and D'Or (13). A new weak and relatively broad absorption band was observed near 526 cm^{-1} for solutions of chlorine dissolved in benzene. The Raman shift for chlorine ($^{35}Cl_2$) in carbon tetrachloride was known (22) to be at 548 cm^{-1}. More quantitative studies of the infrared spectrum of chlorine in benzene were carried out by Person and associates (18, 21).

An attempt was made by Friedrich and Person (26) to interpret the changes in vibrational frequency and intensity of the halogen-halogen stretching vibration when the halogen molecule, an aσ acceptor (37), complexes with benzene, a bπ donor (37) (or with other electron donor molecules) in terms of charge transfer theory (11). They postulated that a relationship existed between the vibrational frequency shift ($\Delta\nu$) and $\underline{b}$ the coefficient of the dative wavefunction:

$$F_{1N} = (b^2 + abS_{01}) \simeq \Delta k/k_0 = 2\Delta\nu/\nu_0 \quad . \qquad (1\text{-}3)$$

Here F_{1N} is the weight of the dative structure in Ψ_N ($F_{1N} = b^2 + 2abS_{01}$), S_{01} is the overlap integral between Ψ_0 and Ψ_1, k is the force constant and ν_0 is the vibrational wavenumber of the isolated molecule, while Δk and $\Delta\nu$ are the changes ($k_0 - k$ or $\nu_0 - \nu$, respectively) in the complex.

In the following, we shall summarize some of the material from Ref. 41 relating to the theories of charge-transfer and of electrostatic effects for the interpretation of the changes in infrared intensity of halogens forming complexes with benzene. The experimental absolute infrared intensity (A_i) of the ith normal vibrational mode of any molecule can be related to the dipole moment derivative $(\partial p/\partial \xi_1)$ by (41)

$$A_i = N\pi g_i/3c^2(\partial p/2\xi_i)^2 = K(\partial p/\partial \xi_i)^2 \quad . \tag{1-4}$$

Here N is the Avogadro's number, g_i is the degeneracy of the ith normal vibration at wavenumber $\tilde{\nu}_i$, $(\partial p/\partial \xi_i)$ is the magnitude of the dipole moment derivative for the ith normal vibration with respect to normal coordinate (ξ_i). The integrated molar absorption coefficient A_i is defined experimentally by:

$$A_i = (1/n\ell)\int \ell n(I_0/I)d\tilde{\nu} \quad . \tag{1-5}$$

Here n is the concentration of the absorbing molecules in liter $mole^{-1}$, ℓ is the pathlength in cm, I and I_0 are the transmitted and incident intensities of monochromatic light at wavenumber $\tilde{\nu}_i$.

Based on charge-transfer theory (11), Friedrich and Person (26) argued that the dipole moment derivative for the Cl-Cl stretching vibration in the complex is given by

$$\partial p/\partial \xi_i \simeq \partial \vec{\mu}_N/\partial \xi_i + (2b)(\partial b/\partial \xi_i)|\vec{\mu}_1 - \vec{\mu}_0| \quad . \tag{1-6}$$

Here $\partial \mu_N/\partial \xi_i$ represents the magnitude of change in the Cl-Cl dipole moment of the uncomplexed Cl_2 molecule when the Cl-Cl coordinate (ξ_i) changes; $|\vec{\mu}_1 - \vec{\mu}_0|$ is the difference between the dipole moment in the

dative state $\vec{\mu}_1$ and that in the no-bond state $\vec{\mu}_0$, and is approximately equal to $\vec{\mu}_{VN}$, the electronic transition moment for the charge-transfer absorption band. The second term $(\partial b/\partial \xi_i)$ is the change in the coefficient b as the Cl-Cl bond length changes (ξ_i) and gives the vibronic charge-transfer effect.

The derivative $(\partial p/\partial \xi_i)$ is related to the derivatives with respect to the internal coordinates (R_j) by:

$$\partial\vec{p}/\partial\xi_i = \sum_j L_{ji}(\partial\vec{p}/\partial R_j) \quad . \tag{1-7}$$

Or conversely,

$$\partial\vec{p}/\partial R_j = \sum_i L^{-1}_{ij}(\partial\vec{p}/\partial\xi_i) \quad . \tag{1-8}$$

Here L_{ji} is the jith coefficient from the normal coordinate transformation, while L^{-1}_{ji} is the corresponding element from the inverse transformation. In analogy with Eq. 1-6 we have

$$\partial\vec{p}/\partial R_j \cong \partial\vec{\mu}_N/\partial R_j + (2b)(\partial b/\partial R_j)|\vec{\mu}_1 - \vec{\mu}_0| \cdot \tag{1-9}$$

Assuming $\partial\vec{\mu}_N/\partial R_j$ is not different from the dipole moment derivative of the free molecule, it has been shown (41) from Eq. 1-9 that the vibronic contribution (M_d') to the infrared intensity change, for the special case $R_j = R_1$, the stretching coordinate of the X-Y bond of a complexed halogen molecule, can be obtained from the following equation:

$$M_d' = (\partial\vec{p}/\partial R_1) - (\partial\vec{\mu}_N/\partial R_1) \cong -(2F_{0N}F_{1N})(\partial E_A^v/\partial R_1)/\Delta|\vec{\mu}_1 - \vec{\mu}_0| \quad . \tag{1-10}$$

Here F_{0N} is the weight of the no-bond structure in Ψ_N $(F_{0N} = a^2 + abS_{01})$, and is related to F_{1N} by $F_{0N} + F_{1N} = 1$; Δ is the difference between the energies of the dative and no-bond structures and E_A^v is the vertical

electron affinity of the acceptor, and appears because $\underline{b}$ depends on E_A^v, so that $\partial b/\partial R_1$ is related to $\partial E_A^v/\partial R_1$. The comparison between the calculated M_d' and the observed values is shown in Table 1.8 of Ref. 41. The agreement is qualitatively good, but the calculated values in some cases are larger than experimental by a factor of 2 to 5.

The defect of the model of Friedrich and Person arises from two sources: one is the oversimplified assumption that $\partial\vec{\mu}_N/\partial R_1$ can be approximated by $\partial p^0/\partial R_1$, the dipole moment derivative of the free molecule, the other is because $\partial E_A^v/\partial R_1$ (and, to a lesser extent, the other parameters such as F_{1N}) cannot be obtained *a priori*.

In an alternative treatment, Hanna and associates (30, 31) attempted to interpret the change in the infrared intensity of halogens in benzene as a purely electrostatic effect. They estimated an induced dipole for chlorine in a complex arising from the interaction of the field along the six-fold z-axis from the benzene molecule with the polarizable halogen molecule:

$$\mu_i = (1/2)\,\alpha''\,(E_1 + E_2). \qquad (1\text{-}11)$$

Here α'' is the polarizability of the halogen parallel to its axis (in the $\underline{z}$ direction); E_1 is the field from the benzene at the nearest halogen atom (X), and E_2 is the field at the halogen atom (Y) further away from the benzene. Taking the derivative of Eq. 1-11 with respect to the internal coordinate R_1 of the halogen,

$$(\partial\mu_i/\partial R_1) = (1/2)(\partial\alpha''/\partial R_1)(E_1 + E_2) + (1/2)\,\alpha''[(\partial E_1/\partial R_1) + (\partial E_2/\partial R_1)]\ . \qquad (1\text{-}12)$$

The calculated infrared intensity for the halogen complexed with benzene from Eq. 1-12 is compared with the observed values (31). Again the agreement is good (within a factor of 2).

The values from the model of Hanna and associates (30, 31) appear to be the right order of magnitude, but the parameters needed for this calculation are not easy to determine. For example, the polarizability derivative $(\partial\alpha''/\partial R_1)$ of chlorine was estimated from the semi-empirical Lippincott model (42); the experimental studies reported here (Chap. IV) found that this estimate is too large. There is also some considerable uncertainty in the parameters chosen for E_1 and E_2 since estimation of the correct values requires quite good molecular wavefunctions of the benzene molecule.

The subject of electrostatic "collision-induced" infrared absorption is an old one, having been studied by Van Kranendonk (43), Fahrenfort (44) and others (45). In the original formulation of collision-induced infrared absorption given by Van Kranendonk (43) and Fahrenfort (44), homonuclear diatomic molecules or nonpolar linear molecules under high pressure are predicted to have induced infrared absorption due to (a) an atomic distortion effect and (b) a quadrupole distortion effect. The former arises from mutual repulsion of electron clouds at small intermolecular separation, while the latter comes from the interaction between one polarizable molecule and the electric field generated by the quadrupole moment of the other molecule. Hanna and associates (30, 31) have considered the second effect in the benzene-halogen case. In line with the correct collision-induced infrared absorption theory (43, 44), the estimated induced infrared absorption intensity for chlorine in benzene solution should be obtained

as an appropriate statistical average over all intermolecular orientations, and not just for one orientation, as assumed by Hanna *et al.*

Using the same argument as Hanna and associates (30, 31), Kettle and Price (33) applied the theory of collision-induced far infrared absorption (46-50) to interpret quantitatively the observed results of their studies on solutions of iodine and bromine in benzene. They reported that the intensities of the far-infrared absorption of iodine and bromine in benzene solutions could be adequately explained by considering only quadrupole-induced dipole moments, but they had to assume different values for the parameters from those given by Hanna and Williams (31).

Meanwhile, a Raman spectroscopic study of iodine in benzene solution had been carried out by Klaeboe (27). He observed only one Raman band in the iodine solution, and did not see a Raman shift for the uncomplexed iodine. Later, Rosen, Shen and Stenman (29, 32) made a more systematic study of the Raman spectrum of iodine in benzene solution. They observed a uniform change in frequency of the Raman shift for iodine as the benzene was increasingly diluted by the addition of the inert solvent; e.g., n-hexane. No change in band shape was observed on dilution. They concluded that the reason for not resolving two Raman peaks, one for the complexed iodine and the other for an uncomplexed one, was the weakness of the charge-transfer interaction between iodine and benzene, so that iodine could interact with more than one donor. If the observed single Raman band for iodine in benzene is due to the weak charge-transfer complex, then the weaker charge-transfer complex of chlorine with benzene may exhibit the same uniform change in vibrational frequency with dilution for both

Raman and infrared spectra.

After reviewing these previous studies of complexes of halogens with benzene, we see there is considerable conflict in the interpretation of the observations of infrared absorption of halogens in benzene. In order to understand better the difference in the interpretations of the spectroscopic phenomena associated with the complexes of halogens with benzene, we decided to re-investigate the benzene-chlorine system. We remeasured the infrared intensity of the complex of chlorine with benzene under carefully controlled experimental conditions, and also studied the infrared absorption spectrum of chlorine in carbon tetrachloride, which is not expected to form a charge-transfer complex with chlorine, in order to compare it with the one in benzene. On the other hand, we re-examined the theory of induced infrared absorption more carefully. With the improved liquid structure theory (51, 52) recently available, we applied the collision-induced infrared absorption theory of Van Kranendonk (43) and Fahrenfort (44) in order to determine whether intensities observed for chlorine in both the benzene and carbon tetrachloride solutions could be explained quantitatively by this theory alone, without any charge-transfer effect.

Secondly, we extended the work of Rosen, Shen and Stenman (29, 32) by studying the Raman spectrum of chlorine in benzene-carbon tetrachloride solutions in order to understand better the nature of weak charge-transfer complexes of halogens with benzene. There are three reasons for our choice of chlorine instead of bromine or iodine for the Raman work: (1) the complex of chlorine with benzene is much weaker than a complex of iodine with benzene (6), so that the negative results for benzene-iodine could be even worse for benzene-chlorine, (2) the

chlorine solution absorbs less of the Raman exciting line because the solution is more transparent, so it could be observed easier in the Perkin-Elmer LR-1 spectrometer, and (3) the infrared absorption of chlorine is in a region which can be studied with less difficulty (13, 17) than for the benzene-iodine solutions.

We repeated the study of the ultraviolet spectrum reported by Andrews and Keefer (6) for two reasons: first, we wanted to see if the equilibrium constant of the complex of chlorine with benzene changes with concentration of chlorine, since the Raman and infrared experiments required a high concentration of chlorine, while the equilibrium constant obtained by Andrews and Keefer was presumably determined in a dilute solution (they did not report their concentrations); secondly, error analysis (53, 54) of the determination of equilibrium constants for weak molecular complexes has shown that equilibrium constants as small as that reported for chlorine with benzene cannot be determined with any meaningful accuracy. For a complex with saturation function (s, the fraction of complexed Cl_2 in the solution) between 0.01 and 0.1, the relative error in both the equilibrium constant and absorptivity (E) will vary between $\pm$ 10 and $\pm$ 100%, respectively (52a). It is thus of interest to compare equilibrium constants obtained from these three different methods (ultraviolet, Raman, and infrared spectra) in order to see the order of agreement that can be achieved.

CHAPTER II

GENERAL EXPERIMENTAL PROCEDURES

Introduction

In this chapter we shall discuss the experimental procedures that were common to all of the different spectroscopic studies. These include the discussion of the source and purity of reagents, the preparation and handling of chlorine solutions, and the cells used, including a description of the specially constructed infrared cells. In the following chapters we shall then describe in detail the special experimental procedures for each different (ultraviolet, Raman and infrared) spectral study.

Source of Reagents

The reagents used for all experiments in this work are listed in Table I. All the solvents were used without further purification. However, these solvents did not have impurities detectable at the conditions of our spectral studies. The two different grades of chlorine gas did not show any differences in our spectra.

Preparation of Chlorine Solutions

The chlorine solutions for all the different spectral studies were prepared in the same way. Chlorine gas was introduced into the solution through a gas dispersion tube connected by Tygon tubing to a trap filled with glass wool to filter any solid impurity and then to the flask of chlorine. The flow rate of the chlorine gas was not regulated by a

TABLE I

SOURCE AND PURITY OF THE REAGENTS

Material	Purity	Source
chlorine gas	research or ultra-high purity grade	Matheson Gas Products
benzene and carbon tetrachloride	(1) spectrophometric grade	(1) Mallinchrodt Chemical Works
	(2) spectro-quality reagent	(2) Matheson Coleman and Bell
chloroform	analytical reagent	Allied Chemical
sodium thiosulfate ($Na_2S_2O_3 \cdot 5H_2O$)	analytical reagent	Fisher Scientific Company
potassium iodate (KIO_3)	analytical reagent	Fisher Scientific Company
Potassium iodide (KI)	reagent grade	Fisher Scientific Company
water	deionized	University of Florida

regulator, but was controlled in such a way that the concentration of the chlorine was around 0.1 M after bubbling Cl_2 for five minutes, around 0.2 M after 10 minutes, and so on. It may be safe to say that this flow rate is about 5 bubbles per second. The bubbling process usually took 5 to 30 minutes depending on the concentration desired. As will be discussed in more detail later, the most serious difficulty with the chlorine solution was preventing the formation of photochemical product. Since this product does not absorb ultraviolet light nor have Raman scattering in the same spectral region as does the complexed chlorine, a small amount does not interfere with those studies. However, it does absorb near the Cl-Cl infrared absorption and the impurity is especially bothersome there.

The chlorine solutions were prepared under ordinary room lights, and the flow rate adjusted as described above during the ultraviolet and Raman experiments. With the experience gained from these two experiments, it was easy to work in the dark in order to prepare chlorine solutions for the infrared experiments, where the photochemical product interfered more seriously. However, when the solutions were exposed to light, we could easily detect formation of large amounts of photochemical product, since the solution would first become a little cloudy, clearing again with time, because the product is very soluble in benzene and in carbon tetrachloride. If this cloudiness was detected, we would then discard the solution and use a freshly prepared one. In the dark, we could monitor the solution by feeling the flask to detect the solution heating up, since we believe that heating was always an indication of extensive photochemical reaction.

Because of this well-known (55) photochemical reaction between

chlorine and benzene, occurring in daylight or under fluorescent lights, it was necessary to keep the room as dark as possible. Actually, we had found that the chlorine concentration in the benzene solution under ordinary fluorescent lights decreased by about 8% in 2 hours when the stock solution was about 0.2 M. The reason for the decreasing concentration of chlorine was partly due to the photochemical reaction, but possibly was also due to chlorine gas escaping from the flask even though the flask was stoppered. After evaporating benzene solutions of chlorine that had been exposed to light, the solid residue was dissolved in carbon tetrachloride. The NMR spectrum of this solution showed the residue was mainly hexachlorocyclohexane ($C_6H_6Cl_6$) because of the peak at 4.7 ppm (see Fig. 1).

To make sure the Raman spectrum and the infrared spectrum that were observed for the chlorine solution were actually due to the chlorine molecule and not to any compound formed between chlorine and the solvent, we removed the chlorine gas from the solvent after running the spectrum either by bubbling nitrogen through the solution in the case of Raman experiments, or by pumping out the chlorine gas (from the solution in the cell) through a vacuum line, in the case of infrared experiments. Following this treatment the spectrum of the clear solution was then taken, so that absorption by the photochemical product could be detected.

We have mentioned briefly earlier that the photochemical product ($C_6H_6Cl_6$) gives more serious problems for the infrared experiment. The absorption of the hexachlorocyclohexane near 510 cm^{-1} could distort the spectrum of chlorine by overlapping the two bands. Therefore, extreme care is necessary to avoid exposing the sample to light. However,

Fig. 1. -- The NMR spectrum of the residue (redissolved in CCl_4) after benzene solutions were evaporated.

filter bandwidth: 4 Hz
R.F. field: 0.05 mG
sweep time: 1000 second
spectrum amplitude: 80

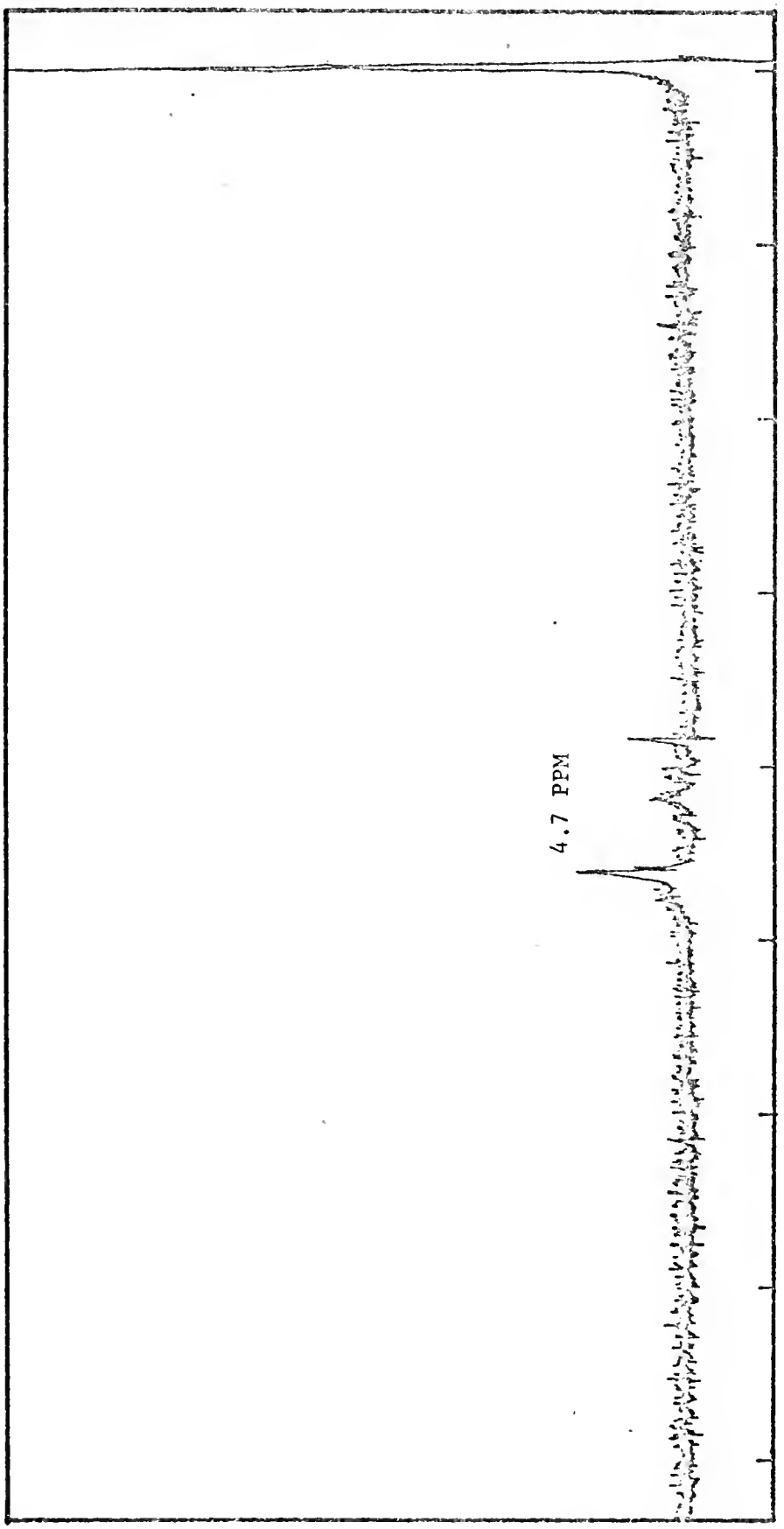
4.7 PPM
0
1.0
2.0
3.0
4.0
5.0
6.0
7.0
8.0
PPM (δ)

one method which can inhibit the formation of $C_6H_6Cl_6$ was to add some oxygen gas in the solvent before chlorine gas was introduced. Oxygen was reported to be a radical quencher (56). Nevertheless, we could not completely inhibit the photochemical reaction by this procedure.

Every chlorine solution was freshly prepared for each experiment. The concentration of chlorine was determined by withdrawing a 5 ml portion of chlorine solution from the stock solution and transferring it into a prepared solution containing excess potassium iodide. The iodine released by the reaction with chlorine was titrated with standard aqueous thiosulfate. The analysis of this stock solution was done before and after the Raman and infrared spectra were taken. As a check, occasionally, a 1 ml portion of chlorine solution from the sample cell was withdrawn after its spectrum had been taken, and its concentration was determined. The concentrations of the chlorine solutions in the two cases (from the cell or from the stock) were not significantly different, but the concentrations after the experiment were about 5-6% lower than at the beginning.

Liquid Cells

We used a set of matched silica cells with a pathlength of 1 cm for the ultraviolet spectroscopic study of chlorine solutions at low concentration (about 1.0×10^{-3} M), and a silica cell with light pathlength of 0.1 mm for studying chlorine solutions of higher concentration (about 1.0×10^{-1} M). The 1 cm ultraviolet absorption cells were rectangular ones with ground-glass stoppers, while the 0.1 mm one was constructed with platinum and tantalum parts, with silica windows, and assembled with teflon spacers. All of them were supplied by Beckman.

A standard 2.5 ml Raman liquid cell from Perkin-Elmer was used

for the Raman experiments.

For the infrared experiments, specially constructed liquid cells were made. In order to eliminate the solvent spectrum, we built two fairly well-matched sets of liquid cells, one with a pathlength of 3 mm and the other with 6 mm pathlength; potassium bromide windows (25 mm in diameter and 3 mm thick) were used. Chlorine did not react very rapidly with KBr in contrast with the solvent we used. This was tested by placing the windows in the chlorine solution for one hour. They did not show a significant change in their infrared spectrum from the original KBr background. However, when we tried intentionally to extend the window contact with the chlorine solution to 24 hours, the baseline did change and we saw actual corrosion of the KBr salt plate. We had tried to use AgCl windows of 1.5 mm thickness, and found the thin windows were too soft to resist the pressure difference on evacuation of the cell.

The infrared liquid cell is shown in Fig. 2. The spacer was made of teflon. Between the KBr window and the thick spacer, we inserted a thin Teflon spacer in order to avoid damage by the rigid contact with the KBr window and the Teflon spacer and in order to minimize leaking of the chlorine solution from the cell. To prevent the KBr windows from cracking when they were fastened by two brass tubes to form the liquid cell, an O-ring was placed between the brass tubing and the KBr window. Finally, we compressed all these components by the two outer brass plates, each with four drilled holes, and tightened them with bolts. A hole of the exact dimension of the glass tubing adaptor to the vacuum line was cut into the side of the Teflon spacer. The filled 3 mm pathlength liquid cell contained 2.5 or 3.0 ml of solution.

Fig. 2. -- Schematic diagram of the infrared liquid cell.

A glass tubing adaptor
B Teflon spacer (3 or 6 mm)
C Teflon spacer (0.001 mm)
D KBr window
E O-ring
F brass tubing
G brass plate
H bolt

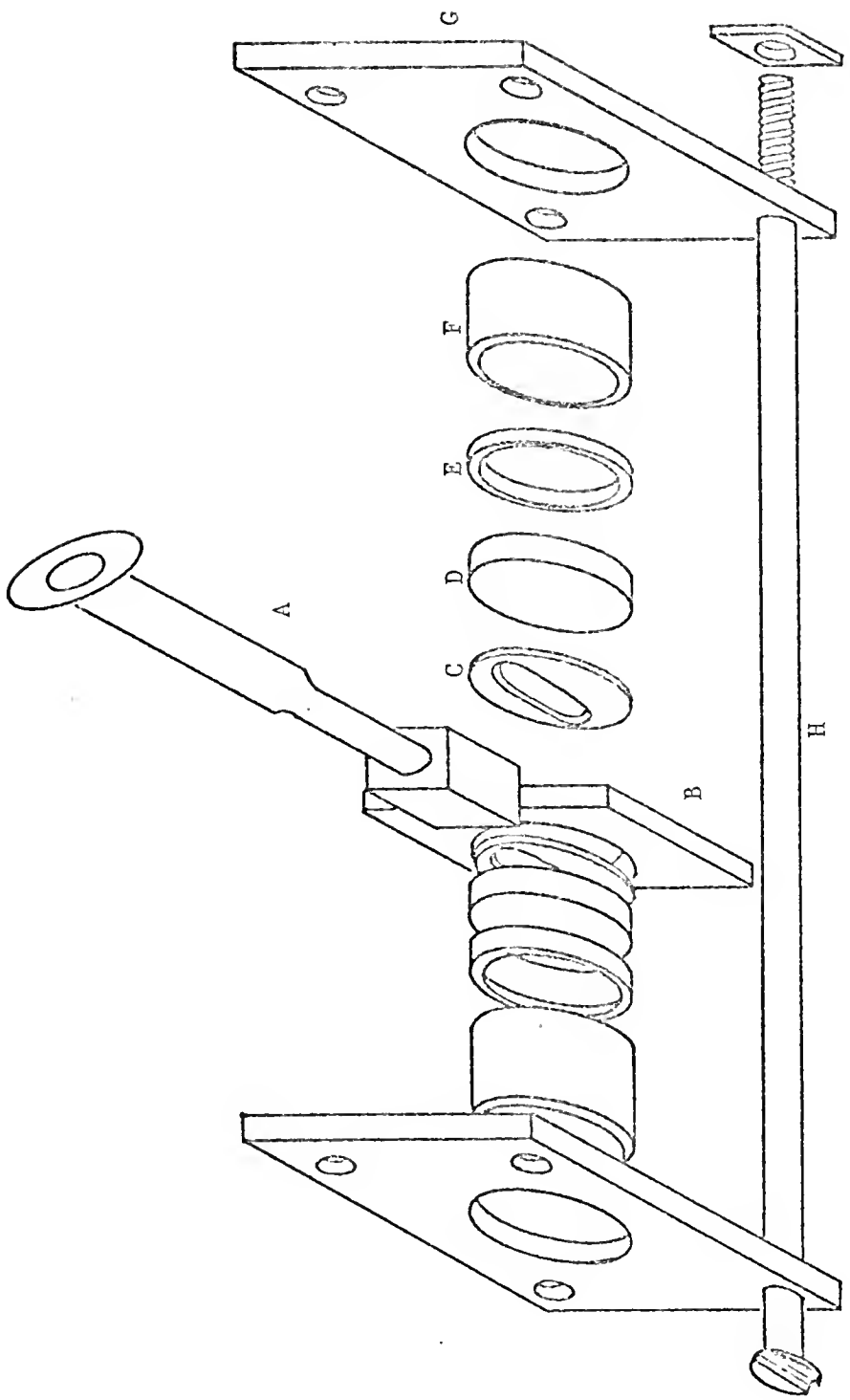
G
F
E
D
C
A
B
H

CHAPTER III

ULTRAVIOLET SPECTROSCOPIC STUDIES OF CHLORINE IN BENZENE SOLUTIONS

Experimental Procedures

The ultraviolet spectrum of the complex of chlorine with benzene dissolved in carbon tetrachloride was studied as a function of benzene concentration at two different chlorine concentrations, one on the order of 0.001 M, and the other in a short path cell (0.1 mm) for solutions around 0.1 M. Five different benzene-carbon tetrachloride mixtures were prepared, ranging from pure benzene to pure carbon tetrachloride, and the chlorine was dissolved in each.

For the chlorine solutions with concentration around 0.001 M, a fairly well-matched set of silica cells was used in the spectral studies. Before any solution was prepared, the Cary Model 15 ultraviolet spectrophotometer was turned on and allowed to warm up. At this point, we started preparing 50 ml of aqueous potassium iodide solution (containing 2 grams of KI) necessary for the titration of the chlorine solution, and the different preparations of solvent needed to dilute the stock chlorine solution. The chlorine solution around 0.1 M was prepared as described in Chap. II. The time was recorded when a 5 ml stock solution was pipetted into the flask containing excess potassium iodide solution; immediately following, we pipetted a 10 ml stock solution into a 125 ml flask containing 90 ml of the same solvent. This solution was diluted to 1/10 the original concentration by adding

10 ml of this solution to a 125 ml flask containing 90 ml of the solvent. Three more dilutions were made to form three different final solutions ranging in concentrations from 0.0005 M to 0.0001 M in chlorine, each with final volume of solution around 60 ml. Each flask containing a chlorine solution was stoppered properly with a glass stopper. At this point, we recorded the baseline of the solvent vs. solvent with the double beam spectrometer. The spectrum (from 320 to 250 nm) of each chlorine solution was then recorded, proceeding from higher to lower concentration, recording the time at the beginning of each spectrum. We repeated each measurement at least three times, proceeding from higher to lower concentration by refilling the sample cell solution from the flask. When all spectra were obtained, the chlorine stock solution already added to the potassium iodide solution was then titrated.

Spectra of chlorine dissolved in pure benzene for several different concentrations of chlorine (each studied as a function of time) are shown in Fig. 3. The time interval between recording any two successive spectra of the same solution was about 20 minutes. The concentration of chlorine indicated for solutions A, B, and C are the values determined by titration of the stock solution, combined with the known volume ratios on dilution, but those values are probably not correct concentrations for the solutions at the time the spectra were taken. From measurements of the baseline (D in Fig. 3) before and after all spectra of the chlorine solutions were taken, we notice that the spectrum is not reliable below 280 nm, where absorption by pure benzene in the sample and reference beams reduces the signal to zero. Each sample spectrum shown in Fig. 3 was measured in a fresh solution formed

by refilling the sample cell from the flask as described above. The decrease in absorbance of each chlorine solution with time (for example, from A-1 to A-3) was most probably due to the changing chlorine concentration, not because of the photochemical reaction between chlorine and benzene (in such dilute solutions), but rather because of the escape of the chlorine gas from the solution into the vapor phase in the flask.

The normalized absorbance at 280 nm (defined as the observed absorbance A_c divided by the concentration of chlorine C_A°) of each chlorine solution was plotted as a function of time. The functions were quite linear as can be seen in Fig. 4. There is a considerable uncertainty in the extrapolated values of the normalized absorbance at time zero because of the long extrapolation. The non-uniform slope for different chlorine solution plots could be due to the difficulty in defining uniquely the procedure for handling the chlorine solutions. When we repeated some measurements for one chlorine solution from freshly prepared solutions, a different slope of the plot was obtained. The best least-squares line through the data in Fig. 4 was used to obtain the extrapolated values of A_c/C_A° at time zero. The results are shown in Table II. These values are then analyzed by the Benesi-Hildebrand or Scott method (as described below) to obtain the formation constant K, and the molar absorptivity ε_{280} for the complex.

For the more concentrated chlorine solutions (around 0.1 M), we used a single silica cell (described in Chap. II) of 0.1 mm pathlength, measuring against air as the reference. Since these solutions were prepared directly without successive dilution as described before, we modified the procedure slightly from the one previously described.

Fig. 3. -- Ultraviolet spectra of chlorine in benzene taken at different concentrations and at different times. (A) 0.00053 M, (B) 0.00027 M, (C) 0.00013 M (all in Cl_2), (D) baseline; (1), (2), and (3) are the order of successive measurements on fresh solutions (see text).

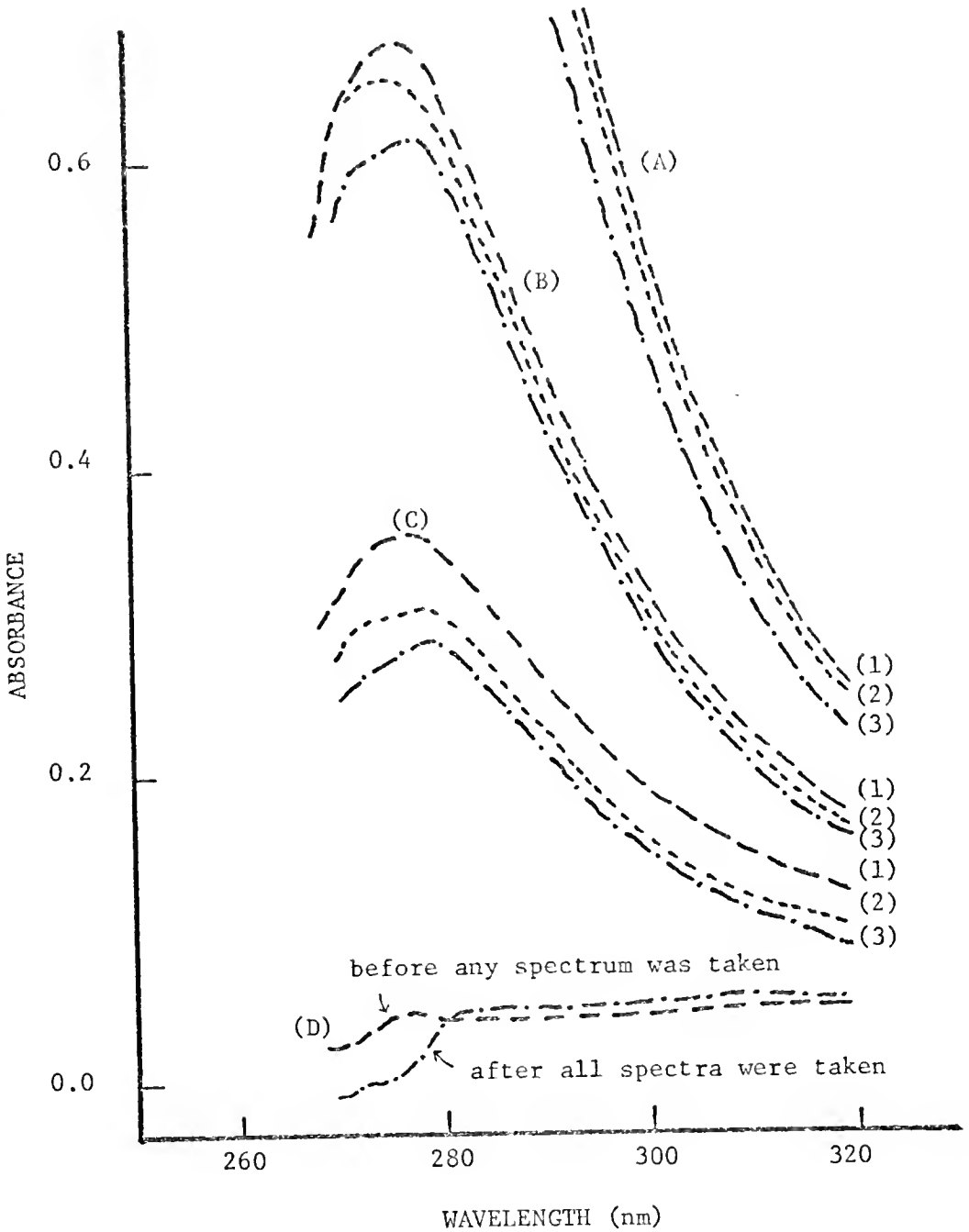
0.6
0.4
0.2
0.0
ABSORBANCE
(A)
(B)
(C)
(D)
(1)
(2)
(3)
(1)
(2)
(3)
(1)
(2)
(3)
before any spectrum was taken
after all spectra were taken
260
280
300
320
WAVELENGTH (nm)

Fig. 4. -- Plots of the normalized absorbance of chlorine at 280 nm vs. time for different chlorine solutions (around 0.001 M).

Δ C_6H_6

o 80% (v/v) C_6H_6, 20% (v/v) CCl_4

⊗ 60% (v/v) C_6H_6, 40% (v/v) CCl_4

⊙ 40% (v/v) C_6H_6, 60% (v/v) CCl_4

□ 20% (v/v) C_6H_6, 80% (v/v) CCl_4

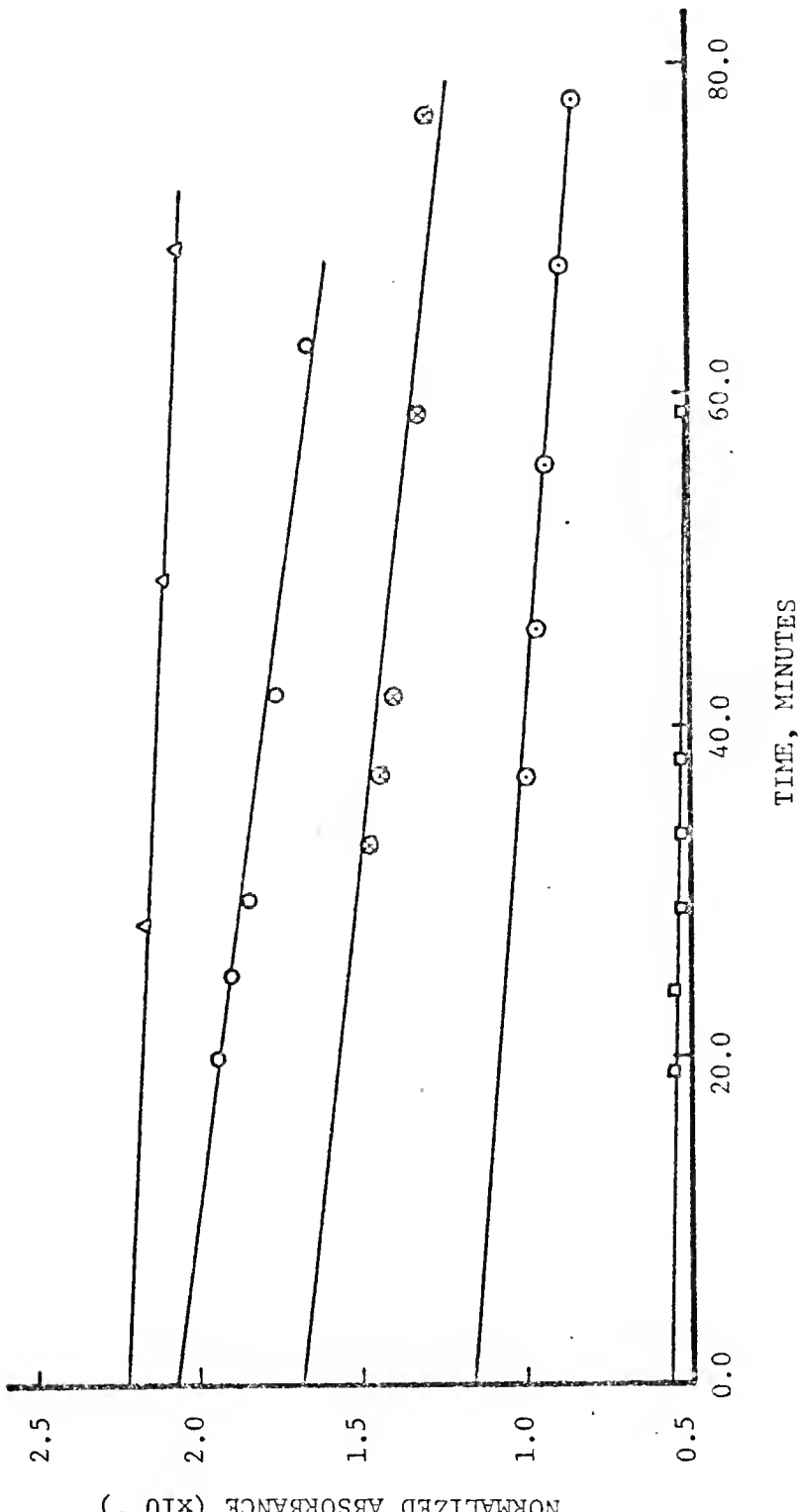
NORMALIZED ABSORBANCE (x10⁻³)
2.5
2.0
1.5
1.0
0.5
0.0
20.0
40.0
60.0
80.0
TIME, MINUTES

TABLE II

EXTRAPOLATED VALUES AT TIME ZERO OF THE NORMALIZED ABSORBANCE (A_C/C_A) FOR DIFFERENT CHLORINE SOLUTIONS

Concentration of Benzene (M)	Extrapolated Values[a] of Normalized Absorbance at 280 nm (A_C/C_A) x 10^{-3}
11.30	2.47
9.03	2.09
6.78	1.68
4.52	1.19
2.26	0.57

a. Values obtained from the intercept (in Fig. 4) of the best least-squares line. The uncertainty of each value is $\pm$ 4% (twice the standard deviation).

This time the concentration of chlorine in the cell could be determined at a time much closer to that of the spectral measurement since the concentration was high enough to be accurately determined. When the sample cell was filled up each time with the syringe and placed in the sample compartment of the spectrometer for the measurement, a 5 ml portion of the chlorine solution was withdrawn within one minute and pipetted into the flask containing excess potassium iodide solution. The measurement was repeated three to four times with fresh solutions from the flask. As before, we measured the baseline before and after the sample spectrum was obtained. Three spectra of chlorine solutions of different concentrations in a 30% (v/v) C_6H_6, 70% (v/v) CCl_4 solvent are shown in Fig. 5. The spectrum A was for a 0.105 M chlorine solution, spectrum B for 0.053 M chlorine, and spectrum C for a 0.026 M chlorine solution; spectra D were taken of the solvent in the cell before and repeated after the spectrum of one of those chlorine solutions was measured. A replotted spectrum for 0.027 M chlorine solution in a 30% (v/v) C_6H_6, 70% (v/v) CCl_4 mixture is shown in Fig. 6. The spectrum is uncertain below 275 nm due to solvent absorption, so that a clear determination of the wavelength of maximum absorbance cannot easily be made, although it appears from Fig. 6 to be near 275 nm.

Analysis of the Ultraviolet Spectroscopic Data from Chlorine-Benzene Solutions

The data at 280 nm from both dilute and concentrated chlorine solutions were analyzed using the Scott equation (14),

$$\ell C_A^\circ C_D^\circ / A_c = C_D^\circ / \varepsilon_{280} + 1/K\varepsilon_{280} \quad . \qquad (3\text{-}1)$$

Here ℓ is the pathlength in cm, C_D° is the initial donor concentration

Fig. 5. -- Ultraviolet spectra of chlorine solutions in a 30% (v/v) C_6H_6 and 70% (v/v) CCl_4 solvent. (A) 0.105 M, (B) 0.053 M, (C) 0.027 M in Cl_2, (D) baseline (solvent vs. air) pathlength = 0.1 mm.

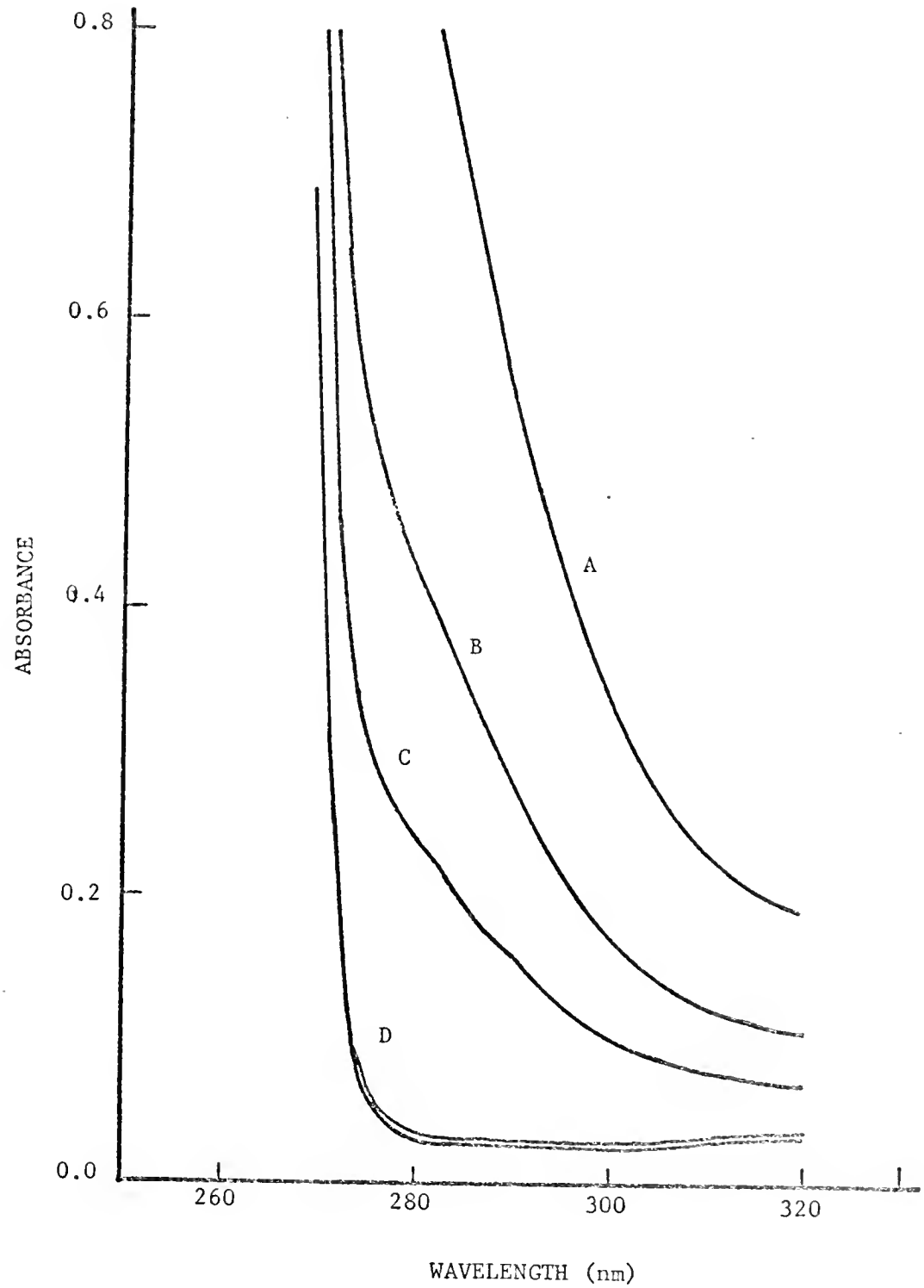
0.8
0.6
0.4
0.2
0.0
ABSORBANCE
A
B
C
D
260
280
300
320
WAVELENGTH (nm)

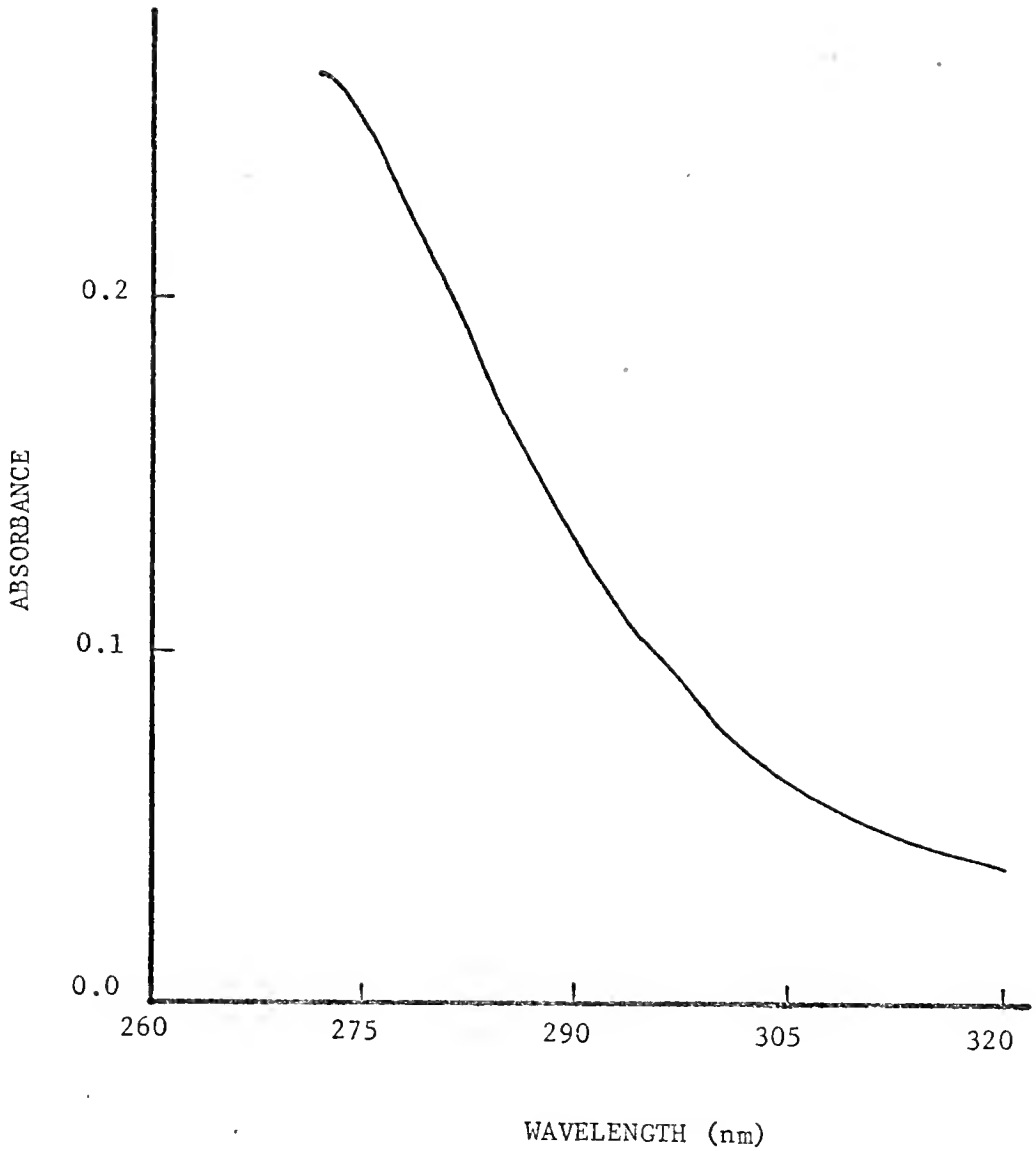

Fig. 6. -- Replotted spectrum of 0.027 M chlorine solution in 30% (v/v) C_6H_6 and 70% (v/v) CCl_4 mixture (0.1 mm path-length).

(M), C_A° is the initial acceptor concentration (M), A_c is the absorbance of the complex at 280 nm, ε_{280} is the molar absorptivity of the complex at 280 nm and K is the equilibrium constant. We assumed the absorption at 280 nm is due to the charge-transfer absorption of the one-to-one complex of chlorine with benzene. The reason absorbance at 280 nm is studied is because that wavelength is the closest to the maximum absorbance that can be studied before the solvent absorption becomes too great.

For the data obtained from the dilute solution in the 1 cm pathlength cell, we used the extrapolated values of A_c/C_A° at time zero (Table II) for the Scott plot, while for those obtained from the concentrated solutions in the short (0.1 mm) pathlength cell, we used the direct absorbance readings and concentrations for the plot. At the same time, we re-analyzed Andrews and Keefer's ultraviolet data (6) by the same Scott plot. The three different sets of the ultraviolet data were plotted on the same graph, and shown in Fig. 7. The error bars for points obtained from the long pathlength cell were estimated from the standard deviation of the least-squares fit to the extrapolation plot (Fig. 4), and from the uncertainty involved in the concentration determination. The error bars for the points obtained from the short pathlength cell are the standard deviations of three to four repeated measurements. There was no way to estimate the uncertainties from Andrews and Keefer's data since they did not report their experimental conditions.

From Fig. 7 we can say that for chlorine solutions of low concentration in chlorine (~ 0.001 M) the agreement between Andrews and Keefer's result and ours is quite good. In particular, we have the

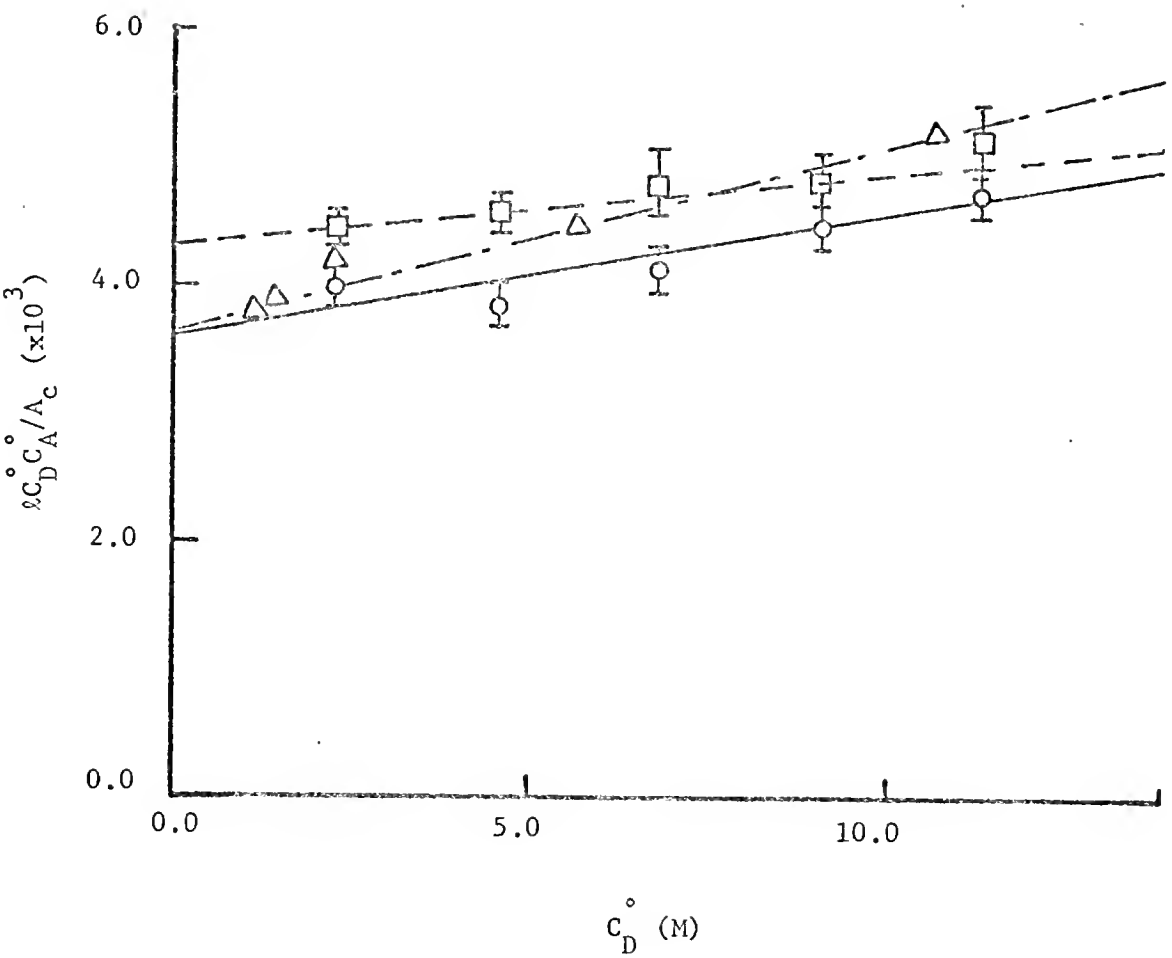

Fig. 7. -- Scott plots of the complex of chlorine and benzene. ○ and — for 1 cm pathlength, □ and – – for 0.1 mm pathlength cell, Δ and —· for Andrews and Keefer's data (Ref. 6).

TABLE III

THE VALUES OF $K\varepsilon_{280}$, K, AND ε_{280} FOR THREE DIFFERENT SETS OF ULTRAVIOLET DATA FROM CHLORINE-BENZENE SOLUTIONS OBTAINED FROM THE SCOTT PLOT

Parameters	Long Pathlength Cell (1 cm)	Short Pathlength Cell (0.1 mm)	Andrews and Keefer's[a] data (probably 1 cm cell)
$K\varepsilon_{280}$ (liter^2 cm^{-1} mole^{-2})	$275 \begin{smallmatrix} +32 \\ -26 \end{smallmatrix}$[b]	321 ± 4[b]	270 ± 11[b]
ε_{280} (liter cm^{-1} mole^{-1})	$13{,}000 \begin{smallmatrix} +23{,}000 \\ -5{,}000 \end{smallmatrix}$[b]	$25{,}000 \begin{smallmatrix} +21{,}000 \\ -8{,}000 \end{smallmatrix}$[b]	$8{,}000 \begin{smallmatrix} +2{,}200 \\ -1{,}400 \end{smallmatrix}$[b]
K[c] (liter mole^{-1})	$0.022 \begin{smallmatrix} +0.012 \\ -0.015 \end{smallmatrix}$[b]	$0.01 \pm .005$[b]	0.034 ± 0.009[b]

a. These values are for ν = 278 nm, not 280 nm.

b. These upper and lower uncertainty limits were twice the calculated standard deviations.

c. The temperature for all measurements of equilibrium constant was 300 °K.

same intercepts of the straight lines which determine the product $K\varepsilon_{280}$. The difference between the plots of the low and the high concentrations of chlorine solutions may not be significant even though the factor of the activity coefficients for solutions of different concentrations could be different (57). However, the experimental uncertainties were so large, we are not in a position to give any definite conclusions about this point.

The values of $K\varepsilon_{280}$, K, and ε_{280} from the Scott plots for the three different sets of ultraviolet data from chlorine solutions are shown in Table III. For each set, the constants were calculated from the best least-squares line. The upper and lower limits of uncertainties listed for each constant were twice the calculated standard deviations.

Despite the fact that the experimental uncertainties were large, the equilibrium constant K of the chlorine-benzene complex is believed to be 0.025 ± 0.015 liter mole^{-1}. The large uncertainty in the value of K is also expected theoretically (53, 54). Nevertheless, the order of the magnitude of K indicates this complex is indeed a very weak one. It is worthwhile to note that the saturation fractions (defined as $s = C_A^c/C_A^\circ$, where C_A^c is the concentration of complexed Cl_2) are between 0.1 to 0.25 in benzene for the above K values.

It has been suggested by Deranleau (54a) that the Scatchard plot is a better method for the analysis of spectral data from weak molecular complexes. In order to check the reliability of the values obtained from the Scott plot, we also used Scatchard's method to analyze the short pathlength ultraviolet data and Andrews and Keefer's data.

The reason for not analyzing the long pathlength cell data was

because the values of the parameters $K\varepsilon_{280}$, ε_{280}, and K of this system were within the range of those obtained from the short pathlength cell data, and those from Andrews and Keefer's data.

The Scatchard equation is given (54a) by

$$A_c/\ell C_A^\circ C_D = K(\varepsilon_{280} - A_c/\ell C_A^\circ) \quad . \tag{3-2}$$

Here C_D is the equilibrium concentration of the donor, ($C_D \simeq C_D^\circ$, the total concentration of the donor for solutions with excess donor), ℓ, C_A°, A_c, K and ε_{280} are the same as defined for Eq. 3-1. We calculated $A_c/\ell C_A^\circ C_D$ and $A_c/\ell C_A^\circ$ for each C_A° at a particular C_D and plotted $A_c/\ell C_A^\circ C_D$ vs. $A_c/\ell C_A^\circ$ for the five different values of C_D. The results are shown in Fig. 8. For the 0.1 mm (short pathlength) cell data, we obtained the average values of $A_c/\ell C_A^\circ C_D$ and $A_c/\ell C_A^\circ$ by averaging all $A_c/\ell C_A^\circ C_D$ and $A_c/\ell C_A^\circ$ values, respectively, at each C_D. The error bars in Fig.8 were obtained from the scatter of the measurements about the average value. There were five sets of ($A_c/\ell C_A^\circ C_D$, $A_c/\ell C_A^\circ$) values at each of the five different C_D values. We estimated K and $K\varepsilon_{280}$ from the slope and the intercept of the best least-squares line through these points. We applied the same technique to analyze Andrews and Keefer's data to estimate K, $K\varepsilon_{278}$ and ε_{278}. The calculated parameters of the Scatchard plots are shown in Table IV. The upper and lower limits were twice the calculated standard deviations.

When we compare Table III and IV, we see that the values of $K\varepsilon_\nu$, K and ε_ν are not significantly different. Again, the value of K from the short pathlength cell may be lower than the value from the more dilute solutions. However, a line can be drawn through the error bars for these data (Fig. 8) that includes the value of K from the long

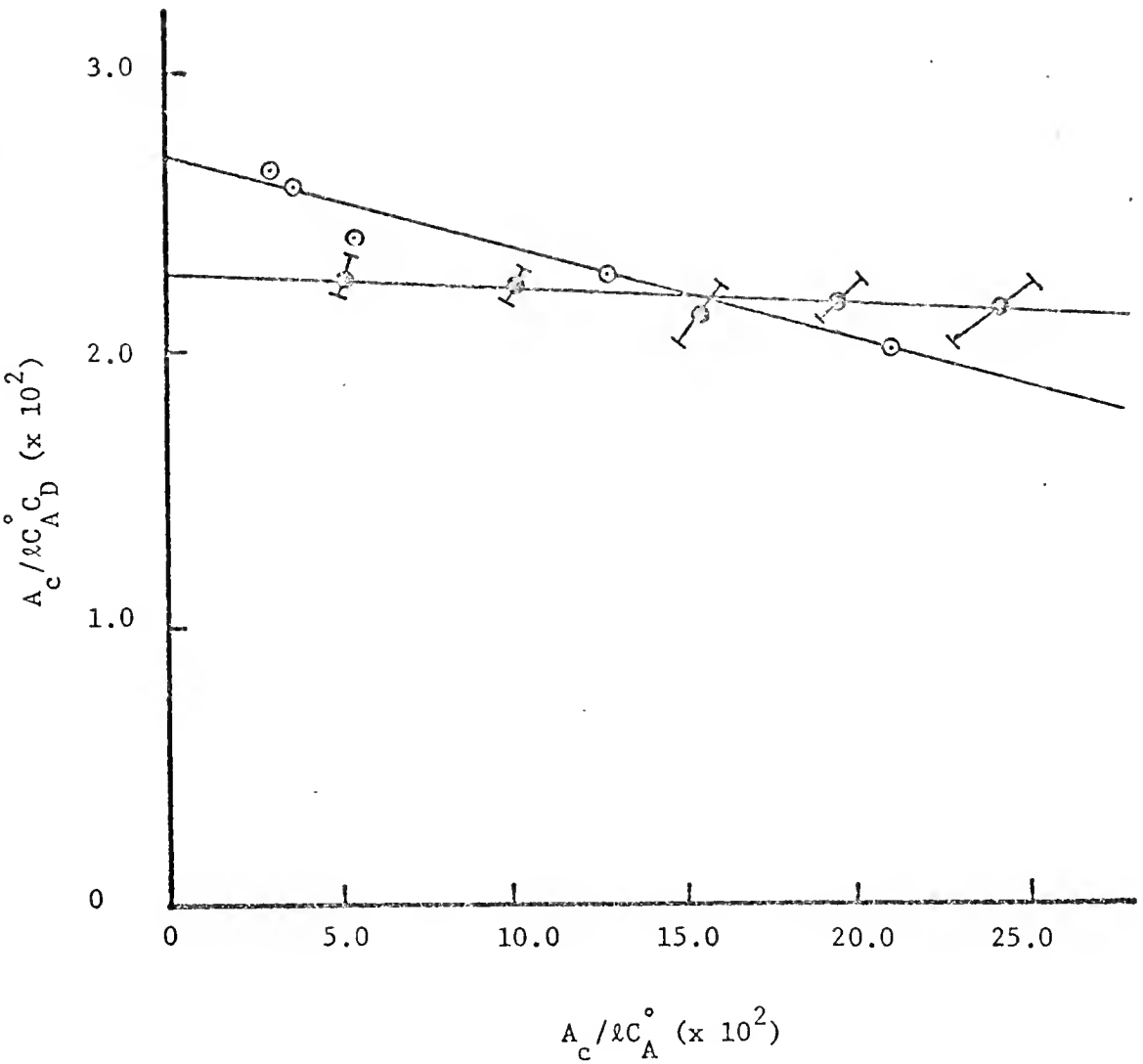

Fig. 8. -- Scatchard plots for the complex of chlorine with benzene. (1) ● 0.1 mm short pathlength data; (2) ⊙ from Andrews and Keefer's data

TABLE IV

VALUES OF $K\varepsilon_\nu$, K AND ε_ν FOR

CHLORINE SOLUTIONS FROM SCATCHARD PLOTS

Parameters	Short Pathlength[a] (0.1 mm)	Andrews and Keefer[b]
$K\varepsilon_\nu$	228 ± 8[c]	269 ± 12[c]
K	0.0064 ± 0.0046[c]	0.034 ± 0.01[c]
ε_ν	$35{,}000 \begin{smallmatrix} + 100{,}000 \\ - 16{,}000 \end{smallmatrix}$[c]	$7{,}300 \begin{smallmatrix} + 4{,}400 \\ - 1{,}300 \end{smallmatrix}$[c]

a. Evaluated at ν = 280 mm.

b. Evaluated at ν = 278 mm.

c. The upper and lower limits were twice the calculated standard deviations.

pathlength studies. We conclude that the value of $K\varepsilon_{280}$ is 280 ± 40, with $K = 0.025 \pm 0.015$ liter $mole^{-1}$ and $\varepsilon_{280} = 13{,}000$, possibly from values as low as 5,000 to values as high as 35,000 liter $cm^{-1}mole^{-1}$. In concentrated solutions, K may possibly be somewhat smaller. It is not possible to reach more definite conclusions about these values from this very weak complex (54).

CHAPTER IV

RAMAN SPECTROSCOPIC STUDIES OF CHLORINE IN BENZENE SOLUTIONS

Introduction

We are particularly interested in studying the Raman frequency shifts and the Raman intensity change of chlorine in solution as the composition of the solvent is gradually changed from benzene by the addition of carbon tetrachloride. The spectral profiles of the Cl-Cl stretching vibration as a function of the composition of the mixture C_6H_6-CCl_4 were carefully examined in order to understand more about the nature of the complex of chlorine with benzene. As a check of the reliability of the equilibrium constant of the complex determined from the ultraviolet spectroscopic measurements, we analyzed the Raman intensity data both by the method of Rosen, Shen and Stenman (32) to estimate the equilibrium constant and also by the method of Bahnick and Person (58). The absolute Raman intensity of chlorine in carbon tetrachloride was carefully determined.

Experimental Procedure

For this study, a Perkin-Elmer LR-1 Raman spectrometer was used with a Ne-He laser with a minimum out-put of 2.7 mw. The Raman shift (Δ cm^{-1}) is proportional to the grating position read in mechanical units (called drum numbers) from the linear spectrometer scale. The actual Raman shift was obtained from a calibration curve of wavenumbers vs. drum number using the known wavenumbers of the emission lines of a Ne lamp.

Three lines at 650.669 nm, 653.308 nm and 659.918 nm (or 433.1 cm^{-1}, 495.1 cm^{-1} and 648.5 cm^{-1} from the Raman exciting line at 15,802.7 cm^{-1} or 632.8 nm) were chosen for this purpose because they had been well studied (59). The Ne lamp source was a Pen-Ray quartz lamp operated with a 115 volt 60 cycle/second power supply (Model No. SCT2, with maximum current of 4 amperes from Ultra Violet Products, Inc., San Gabriel, California). In practice, we placed the lamp in the sample cell position in the sample compartment of the Raman spectrometer, opened the mechanical slit to 5 microns and recorded the spectrum just as though we were making a Raman measurement except the laser was not turned on. As mentioned in Chap. II, the standard Perkin-Elmer 2.5 ml multiple-path cell was used.

Because of the chemical instability of the chlorine solution, it was desirable to work with low chlorine concentrations (around 0.1 M) and to scan the spectrum quite rapidly. In order to obtain a spectral resolution of 7.5 cm^{-1} at a 5% peak-to-peak noise level, the spectral scan rate was about 6 cm^{-1} per minute, or 15 to 20 minutes to measure a complete chlorine Raman spectrum from 480 cm^{-1} to 600 cm^{-1}.

Before studying the Raman spectra of chlorine solutions, we investigated the solvent background in the region where the Raman band of chlorine would appear. The Raman spectrum for the solvent mixture of C_6H_6-CCl_4-$CHCl_3$ in a 6:3:1 ratio is shown in Fig. 9. The Raman shift for chlorine is expected to appear between the two bands (ν_1 of carbon tetrachloride at 461 cm^{-1} on the low frequency side and ν_{18} of benzene at 606 cm^{-1} on the high frequency side) with only slight overlap with these two solvent bands. Nevertheless, that overlap results in the loss of most of the spectral information from the wings of the

Fig. 9. -- Raman spectrum of the C_6H_6-CCl_4-$CHCl_3$ mixture at a ratio of 6:3:1.

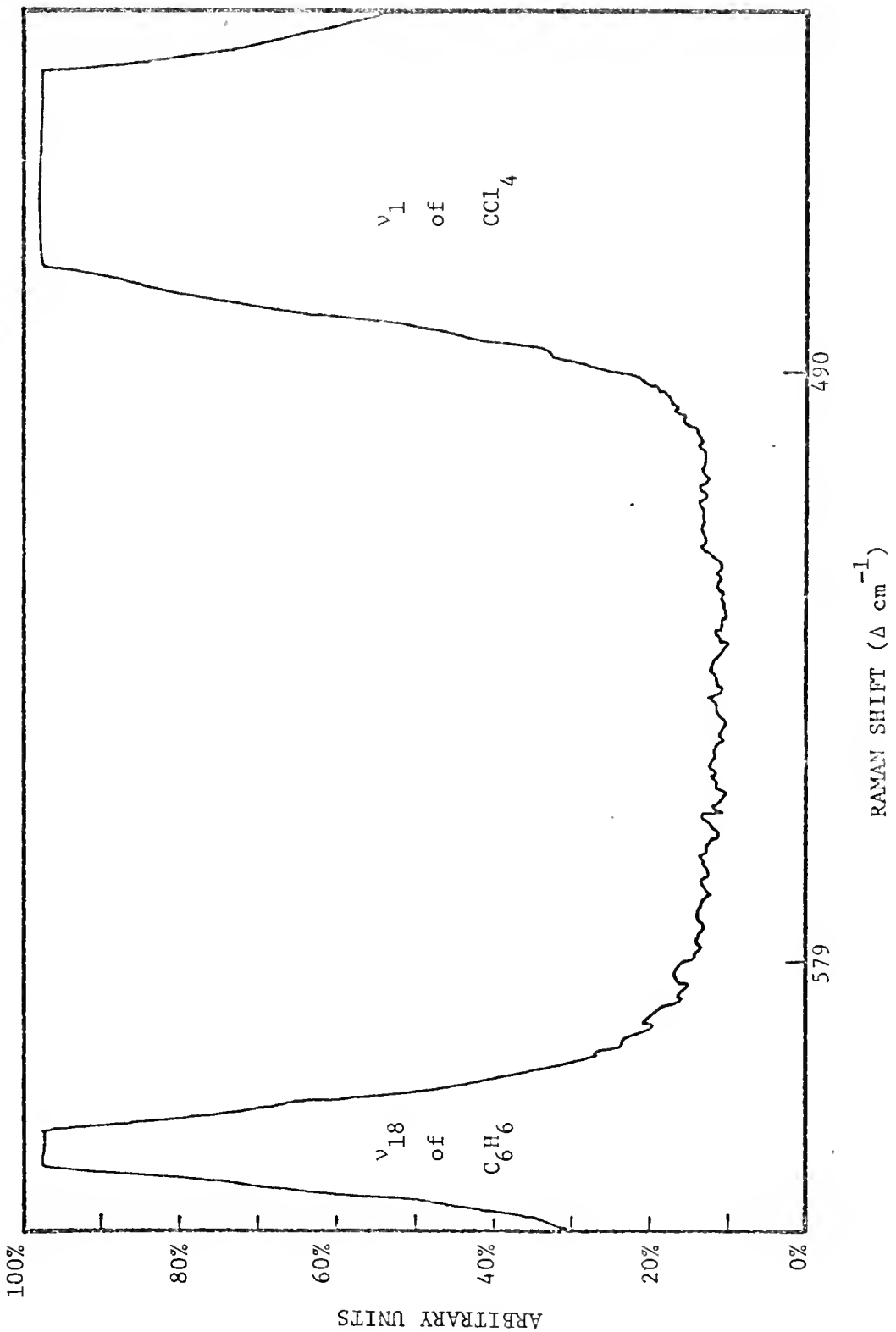
100%
80%
60%
40%
20%
0%
ARBITRARY UNITS
ν_{18} of C_6H_6
ν_1 of CCl_4
579
490
RAMAN SHIFT (Δ cm^{-1})

chlorine band. The extent of the overlap of the chlorine band with the two solvent bands is shown in Fig. 10, where the spectrum was obtained from a 0.12 M chlorine solution in the mixture of C_6H_6-CCl_4-$CHCl_3$ at a ratio of 8:1:1.

Secondly, since we knew that it was very difficult to prevent the photochemical reaction from occurring, especially when the chlorine solution was irradiated by the laser in order to obtain the Raman spectrum, we studied the Raman spectrum of the photochemical product ($C_6H_6Cl_6$) in order to determine its interference with the chlorine band. We found that the hexachlorocyclohexane (and also any other unidentified photochemical products) did not have any observed Raman shift near the chlorine band. This was done by an experiment in which we let the chlorine solution (around 0.5 M) in a 6:4 C_6H_6-CCl_4 mixture stand under the fluorescent room lights for several hours before taking the Raman spectrum of the solution. Afterwards we eliminated the chlorine by bubbling N_2 gas through the same solution (but not from the sample cell solution) and measured the Raman spectrum of the resulting chlorine-free stock solution. We knew that the photochemical product did form in the experiment, since the solid residue after evaporating the solvent was dissolved in carbon tetrachloride and the NMR spectrum showed its existence. The Raman spectrum of this particular chlorine solution (approximately 0.5 M) in the C_6H_6-CCl_4 mixture at a ratio of 6:4 is shown in Fig. 11. The Raman spectrum of the chlorine-free stock solution at the same experimental condition is shown in Fig. 12. The apparent reduction in the Raman intensity, both for ν_{18} of benzene and ν_1 of carbon tetrachloride bands in the chlorine solution (Fig. 11) compared to the intensities in the colorless solution

Fig. 10. -- Raman spectrum of 0.12 M chlorine in a C_6H_6-CCl_4-$CHCl_3$ mixture at a ratio of 8:1:1.

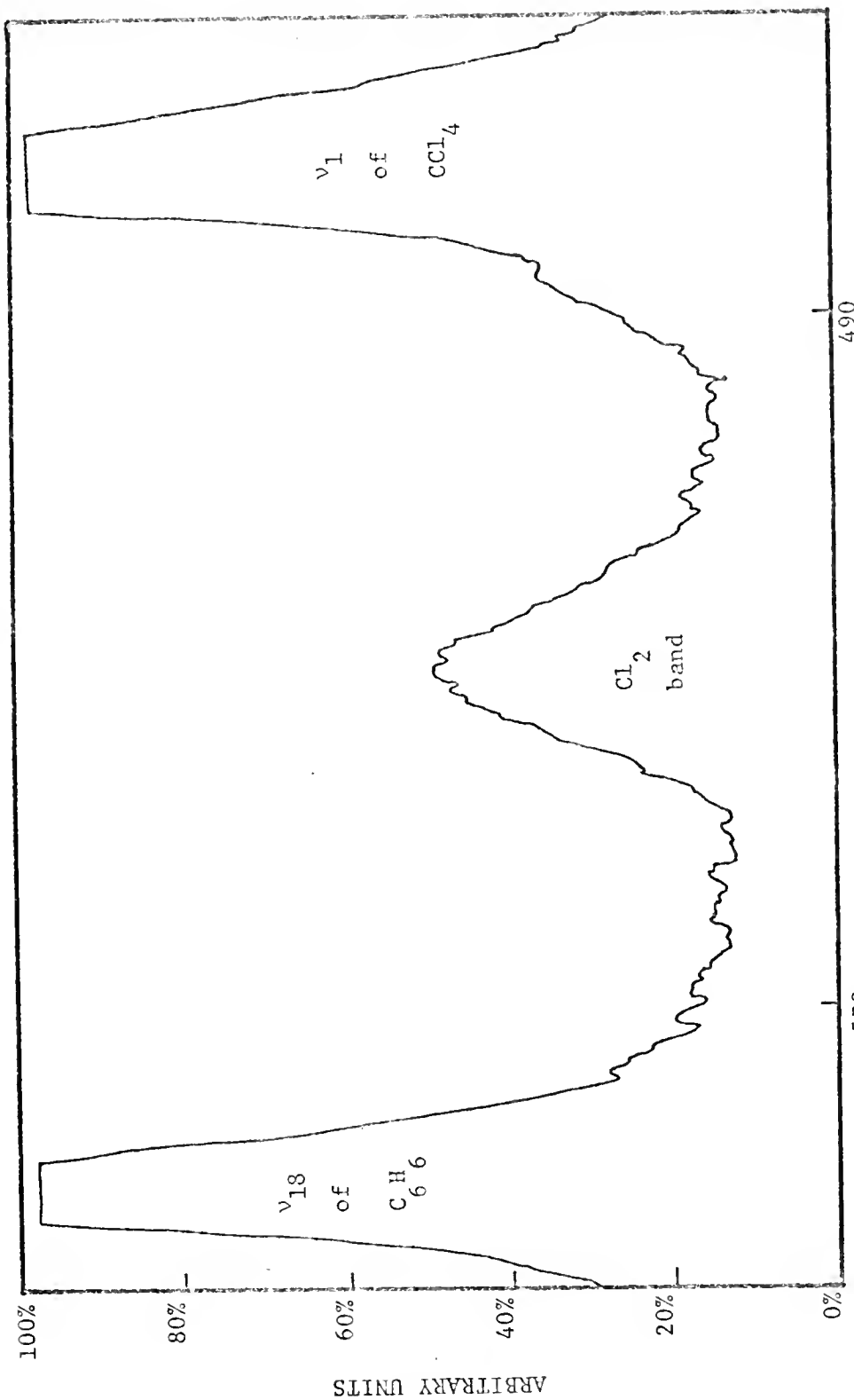
100%
80%
60%
40%
20%
0%
ARBITRARY UNITS
579
490
RAMAN SHIFT (Δ cm⁻¹)
ν18 of C6H6
Cl2 band
ν1 of CCl4

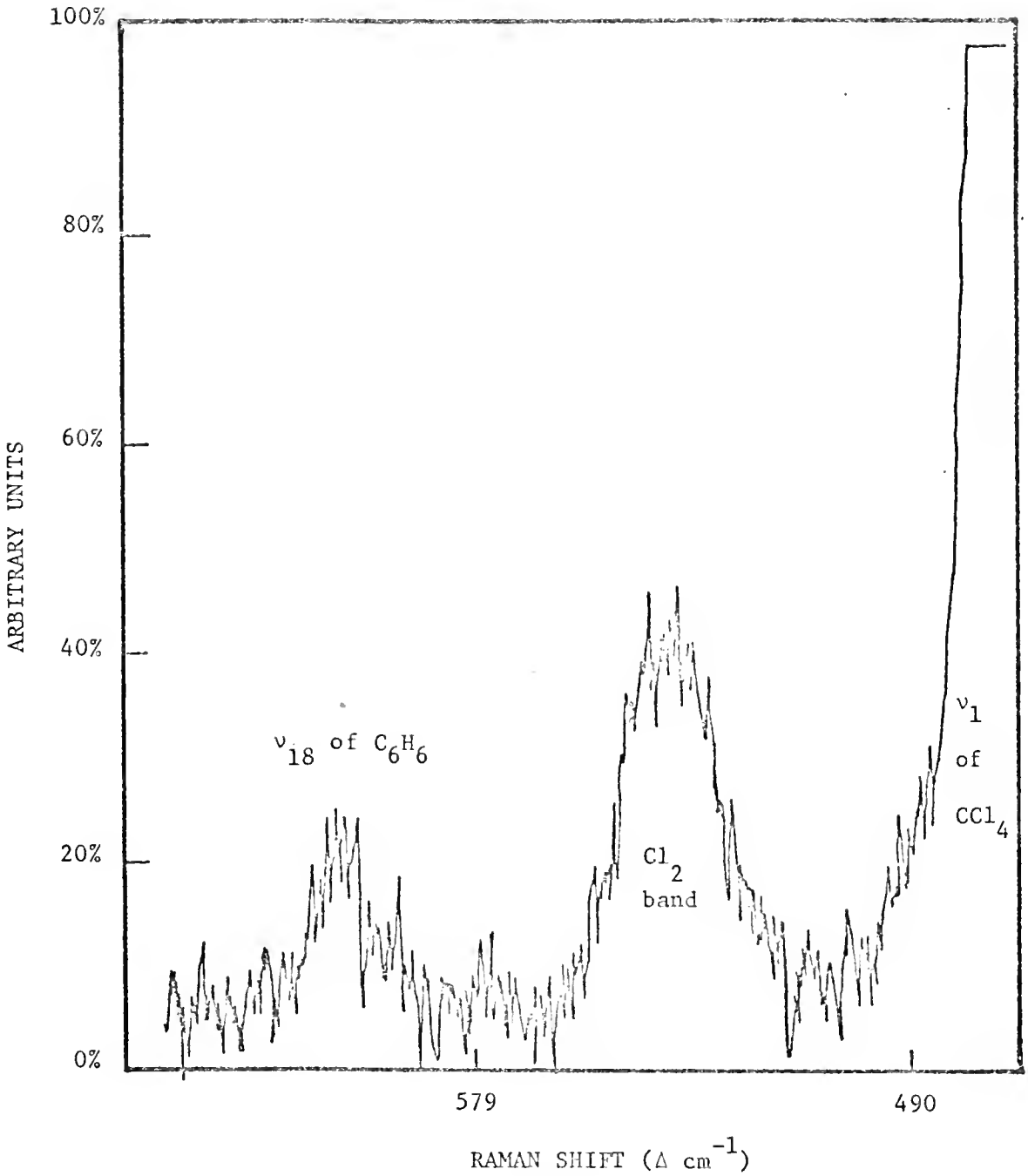

Fig. 11. -- Raman spectrum of 0.5 M chlorine in 6:4 C_6H_6-CCl_4 .

(Fig. 12), is most probably due to the absorption of the existing or scattered light in the dark-colored solution. Within the experimental error we can say that there is no observable Raman band due to photochemical products in this spectral region (between ν_1 of CCl_4 and ν_{18} of C_6H_6).

At this point we were ready to measure the Raman spectra of chlorine solutions. We warmed up the spectrometer for one hour. During this period, we prepared 100 ml of solvent, which always contained 10 ml of chloroform. When the spectrometer was ready, we bubbled chlorine into the solvent for 5 minutes (to prepare a solution about 0.1 M in chlorine). A 5 ml sample of the chlorine solution was withdrawn for titration and the Raman liquid cell was immediately filled with the chlorine solution and placed in the spectrometer. After the Raman spectrum of that chlorine solution was recorded, a 5 ml sample of solution was again withdrawn from the stock solution for concentration determination. We also determined (once only) the chlorine concentration for some solution taken directly from the Raman cell after its Raman spectrum had been recorded. The result was the same as the concentration from the stock solutions within the experimental error.

The depolarization ratio (ρ) of the Raman band of chlorine was measured for three different chlorine solutions (one of chlorine in pure C_6H_6, one in a 1:1 C_6H_6- CCl_4 mixture, and one in pure CCl_4). The concentrations of these chlorine solutions were not determined but they were believed to be around 0.2 M. For these measurements, we used an Ahrens prism placed between the sample housing and the monochromator as described in the Perkin-Elmer manual (60). The spectral resolution was the same as before. The intensity of the parallel component was

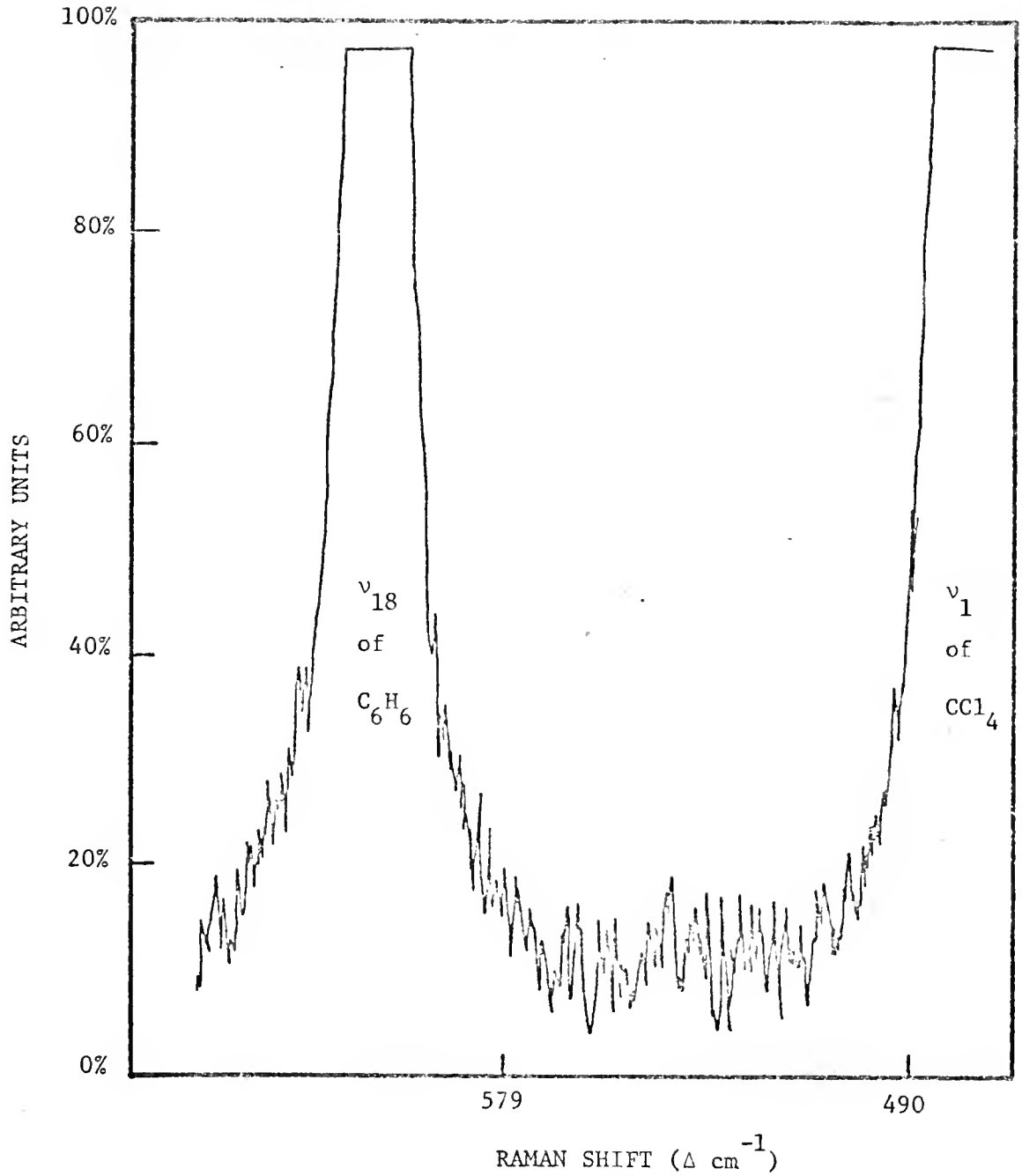

Fig. 12. -- Raman spectrum of the chlorine-free 6:4 C_6H_6-CCl_4 solution.

measured first by adjusting the experimental parameters so that the maximum Raman scattering of this component was around 70% on the chart paper scale. (We did not turn the gain higher because we wanted to keep the peak-to-peak noise level less than 10%.) Then we measured the intensity of the perpendicular component. In order to compensate for the fluctuation of the laser power and the change in chlorine concentration during the measurement, we measured again the intensity of the parallel component immediately after we had measured the perpendicular one. To obtain the depolarization ratio, we divided the band area of the perpendicular component by the average band area of the two measurements of the parallel component. Because the Raman band of chlorine was weaker as more carbon tetrachloride was added to the solvent mixture, the peak-to-peak noise level was higher for Cl_2 in CCl_4. As we tried to increase the amplifier gain in order to obtain a comparable signal for different chlorine solutions, the depolarization ratio of the Raman band of chlorine had larger uncertainty (for solutions containing more CCl_4). In particular, the noise level was so high that the intensity of the perpendicular component could not be measured with certainty for the chlorine solution in pure carbon tetrachloride. Hence, only an upper limit can be given for ρ for Cl_2 dissolved in pure CCl_4.

Results of the Raman Measurements on Chlorine Solutions

The Raman shifts (in cm^{-1}) observed for chlorine solutions are shown in Table V as a function of the benzene concentration. The values listed here are believed to be accurate within $\pm$ 0.5 cm^{-1}, and were obtained from the positions of the band maxima. The concentration of benzene was estimated from a knowledge of the volume of benzene

TABLE V

OBSERVED RAMAN SHIFTS, HALF-BAND WIDTHS AND RELATIVE INTENSITIES OF CHLORINE SOLUTIONS IN C_6H_6-CCl_4 SOLVENT MIXTURES AS A FUNCTION OF BENZENE CONCENTRATION

Concentration of Benzene (M)	Concentration of Chlorine (M)	Raman Shift[a] (cm^{-1})	Raman Half-Band Width (cm^{-1})	Relative Raman Intensity[b]
10.7	0.138	530.2	19.3 ± 0.3	13.7
9.04	0.123	531.2	18.3 ± 0.7	11.0
6.78	0.181	533.2	19.3 ± 0.4	8.4
4.52	0.102	535.6	18.6 ± 0.3	7.1
2.26	0.123	539.7	17.8 ± 0.4	6.3
1.13	0.205	542.0	15.5 ± 0.3	3.7
0.0	0.129	543.3	12.4 ± 0.5	2.75

a) The uncertainty is about ± 0.5 cm^{-1}

b) As defined in Eq. 4-1; the uncertainty is about ± 9.3%

added, and the total volume of the solvent. The concentration of pure liquid benzene was taken to be 11.3 M at room temperature. The concentration of benzene in the solvent mixture was calculated by multiplying this number by the volume fraction of benzene in the mixture (assuming no volume change as benzene was dissolved in CCl_4).

At our rather poor spectral resolution of 7.5 cm^{-1}, we could not observe (for any solvent mixture) two clearly separated Raman peaks, one for complexed chlorine and the other for the uncomplexed molecule, so we examined the spectral profile of the chlorine band as a whole. The half-band widths of the chlorine solutions were measured and are also shown in Table V. The corresponding values are plotted vs. the concentration of benzene in Fig. 13, where we see clearly the broadening of the chlorine Raman band that occurs as the ratio of C_6H_6 to CCl_4 approximates 1:1. This behavior may be an indication of two overlapping bands, one for complexed chlorine and the other for the uncomplexed chlorine.

The relative integrated intensity $I_{R(\nu)}$ of the Raman band of chlorine was defined as given by Bahnick and Person (58),

$$I_{R(\nu)} = I_{\nu}/I_{Ref}M \quad . \tag{4-1}$$

Here I_{ν} is the band area of the chlorine band, I_{Ref} is the band area of the 366 cm^{-1} chloroform reference band (an internal standard, always at 10% by volume), and M is the total molar concentration of chlorine. The band area was measured by a planimeter (Keuffel and Esser Co.). The most difficult thing in defining the band area was the decision on how to draw a baseline. We estimated by different assumed baselines

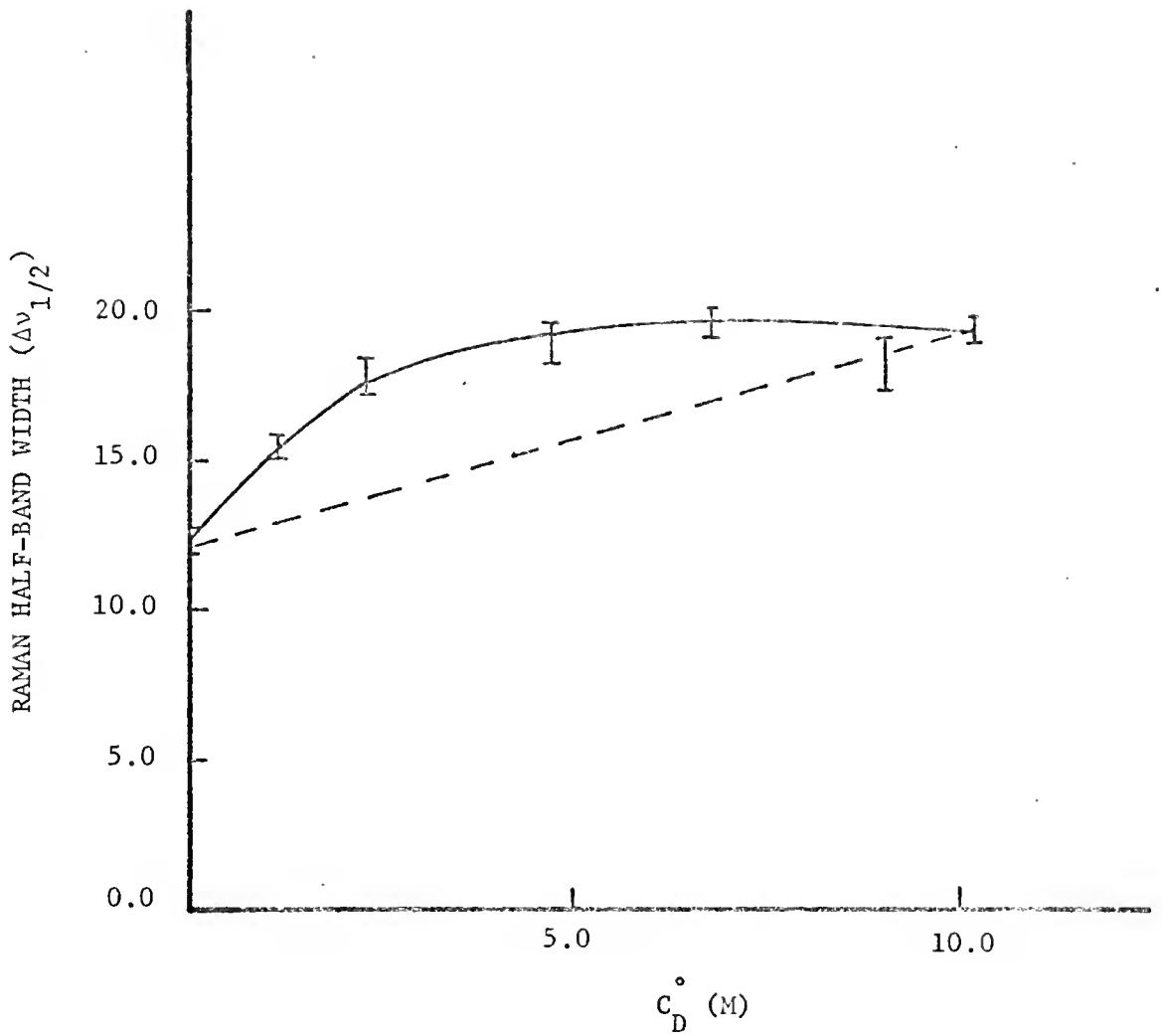

Fig. 13. -- Plot of the Raman spectral half-band width of chlorine vs. the concentration of benzene (C_D°).

that the choice of the baseline might lead to an uncertainty of ± 5-10% in band area. In general, we drew a baseline through the average background noise level in the two wings of the band. The relative integrated intensities obtained according to Eq. 4-1 for chlorine solutions are shown in column 5 of Table IV. The corresponding values of $I_{R(\nu)}$ are plotted in Fig. 14 as a function of benzene concentration.

The uncertainties in the values of the relative intensities of chlorine were estimated by propagation of errors. From Eq. 4-1 the relative error is given by

$$\delta I_{R(\nu)}/I_{R(\nu)} = [(\delta I_{\nu}/I_{\nu})^2 + (\delta I_{ref}/I_{ref})^2 + (\delta M/M)^2]^{1/2} \quad . \tag{4-2}$$

From the scatter in measurements, we estimated that the individual error is ± 4.3% for $(\delta I_{\nu}/I_{\nu})$, ± 6.8% for $(\delta I_{ref}/I_{ref})$ and 4.6% for $(\delta M/M)$, so that the uncertainty in the relative intensity $(\delta I_{R(\nu)}/I_{R(\nu)}$ was then found from Eq. 4-2 to be ± 9.3%.

From Fig. 14 we see that there is a drastic intensification of the relative Raman intensity of the Cl-Cl stretching vibration of chlorine as the solvent is changed from pure CCl_4 to pure benzene. The enhancement in intensity is found to be approximately by a factor of 5 based on a total chlorine concentration or by a factor of 20 based on the concentration of complexed chlorine. (Note: The fraction of chlorine in pure benzene solution that is complexed is about 0.2 of the total concentration, based on a value for the equilibrium constant of 0.03 liter $mole^{-1}$.) There appear to be only two possible explanations for this dramatic intensity increase -- one due to the non-specific solvent effects and the other due to the effects from the formation of the charge-transfer complex. A more detailed discussion

Fig. 14. -- The relative Raman intensity of chlorine $I_{R(\nu)}$ as function of the benzene concentration (M).

⊠ Measured values

⊗ Calculated values from K and I_R° determined from Rosen plot and measured value of $I_{R(\nu)}$

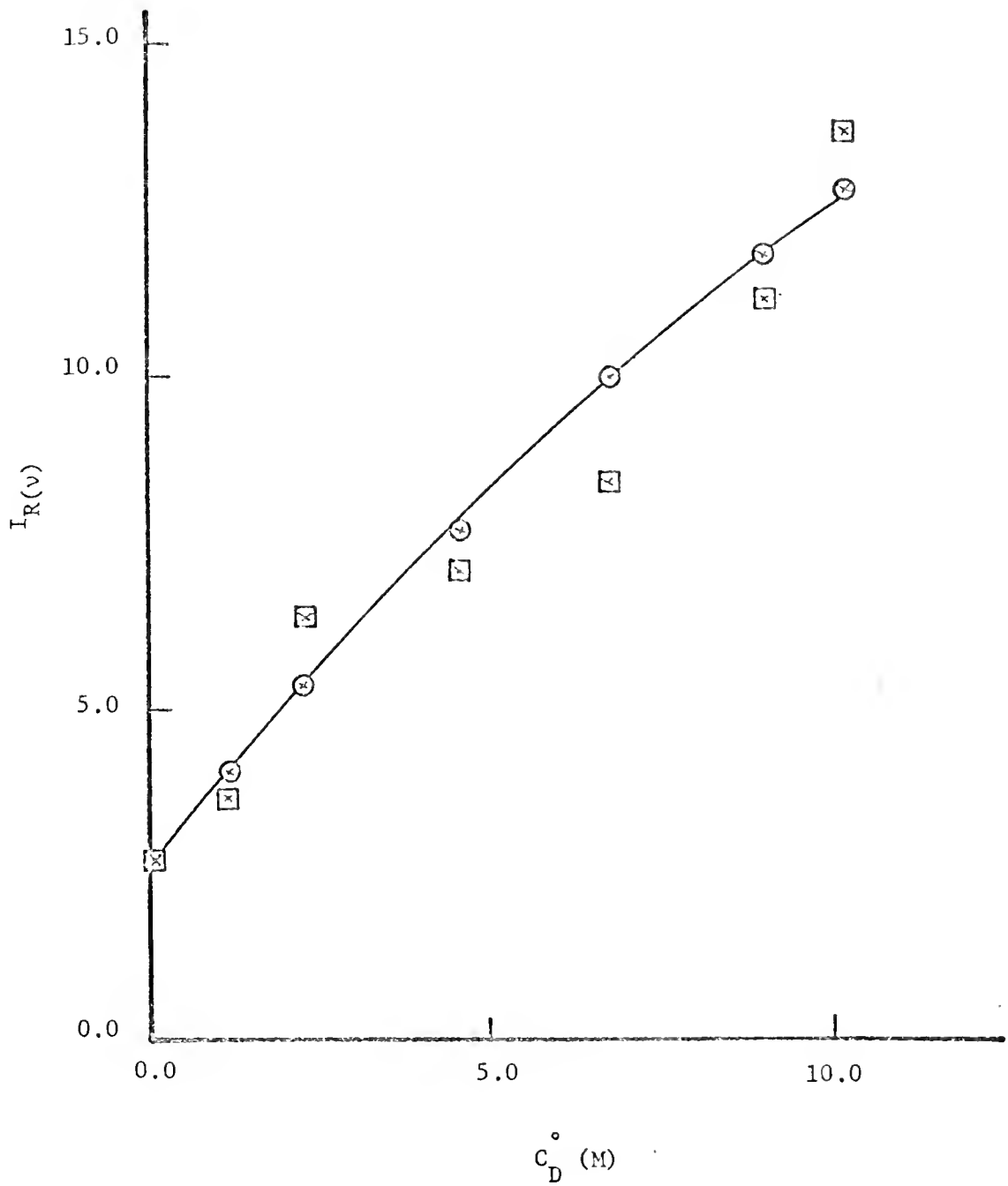
15.0
10.0
5.0
0.0
$I_{R(v)}$
0.0
5.0
10.0
C_D° (M)

will be given in Chap. VII.

Rosen, Shen and Stenman (32) have derived an equation which can be used to analyze the Raman spectroscopic data from the complex, which may not necessarily be a charge-transfer complex. Their equation was derived from a statistical mechanical treatment assuming that the properties of the acceptor are a statistical average over all possible configurations between acceptors and donors weighed by an appropriate distribution function. For a one-to-one complex, the Benesi-Hildebrand type equation for Raman intensity data of the acceptor was found by Rosen, Shen, and Stenman to be

$$1/[(I_{R(\nu)} - I'_{R(\nu)}] = \rho_B^{\circ}/I_R^{\circ}K'\rho_B + 1/I_R^{\circ} \quad . \qquad (4\text{-}3)$$

Here $I_{R(\nu)}$ is the total relative intensity of the Raman band of the acceptor at some particular donor concentration, $I'_{R(\nu)}$ is the relative intensity of the acceptor Raman band at zero donor concentration (i.e., the pure CCl_4 solution), ρ_B° is the molar concentration of the pure donor, ρ_B is the molar concentration of the donor in the solvent mixture, I_R° is the Raman intensity statistically averaged over all possible orientations of the one-to-one interactions between donor and acceptor, and K'/ρ_B° (= K) is the statistically averaged "equilibrium constant" over all the one-to-one interactions.

In applying Eq. 4-3, we assumed that only one-to-one interactions between chlorine and benzene have a significant effect on the Raman spectrum. Using the relative Raman intensity data for chlorine in this system, reported in the last column of Table IV, a plot of Eq. 4-3 is shown in Fig. 15, where the error bar for each point indicated the uncertainty of the measured relative Raman intensity of chlorine. The

Fig. 15. -- Plot of $1/[I_{R(\nu)} - I'_{R(\nu)}]$ vs. ρ_B°/ρ_B for chlorine in benzene solutions.

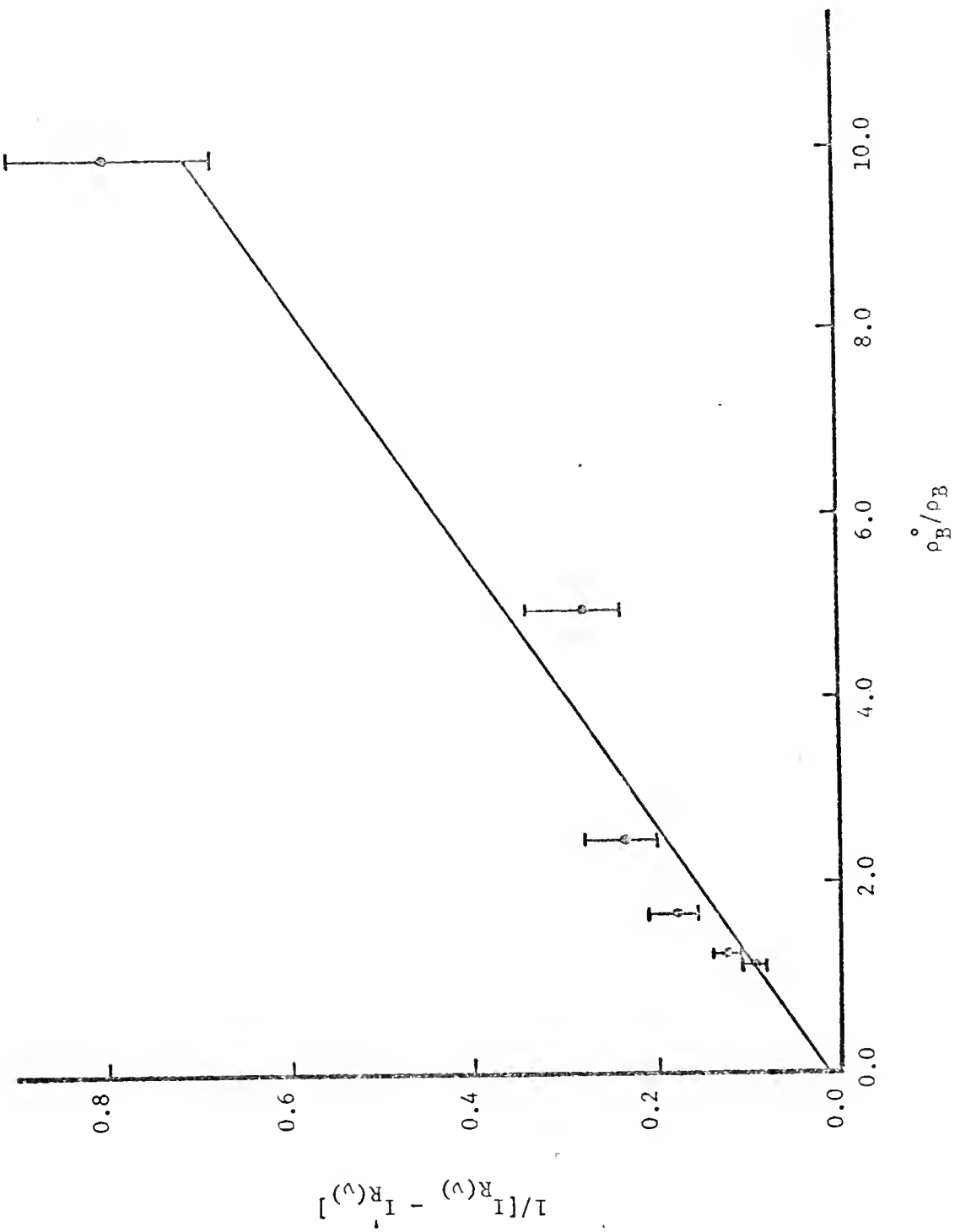
0.0
0.2
0.4
0.6
0.8
1/[I_R(υ) - I'_R(υ)]
0.0
2.0
4.0
6.0
8.0
10.0
ρ°_B/ρ_B

constant I_R° is found from the intercept of Fig. 15, by a least-squares fit to be $54.7 \pm \infty_{3.7}$ (the upper limit is undefined because the standard deviation is larger than the magnitude of the intercept), and the constant $K' I_R^\circ/\rho_B^\circ$ is calculated from the slope to be 1.2 ± 0.15. Taking the ratio, we estimated that the equilibrium constant K ($= K'/\rho_B^\circ$) is $0.022 \begin{smallmatrix} + 0.055 \\ - 0.02 \end{smallmatrix}$ liter mole^{-1} (the lower limit is undefined because the upper limit of I_R° is undefined). The undertainties here are the standard deviations. Even though the uncertainty in K is large, its value (0.022 liter mole^{-1}) is almost identical with the equilibrium constant determined from the ultraviolet spectroscopic measurements given earlier in Chap. III.

In order to gain some confidence in our measured relative Raman intensities of chlorine in different benzene solutions, we substituted the values found here for I_R° and K'/ρ_B° back into Eq. 4-3 together with the measured value for $I'_{R(\nu)}$ (2.75 liter mole^{-1}) to obtain values for $I_{R(\nu)}$ vs. ρ_B to be compared in Fig. 14 with the measured values of $I_{R(\nu)}$. Comparing these calculated values of $I_{R(\nu)}$'s with the observed ones, we see that the measured $I_{R(\nu)}$'s are reasonably good.

Earlier, Bahnick and Person (58) had derived a different expression for the analysis of the Raman spectroscopic data of a complex to obtain the formation constant. By analogy to the derivation of the method for analysis of ultraviolet spectroscopic data by Tamres (61), they obtained an equation for a one-to-one complex (assumed to be in a particular configuration):

$$\rho_B/[I_{R(\nu)} - I'_{R(\nu)}] = (\rho_B + C_A^\circ - C)/[I_R^\circ - I'_{R(\nu)}] + 1/K[I_R^\circ - I'_{R(\nu)}] \quad . \tag{4-4}$$

Here $I_{R(\nu)}$, $I'_{R(\nu)}$, I_R° are the same as those defined for Eq. 4-3; ρ_B is

still the molar concentration of the donor and C_A° is the total molar concentration of the acceptor, while C is the molar concentration of the complex (or the molar concentration of the complexed acceptor for the one-to-one complex). The difference between Eq. 4-3 and Eq. 4-4 is that the former is equivalent to the Benesi-Hildebrand equation (2), while the latter is similar to the Scott equation (14).

In order to apply Eq. 4-4, a trial value of K has to be assumed, and C is then computed for each solution. The left-hand side of Eq. 4-4 is then plotted vs. $(\rho_B + C_A^\circ - C)$, and the best straight line is fitted to the points by least squares. The value of K calculated from this line was used to recompute C and so on until K converges to a constant value (for more detailed procedure, see Ref. 58). Since C for the complex of chlorine with benzene is very small (since it was found from the ultraviolet spectroscopic data that the equilibrium constant was very small), $(\rho_B + C_A^\circ - C)$ is almost equal to $(\rho_B + C_A^\circ)$, so we used the value of K (0.022 liter $mole^{-1}$) obtained from the plot of Eq. 4-3 to calculate C and then made a least-squares fit to the points calculated. The formation constant K and the values of I_R° were then estimated from this best straight line (as shown in Fig. 16) to be $0.034 \begin{smallmatrix} + 0.045 \\ - 0.03 \end{smallmatrix}$ liter $mole^{-1}$ and $38.9 \begin{smallmatrix} + 180.0 \\ - 15.0 \end{smallmatrix}$ respectively.

Thus both methods for analyzing the Raman intensity data gave almost the same equilibrium constant K for the complex of chlorine with benzene and nearly equal values for the relative molar Raman intensity I_R° for the complexed chlorine. The slight differences in K and I_R° obtained from the two methods could be due just to the differences between the two procedures (Benesi-Hildebrand and Scott), since the two methods weigh the experimental points differently.

The results of the depolarization ratio measurements (ρ) for the Cl-Cl stretching vibration measured in these different chlorine-benzene solutions are shown in Table VI. ρ was estimated from the ratio of the band area of the perpendicular component to that of the parallel one. As mentioned in the experimental procedures section, the perpendicular band of chlorine in carbon tetrachloride was weak and the noise level was so high that it was impossible to obtain a reliable value of ρ in this solvent. We believe these results show a tendency for the depolarization ratio to increase as the benzene concentration increases, possibly because more chlorine molecules are complexed as more benzene is added. However, we cannot make a definite conclusion about whether any real increase in the depolarization ratio occurs as benzene is added, since the value of ρ for chlorine in carbon tetrachloride could not be determined accurately. In order to give some indication as to what the value of ρ for chlorine in carbon tetrachloride might be, we listed the gas phase value in Table VI.

Absolute Raman Intensity of Chlorine in Carbon Tetrachloride

It is possible to obtain the absolute Raman intensity and hence the values of the average polarizability derivative α' and of the anisotropic polarizability derivative γ' from the measured relative Raman intensity. This had been demonstrated first by Bernstein and Allen (62) and confirmed later by Long, Gravenor and Milner (63). In order to calculate α' and γ' we have to know both P_ν^s (which will be defined in the following) and the depolarization ratio ρ_ν of the band at ν. Bernstein and Allen (61) showed that a standard intensity P_ν^s (for a Raman band at ν) of a compound could be defined by comparing

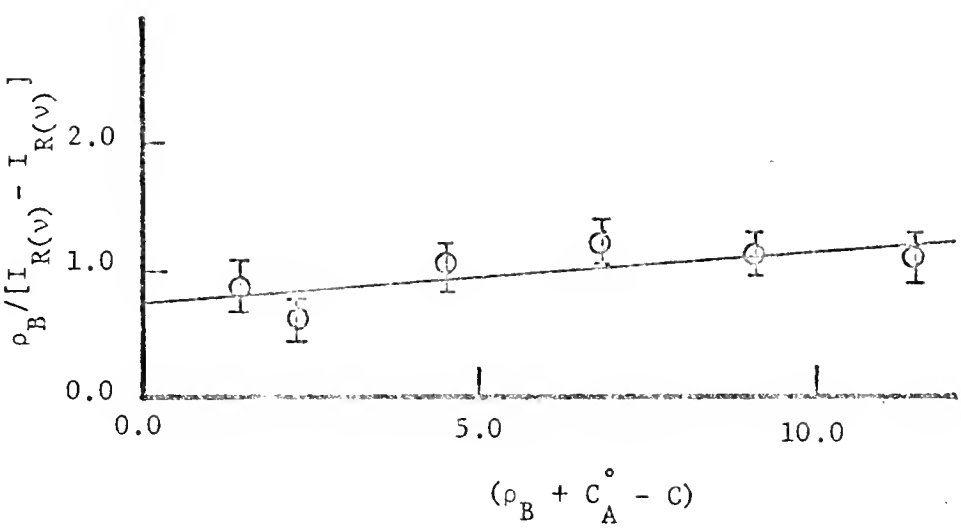

Fig. 16. -- Plot of $\rho_B/[(I_{R(\nu)} - I'_{R(\nu)}]$ vs. $(\rho_B + C^\circ_A - C)$ for Eq. 4-4.

TABLE VI

DEPOLARIZATION RATIO OF
CHLORINE IN DIFFERENT CHLORINE SOLUTIONS

Concentration of Benzene (M)	Depolarization (ρ)[a] of chlorine
11.3	0.27 ± 0.03
5.65	0.25 ± 0.04
0.0[b]	< 0.22[c] ± 0.04
gas phase[d]	0.14

a. ρ = band area of perpendicular component divided by band area of parallel component.

b. In carbon tetrachloride.

c. It was difficult to measure the perpendicular band of chlorine in this solvent with certainty, so the upper limit is listed (see text).

d. See Ref. 63, 64, 65 and others.

this band with the measured intensity of the 459 cm^{-1} band of carbon tetrachloride in the pure liquid:

$$P_\nu^s = [45\alpha'^2 + 7\gamma'^2]_\nu^{compound} / [45\alpha'^2 + 7\gamma'^2]_{459}^{CCl_4} \quad . \qquad (4\text{-}5)$$

By taking arbitrarily the value of $[45\alpha'^2 + 7\gamma'^2]_{459}^{CCl_4}$ to be 1, P_ν^s of the $\nu = 366$ cm^{-1} chloroform band was estimated to be 0.28 by Long Gravenor and Milner (63). From our measurement, we obtained the relative molar intensity of chlorine in carbon tetrachloride with respect to the 366 cm^{-1} band of 1.25 M chloroform to be $I_R = 2.75 \pm 0.26$ (as given in Table V. Analytically, this means that

$$[45\alpha'^2 + 7\gamma'^2]_{543}^{Cl_2} / [45\alpha'^2 + 7\gamma'^2]_{366}^{CHCl_3} =$$

$$(2.75 \pm 0.26) \times 1.25 = 3.46 \pm 0.30 \quad . \qquad (4\text{-}6)$$

From the value of P_{366}^s for chloroform (63) and the results in Eq. 4-6, we then obtained the standard Raman intensity of the Cl-Cl stretching vibration at 543 cm^{-1} to be:

$$P_{543}^s = [45\alpha'^2 + 7\gamma'^2]_{543}^{Cl_2} / [45\alpha'^2 + 7\gamma'^2]_{459}^{CCl_4} = 0.969 \pm 0.084. \qquad (4\text{-}7)$$

Often in the literature, γ'^2 of the 459 cm^{-1} band of carbon tetrachloride has been assumed to be zero [for example, Long, Gravenor and Milner (63)] defined P_ν^s explicitly with the assumption that $(\gamma')^2$ is 0 for this band. We verified the reasonableness of this assumption by calculating $(\gamma')^2$ from Bernstein's value 0.015 for ρ, finding that $7\gamma'^2$ contributed only 2% to the total intensity of this particular band. Therefore, we can assume in practice that:

$$[45\alpha'^2 + 7\gamma'^2]^{CCl_4}_{459} \simeq [45\alpha'^2]^{CCl_4}_{459} \quad . \tag{4-8}$$

The value of $[45\alpha'^2]^{CCl_4}_{459}$ had been measured in liquid CCl_4 and found (64) to be $(33.71 \pm 9.63) \times 10^{-8}$ cm^4/g. From this value and Eq. 4-7 we obtain

$$[45\alpha'^2 + 7\gamma'^2]^{Cl_2}_{543} = (32.3 \pm 10.0) \times 10^{-8} \text{ cm}^4/\text{g} \quad . \tag{4-9}$$

(Here the major uncertainty is in the value for the absolute intensity of the CCl_4 band.)

As has been mentioned, the depolarization ratio of chlorine in carbon tetrachloride was difficult to determine with our spectrometer. However, the gas phase value ($\rho = 0.14$) (65) for chlorine is most probably the lower limit for the values (see Table VI). Using this value, we then obtained

$$\rho = 3\gamma'^2/(45\alpha'^2 + 4\gamma'^2) = 0.14 \quad . \tag{4-10}$$

Solving Eqs. 4-9 and 4-10, we find that the absolute intensity of chlorine is given by

$$\alpha'^2 = (0.512 \pm 0.159) \times 10^{-8} \text{ cm}^4/\text{g} = [(\partial\alpha/\partial\xi_1)_0]^2 \tag{4-11a}$$

$$\gamma'^2 = (1.32 \pm 0.41) \times 10^{-8} \text{ cm}^4/\text{g} = [(\partial\gamma/\partial\xi_1)_0]^2 \quad . \tag{4-11b}$$

We may convert from unit of cm^4/g to cm^4, by multiplying α'^2 and γ'^2 each by the reduced mass of chlorine (29.426×10^{-24} g). When this was done, we found

$$\alpha'^2 = (0.15 \pm 0.047) \times 10^{-30} \text{ cm}^4 = [(\partial\alpha/\partial r_1)_0]^2 \tag{4-12a}$$

$$\gamma'^2 = (0.39 \pm 0.12) \times 10^{-30} \text{ cm}^4 = [(\partial\gamma/\partial r_1)_0]^2 \tag{4-12b}$$

or

$$\alpha' = (3.9 \pm 0.6) \times 10^{-16} \text{ cm}^2 \qquad (4\text{-}13a)$$

$$\gamma' = (6.2 \pm 0.9) \times 10^{-16} \text{ cm}^2 \quad . \qquad (4\text{-}13b)$$

However, the depolarization ratio of chlorine in benzene was measured to be 0.27 (see Table VI) which may be an upper limit for ρ for chlorine in carbon tetrachloride. With this value we found

$$\alpha' = (3.3 \pm 0.46) \times 10^{-16} \text{ cm}^2 \qquad (4\text{-}14a)$$

$$\gamma' = (8.2 \pm 1.2) \times 10^{-16} \text{ cm}^2 \quad . \qquad (4\text{-}14b)$$

We believe that the depolarization ratio of chlorine in carbon tetrachloride may be much closer to the value found for the gas phase than it is to the value obtained in benzene solution, since carbon tetrachloride is expected to be a relatively inert solvent. Therefore the values of α' and γ' for chlorine in carbon tetrachloride given by Eqs. 4-13a and 4-13b are expected to be more reliable, although the range of possible values for these parameters allowed by the uncertainties in ρ (compare Eq. 4-13 to Eq. 4-14) is not very large.

CHAPTER V

INFRARED SPECTROSCOPIC STUDIES OF CHLORINE IN BENZENE SOLUTIONS

Experimental Procedure

The concentrations of chlorine solutions required for infrared studies (0.3 M to 0.9 M) were higher than those for ultraviolet and Raman studies. At these concentrations, we found that the photochemical reaction occurs very easily. When we exposed the solution of chlorine in benzene to fluorescent light, and determined the infrared spectrum as a function of the time after it was prepared, an increase in the concentration of photochemical product was observed as illustrated in Fig. 17. Since it was impossible to prepare the solution and to fill the sample cell in complete darkness, there was no way to prevent the photochemical reaction from occurring. At last we tried adding oxygen gas to the solution to act as a radical quencher (56). As a result, the photochemical reaction was inhibited considerably, if not completely. A small amount of iodine in addition to oxygen was reported to be even more effective in quenching the radicals (56). Since iodine itself forms a stronger complex with benzene than does the chlorine, we did not try to use iodine as radical quencher in our studies for fear of further complicating the system.

The infrared spectrometer we used was a Perkin-Elmer Model 621. In order to minimize the change in chlorine concentration during the

Fig. 17. -- Infrared spectra of chlorine (about 0.6 M) in benzene solutions as a function of the exposure to fluorescent lights.

A baseline: benzene vs. benzene (pathlength, 1 mm)

B freshly prepared chlorine solution

C chlorine solution exposed to fluorescent lights for one hour

D chlorine solution exposed to fluorescent lights for two hours

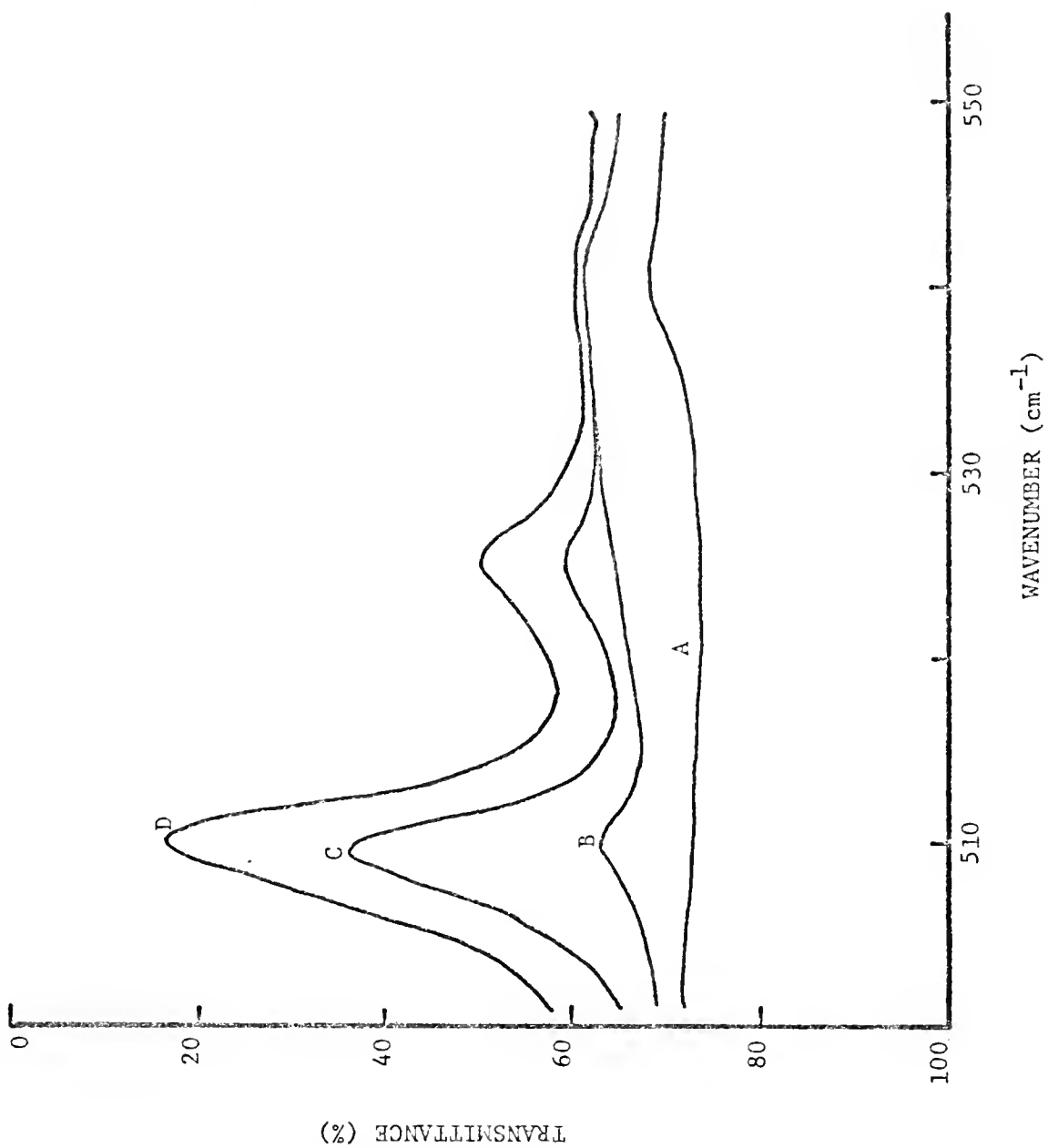
TRANSMITTANCE (%)
0
20
40
60
80
100
510
530
550
WAVENUMBER (cm^{-1})
A
B
C
D

course of recording the spectrum and the growth of the photochemical product sufficient to distort the absorption band from the Cl-Cl stretching vibration, we chose to sacrifice the signal-to-noise ratio (S/N), reducing it to around 125, with a spectral resolution of about 2 cm^{-1}. The total scan time for each measurement from 650 cm^{-1} to 350 cm^{-1} was about 15 to 20 minutes.

Before the preparation of the chlorine solution, we warmed up the spectrometer and covered the sample compartment with a black polyethylene sheet. The baseline was recorded beforehand to give the apparent transmittance of solvent vs. solvent in the matched cells described earlier in Chap. II. At this point, we prepared the chlorine solution, withdrew a 5 ml portion for determination of the chlorine concentration, and immediately filled the liquid cell with the chlorine solution using a micropipette (5 3/4 inches long, P5205-1 Scientific Products, Evanston, Illinois). The sample cell was carried to the spectrometer in a box covered with a black polyethylene sheet. All lights in the room were turned off (note the sample preparation room was separated from the laboratory containing the spectrometer), since the light emitted from the infrared glower source was sufficient to permit the alignment of the cells in the sample compartment. A special holder was made to fit the sample compartment so that we could reproducibly align the sample each time with little light. After the spectrum of the chlorine solution was taken, the sample cell was placed in the box mentioned before, and connected to the vacuum line in order to pump out the chlorine. The chlorine solution always filled the cell up to the top of the glass tubing, so that the pumping process did not reduce the liquid level below the upper edge of the light path. It usually took

about half an hour to eliminate the chlorine gas from the solution. The baseline spectrum of clear solution vs. solvent was then recorded. The baseline always changed a little from that recorded at the beginning but not enough to affect the total band area of the chlorine absorption by as much as 2%. Most importantly, if enough of the photochemical product was present in the original chlorine solution, we could detect it by its infrared absorption spectrum in the second clear solution after the chlorine was removed. If that product was detected, then we would have to repeat the measurement. Occasionally, instead of pumping out the chlorine gas in the sample cell, we withdrew a 1 ml portion of the chlorine solution and determined the concentration of chlorine by titration to find out how much had been lost by both the photochemical reaction and the escape of chlorine gas from the cell.

We had actually tried three liquid cells with different pathlengths. The 1 mm liquid cell was made specially of tantalum metal in our machine shop. Its construction was not much different from an ordinary standard round liquid cell with Teflon spacer (Barnes cell # 0004-035) such as that used to take the spectrum shown in Fig. 17. Since the intensity of the chlorine absorption (spectrum B in Fig. 17) with this 1 mm pathlength cell was so small, it was difficult to observe especially the very weak absorption by chlorine in benzene solutions diluted very much with carbon tetrachloride. Furthermore, it was difficult to distinguish between the baseline shift due to the photochemical reaction and the absorption by the chlorine. The 6 mm pathlength liquid cell described in Chap. II also had been used to measure the absorption by chlorine, but the benzene absorption in this long path cell was so high in this region, and the actual signal-to-

noise ratio was so low, that we could not measure a reliable chlorine absorption band with this 6 mm cell. Hence, the 3 mm pathlength liquid cell (also described in Chap. II) was the most suitable for this kind of measurement. The pathlength (3 mm) was obtained by measuring the thickness of the Teflon spacer with a micrometer. Since the absorption by carbon tetrachloride was less than that by benzene in the infrared region near the chlorine absorption band, we were able to measure the absorption by chlorine dissolved in carbon tetrachloride in the 6 mm pathlength liquid cell by making a special effort (more discussion will be given later in this chapter).

The spectrum of 0.33 M chlorine in benzene in the 3 mm cell is shown in Fig. 18 (recorded vs. pure benzene in the reference beam in a matched cell), where it is compared with the spectrum of benzene in that same cell, recorded with air in the reference beam, and with a baseline of benzene vs. benzene. Benzene absorbs almost totally above 575 cm^{-1} and below 410 cm^{-1}, so that we lost all the spectral information for the chlorine-benzene solution outside the region from 410 to 575 cm^{-1}. However, within that spectral region, we were able to work at quite a good signal-to-noise ratio (a ratio of 125), and so we could obtain a reliable spectrum. (The spectra were recorded in the transmittance mode rather than in the absorbance mode because operation of our Perkin-Elmer 621 in the absorbance mode was not reliable at the time of the experiment.)

Spectra of chlorine solutions in benzene diluted by carbon tetrachloride are shown in Figs. 18-21. As benzene was gradually diluted by the addition of carbon tetrachloride, less solvent absorption was found above 575 cm^{-1}, so that more spectral information was

Fig. 18. -- Infrared spectra of 0.33 M chlorine in benzene. The pathlength of the cells for all studies is 3 mm.

A spectrum of benzene vs. air

B spectrum of chlorine (0.33 M) in benzene vs. benzene in a matched cell

C baseline of pure-liquid benzene in matched cells

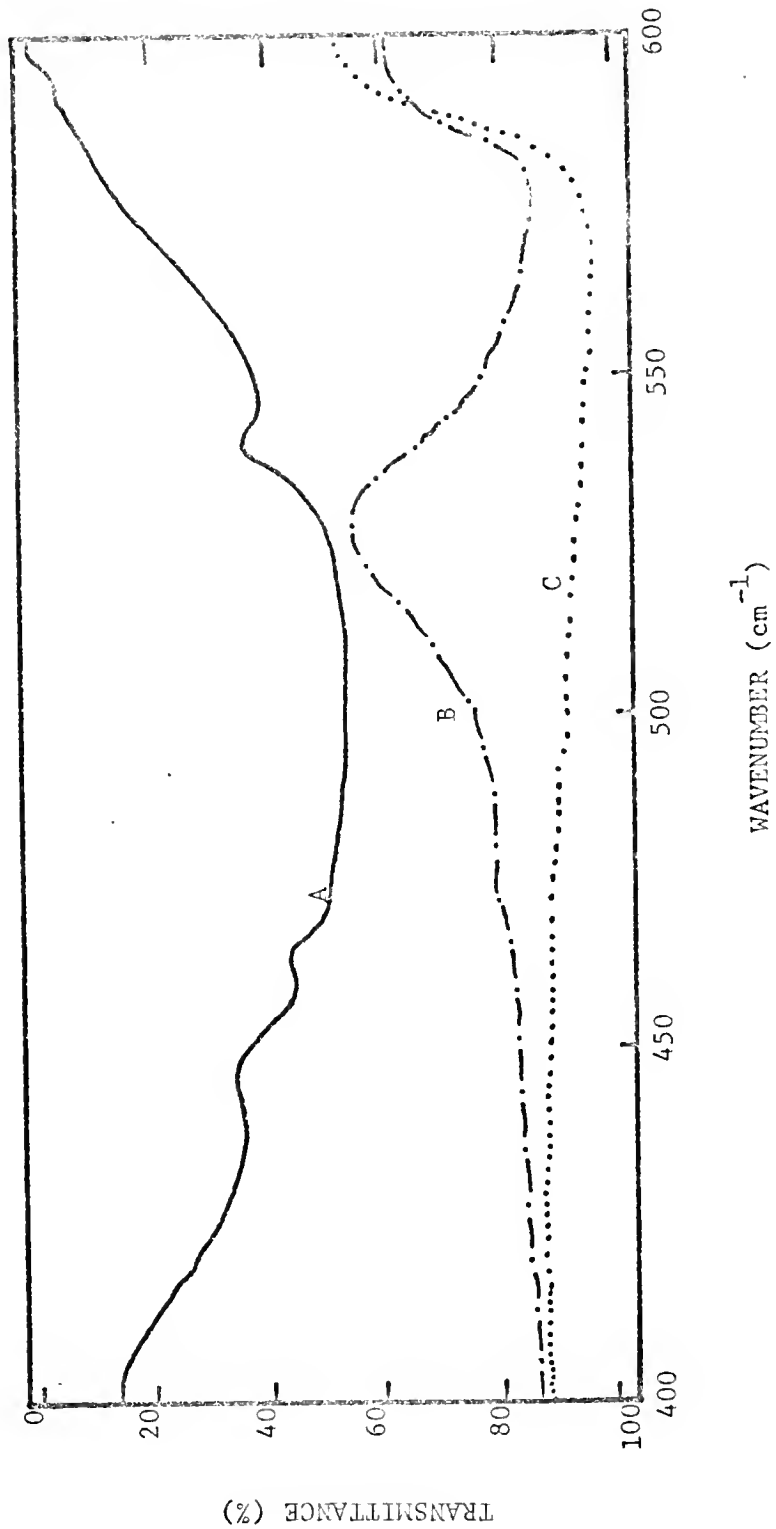
TRANSMITTANCE (%)
0
20
40
60
80
100
400
450
500
550
600
WAVENUMBER (cm^{-1})
A
B
C

Fig. 19. -- Infrared spectrum of chlorine in 60% (v/v) benzene and 40% (v/v) carbon tetrachloride. The pathlength is 3 mm for all spectra.

A spectrum of the solvent vs. air

B spectrum of 0.445 M chlorine vs. solvent

C baseline of solvent vs. solvent

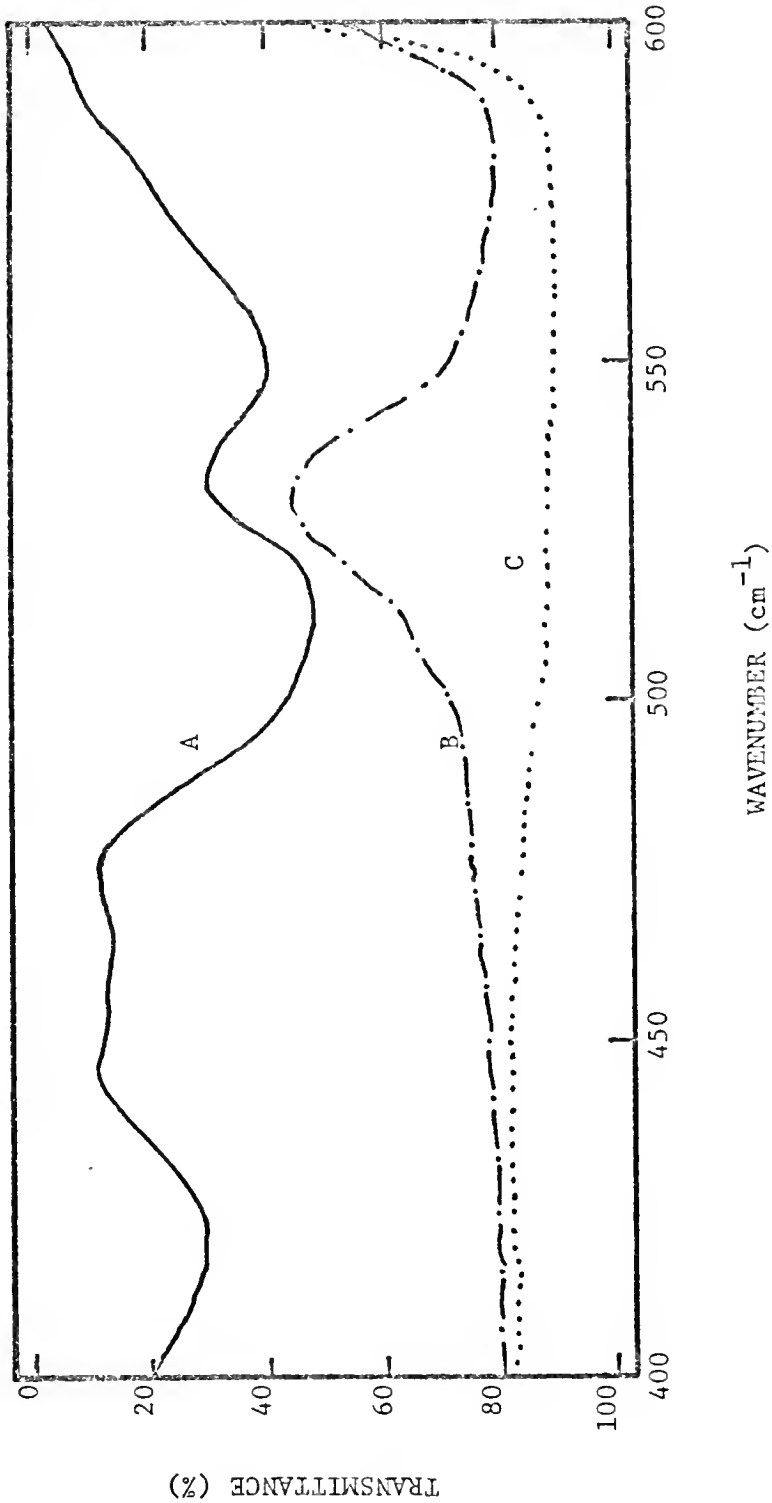
TRANSMITTANCE (%)
0
20
40
60
80
100
400
450
500
550
600
WAVENUMBER (cm⁻¹)
A
B
C

Fig. 20. -- Infrared spectrum of chlorine solution in 20% (v/v) benzene and 80% (v/v) carbon tetrachloride. Pathlength is 3 mm. (Note scale change from Fig. 18-19)

A spectrum of solvent vs. air

B spectrum of 0.99 M chlorine solution vs. solvent

C spectrum of 0.296 M chlorine solution vs. solvent

D baseline of solvent vs. solvent

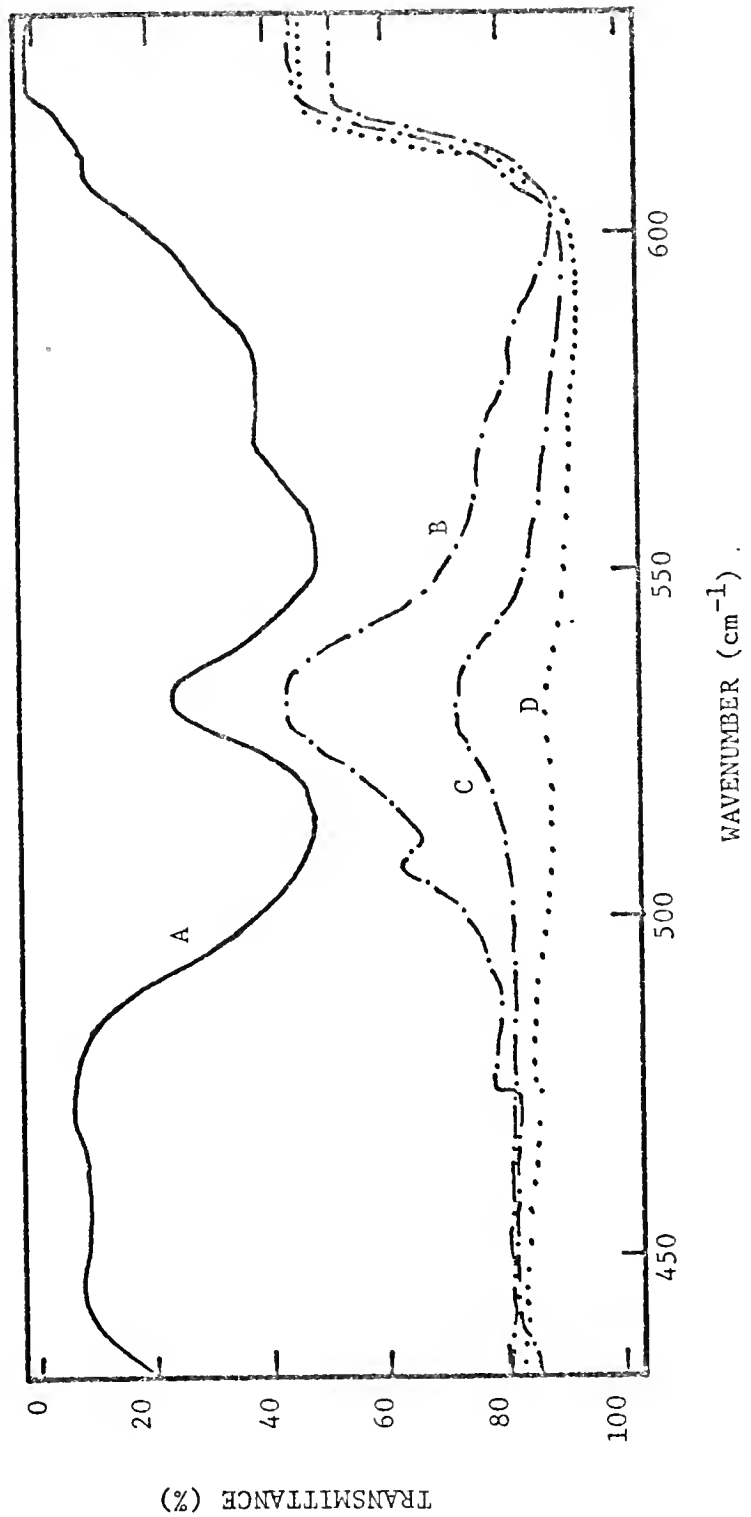
TRANSMITTANCE (%)
0
20
40
60
80
100
450
500
550
600
WAVENUMBER (cm^{-1})
A
B
C
D

Fig. 21. -- Spectrum of chlorine in carbon tetrachloride. Pathlength is 3 mm for all spectra.

A spectrum of carbon tetrachloride vs. air

B spectrum of 0.33 M chlorine in carbon tetrachloride vs. carbon tetrachloride

C baseline of carbon tetrachloride vs. carbon tetrachloride

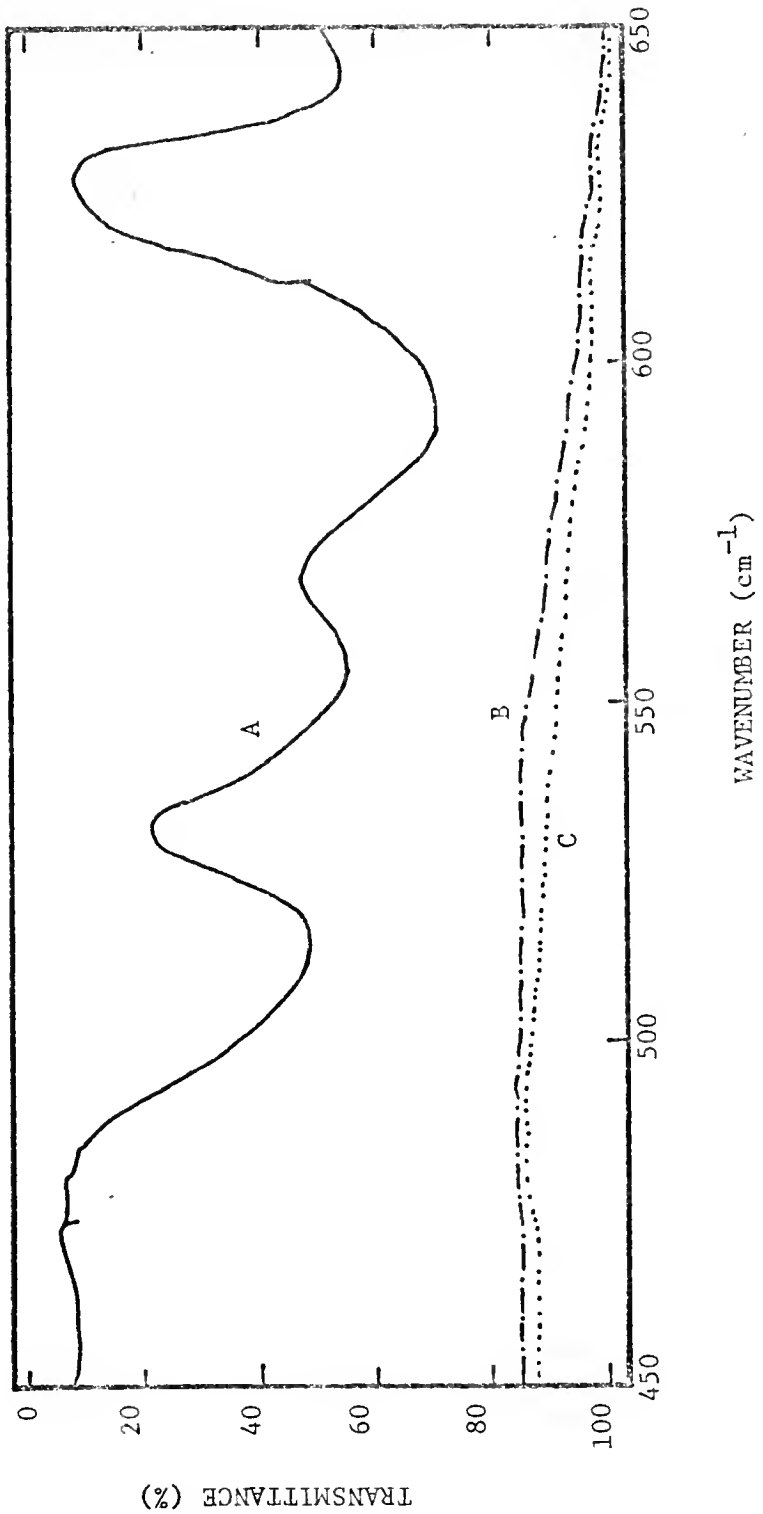
TRANSMITTANCE (%)
0
20
40
60
80
100
450
500
550
600
650
WAVENUMBER (cm^{-1})
A
B
C

unveiled concerning the high frequency wing of the chlorine absorption band. However, the strong absorption by carbon tetrachloride in the 3 mm cell below 500 cm^{-1} made it difficult to observe the low frequency wing of the chlorine absorption band. This situation is illustrated in Fig. 20 and Fig. 21. The weak absorption band near 510 cm^{-1} in Fig. 20B was due to the hexachlorocyclohexane.

One of the most exciting things in this work was the observance of the infrared absorption band of chlorine in carbon tetrachloride shown in Fig. 21. To the author's knowledge, this was the first time that the infrared absorption by chlorine has been observed for a chlorine solution in a solvent whose molecules have tetrahedral symmetry. This spectrum is quite different from that of chlorine in benzene (Fig. 18) or those of chlorine in different benzene-carbon tetrachloride mixtures (Figs. 19-20). It is very broad and weak. If one did not use a long pathlength liquid cell, this broad and weak absorption could easily be confused with some baseline shift of unknown origin. To make clear that the absorption in Fig. 21B is due to chlorine in carbon tetrachloride, we measured this absorption band at several different concentrations of chlorine, as shown in Fig. 22. The dependence of the absorption on the concentration of chlorine was clearly demonstrated. To be more convincing, the spectrum of 0.33 M chlorine in carbon tetrachloride was measured with the longer pathlength (6 mm) cell. The spectrum obtained is shown in Fig. 23 where the absorption is seen to be twice as large (within experimental error) as that shown for the same solution in Fig. 21 in a 3 mm cell.

Fig. 22. -- Infrared spectra of chlorine in carbon tetrachloride. The pathlength is 3 mm for all measurements. Compare these spectra also with Fig. 21 and Fig. 23.

A spectrum of carbon tetrachloride vs. air

B spectrum of 1.2 M chlorine in carbon tetrachloride vs. carbon tetrachloride

C spectrum of 0.66 M chlorine in carbon tetrachloride vs. carbon tetrachloride

D baseline of carbon tetrachloride vs. carbon tetrachloride

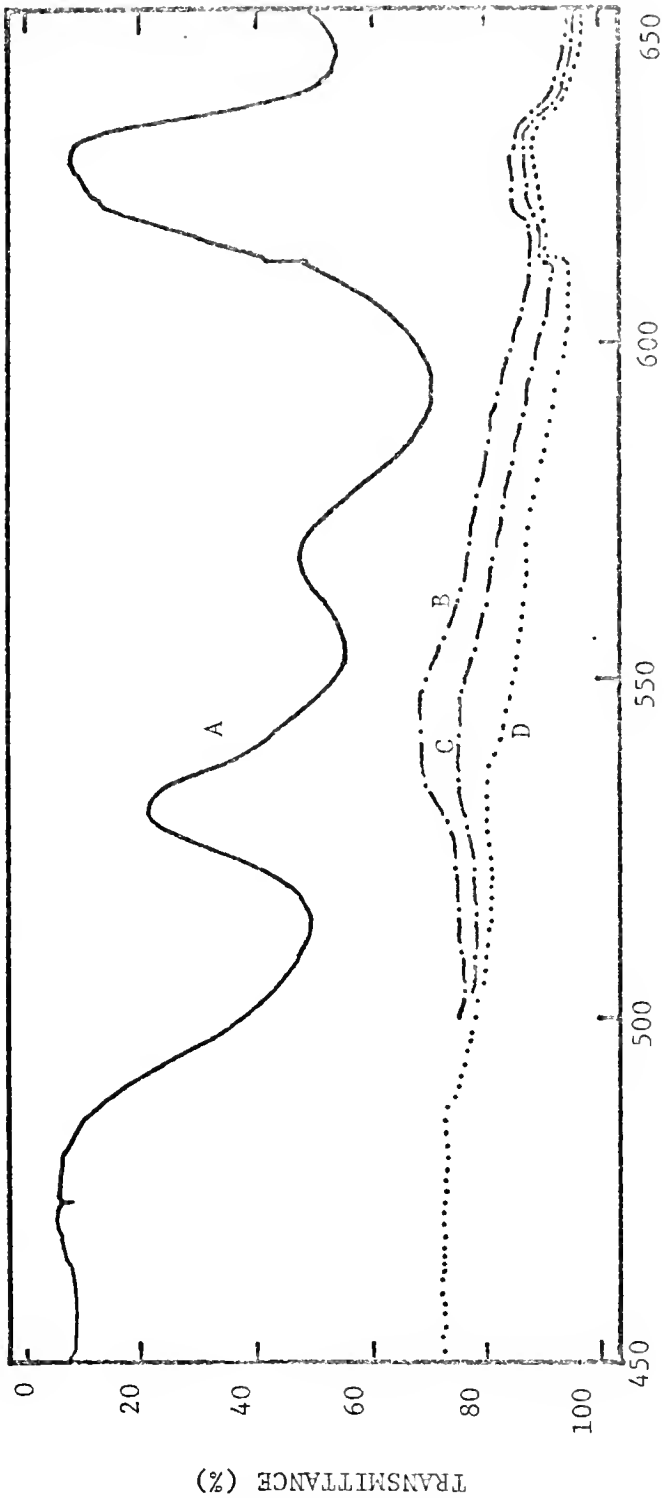
TRANSMITTANCE (%)
0
20
40
60
80
100
450
500
550
600
650
WAVENUMBER (cm⁻¹)
A
B
C
D

Fig. 23. -- Infrared spectrum of chlorine in carbon tetrachloride solution with 6 mm pathlength liquid cell.

A spectrum of carbon tetrachloride vs. air

B spectrum of chlorine (0.31 M) vs. carbon tetrachloride

C baseline of carbon tetrachloride vs. carbon tetrachloride

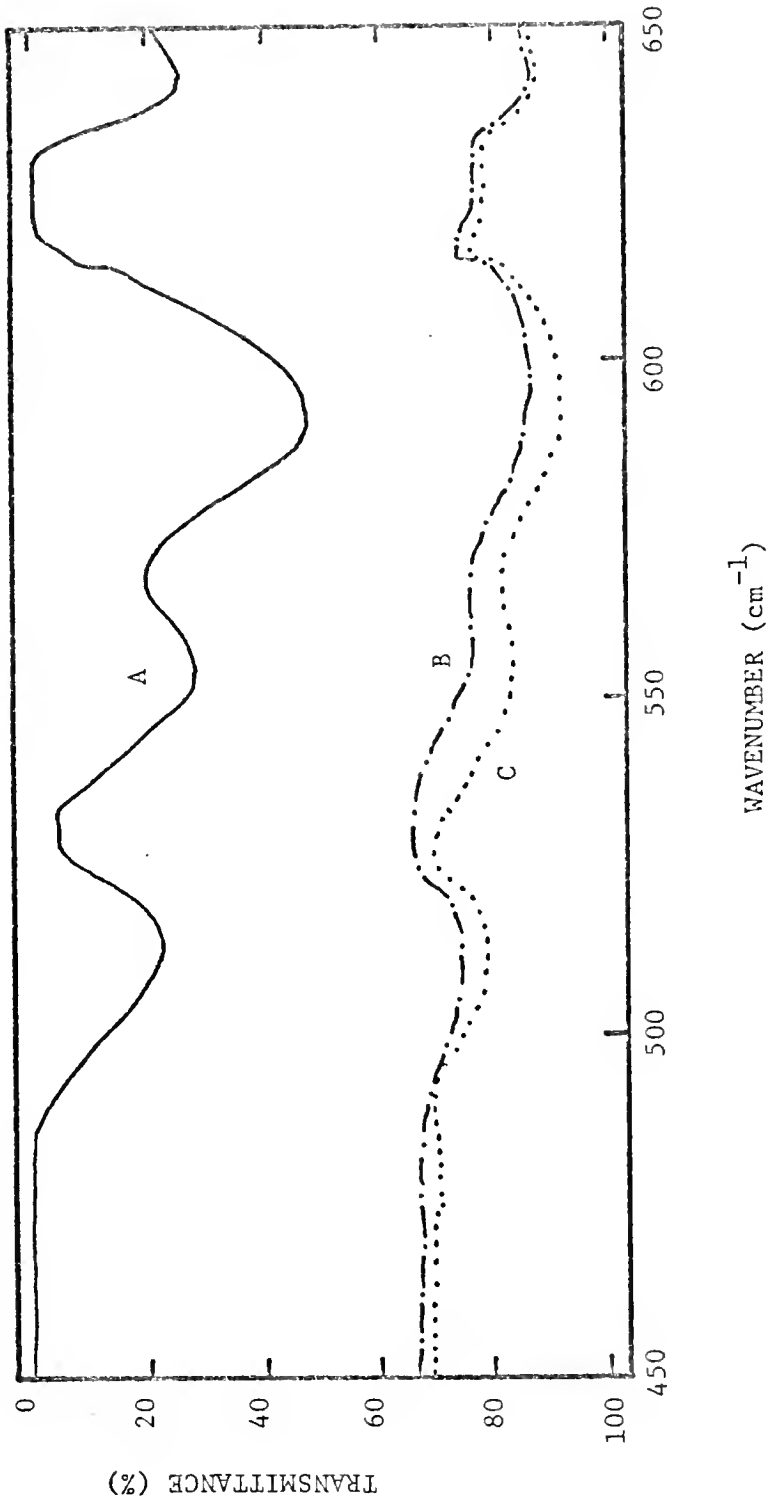
A
B
C
0
20
40
60
80
100
450
500
550
600
650
TRANSMITTANCE (%)
WAVENUMBER (cm^{-1})

Analysis of the Experimental Results

The absorption band of the chlorine solutions recorded on the transmittance scale was converted to a plot of absorbance vs. wavenumber in a point-by-point replot by calculating the natural logarithm of the ratio of the transmittance of the chlorine to that of the baseline. Tha absorbance of chlorine in each solution was calculated at 0.5 M chlorine by assuming the absorbance obeyed Beer's law semi-quantitatively. The interval between any two points was 2 cm^{-1}; the total spectral range was about 200 cm^{-1}. The spectra of chlorine in different benzene solutions were then replotted as absorbance vs. wavenumber by Calcomp Plotter. All these were done in one computer program with only one set of initial input data: the readings of the transmittance of the chlorine solution and of the baseline. Some of the replotted spectra are shown in Fig. 24. It can be seen in Fig. 24 that none of the spectra were complete because the solvent absorption damaged the determination of the spectral information in the wings of the chlorine absorption band.

The incompleteness of the chlorine absorption band made it difficult to measure directly the absorption intensity of the chlorine in different benzene-carbon tetrachloride mixtures by measuring the band area. To solve this problem, we tried to fit different known theoretical curves to the measured absorption band contour. The first and most successful theoretical curve we tried to fit was a Lorentzian function, since most infrared absorption bands can be fit quite well by that function (66-70). The Lorentzian function is

$$L(\tilde{\nu}) = a/[(\tilde{\nu} - b)^2 + c^2] \quad . \qquad (5\text{-}1)$$

Fig. 24. -- Replotted infrared spectra of chlorine in benzene solutions; the concentration of chlorine in each solution is 0.5 M and the pathlength is 3 mm.

---- This line indicates the wavenumber reading of 530 cm^{-1} in order to observe the frequency shift easily.

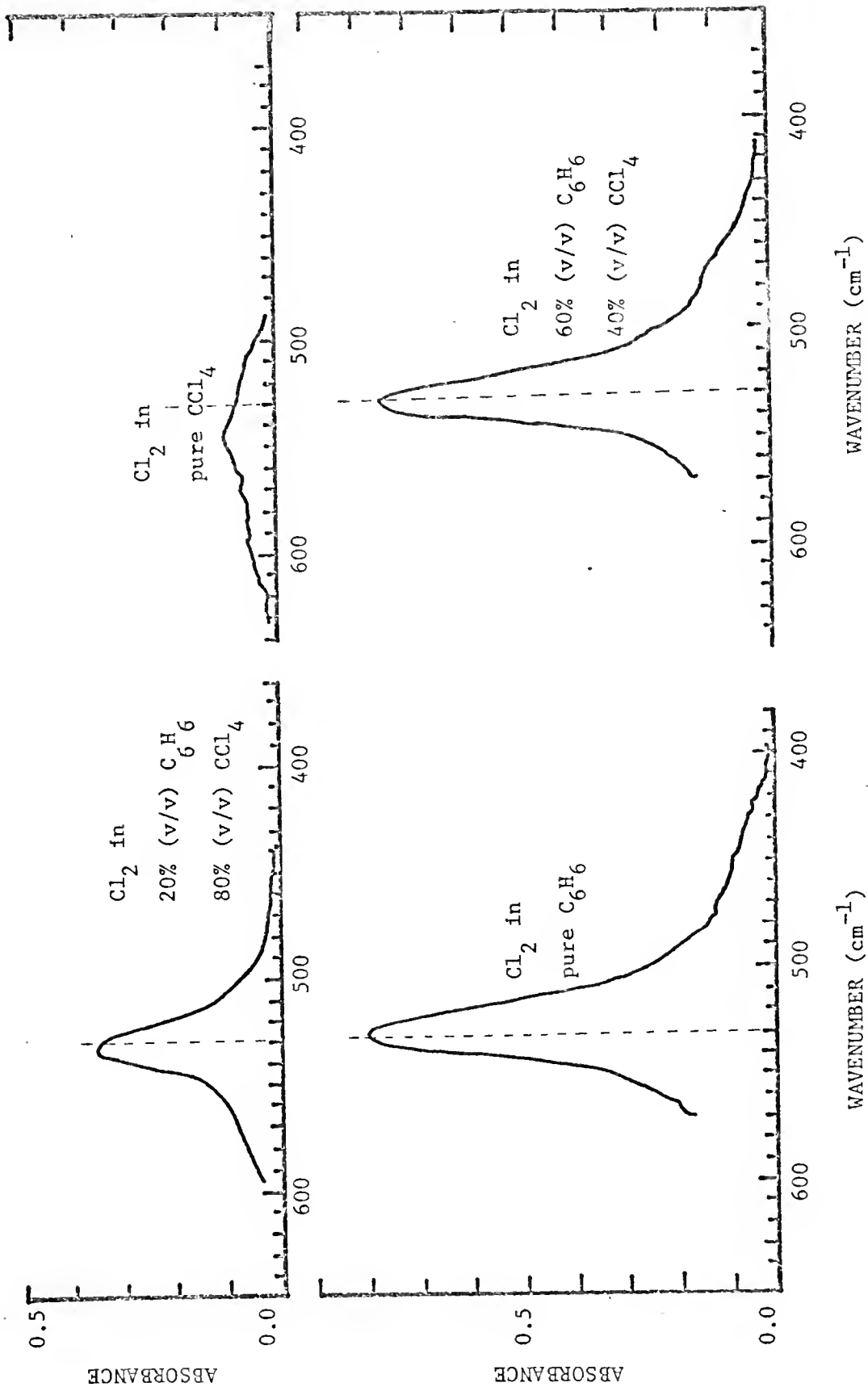
Cl_2 in
pure CCl_4
Cl_2 in
60% (v/v) C_6H_6
40% (v/v) CCl_4
Cl_2 in
20% (v/v) C_6H_6
80% (v/v) CCl_4
Cl_2 in
pure C_6H_6
ABSORBANCE
0.0
0.5
400
500
600
WAVENUMBER (cm^{-1})

Here, a, b, and c are constants related to the infrared absorption band by the following relationships (69):

$$a = S\ \Delta\nu_{1/2}/2\pi \quad , \tag{5-2}$$

$$b = \tilde{\nu}_0 \quad , \tag{5-3}$$

and

$$c = (1/2)(\Delta\tilde{\nu}_{1/2}) \quad . \tag{5-4}$$

Here S is the total integrated intensity of the absorption band, $\Delta\tilde{\nu}_{1/2}$ is the true half-band width and $\tilde{\nu}_0$ is the wavenumber of the absorption maximum. The nonlinear least-squares curve fit of Eq. 5-1 to the observed spectrum was carried out with Quantum Chemistry Exchange Program No. 60 (71) at the Computing Center of the University of Florida. We tried with at least five different sets of initial parameters (a, b and c) for each curve fitting program. We selected the set (a, b and c) generated by the program which gave the best fit. In most of the cases, almost all of the initial parameters gave the same final results. Some of the results of the Lorentzian curve fitting are shown in Figs. 25-27. where the ordinate scale is linearly proportional to the absorbance. We obtained the recalculated absorbances (A_{cc}) in each of Figures 25-27 by the equation

$$A_{cc} = 5.3\ A_{co}/(A_{co})_{max} \quad . \tag{5-5}$$

Here A_{cc} is the recalculated absorbance at wavenumber $\tilde{\nu}$, A_{co} is the observed absorbance at wavenumber $\tilde{\nu}$, $(A_{co})_{max}$ is the maximum observed absorbance of chlorine in each chlorine solution. The factor 5.3 is a scaling factor for the plot to utilize the full scale. The reason

Fig. 25. -- Lorentzian curve (F) fitted to the observed absorption spectrum of chlorine in benzene (I). Curve E is the difference (absolute value) between I and F.

E ...

F ---

I ooo

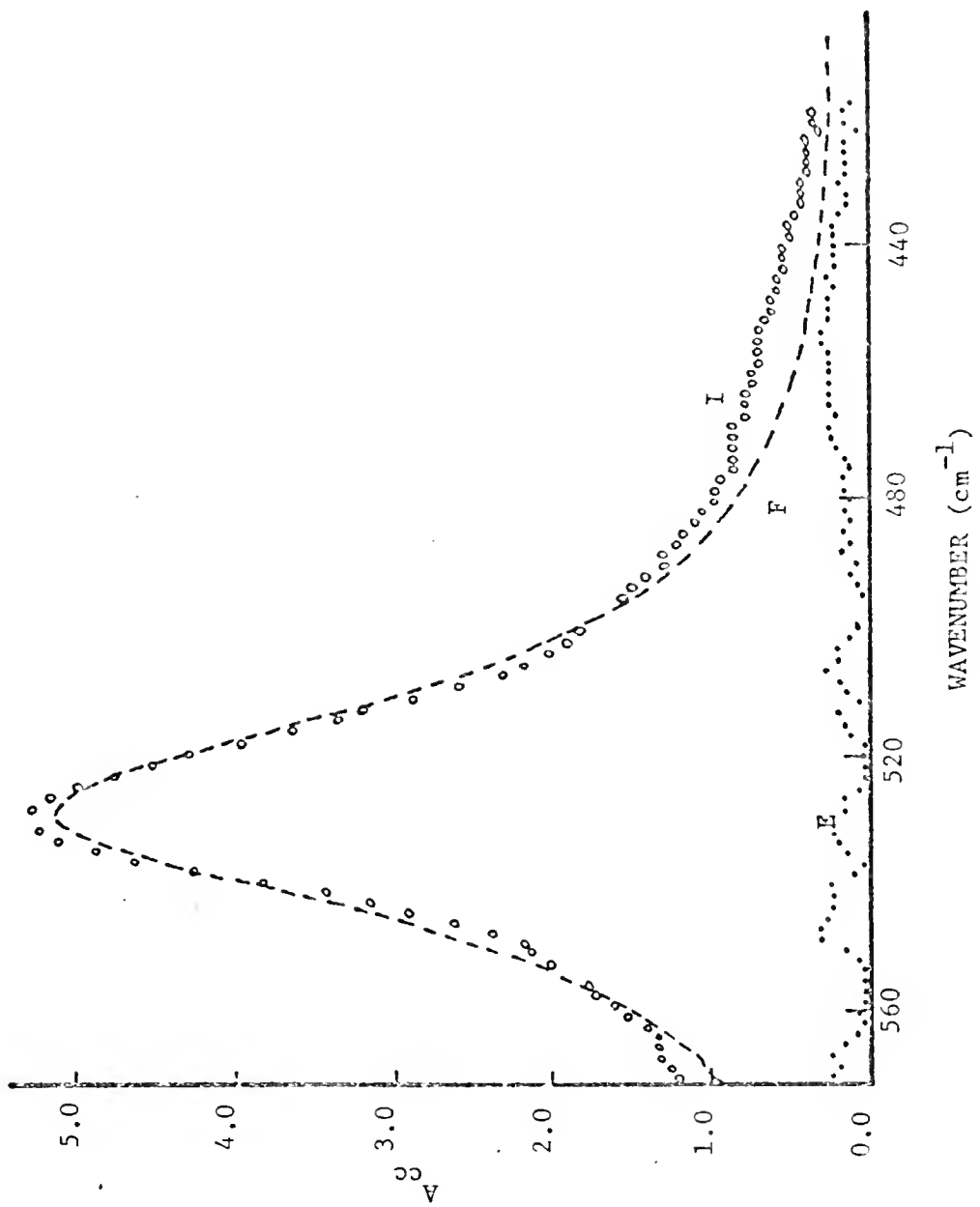
5.0
4.0
3.0
2.0
1.0
0.0
A_{cc}
560
520
480
440
WAVENUMBER (cm^{-1})
I
F
E

Fig. 26. -- Lorentzian curve (F) fitted to the observed absorption band (I) of chlorine in 60% (v/v) benzene and 40% (v/v) carbon tetrachloride. Curve E is the difference (absolute value) between I and F.

E ...

F ---

I °°°

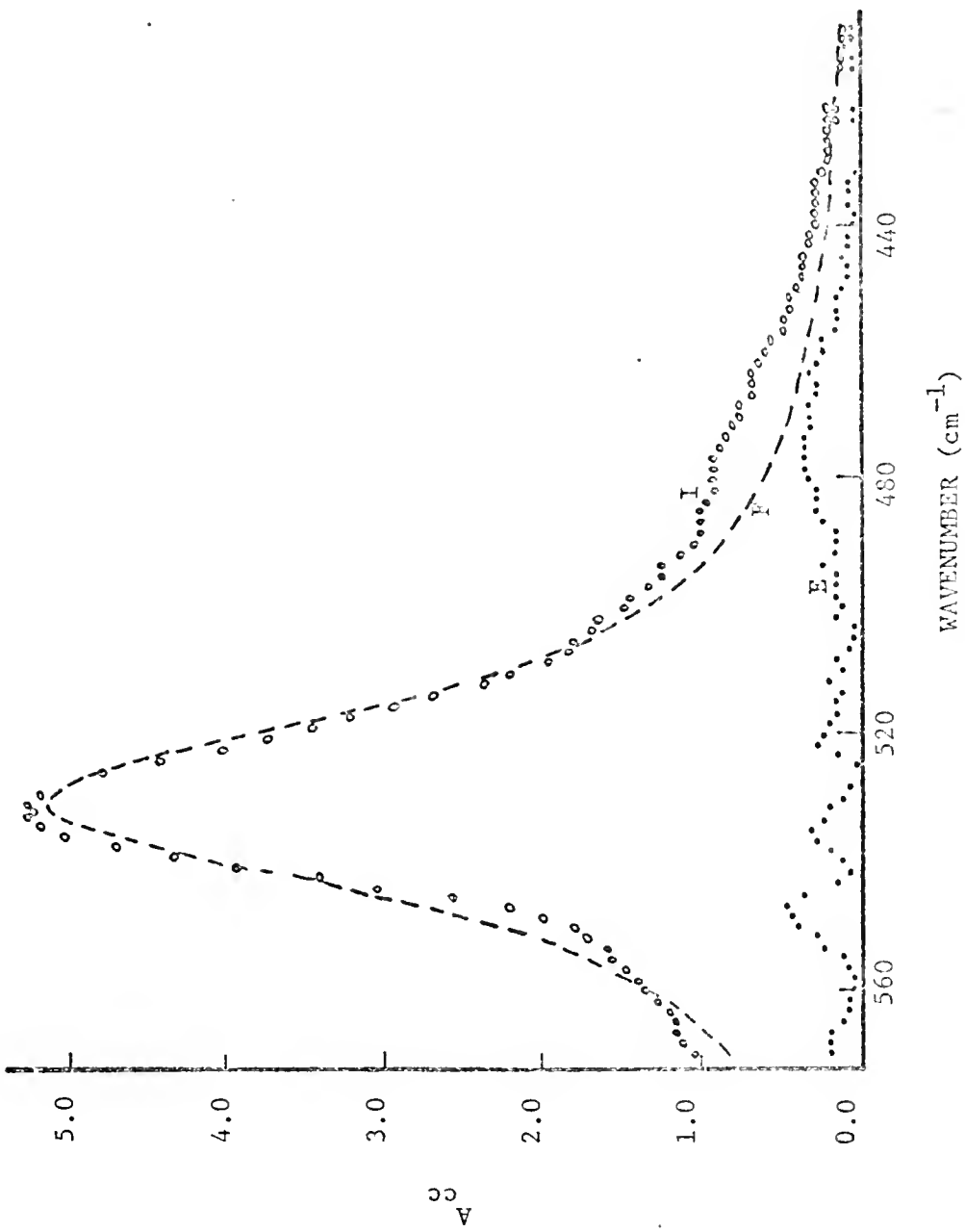
5.0
4.0
3.0
2.0
1.0
0.0
A_{cc}
560
520
480
440
WAVENUMBER (cm^{-1})
I
F
E

Fig. 27. -- Lorentzian curve (F) fitted to the observed absorption band (I) of chlorine in carbon tetrachloride. Curve E is the difference (absolute value) between I and F.

E ...

F ---

I ooo

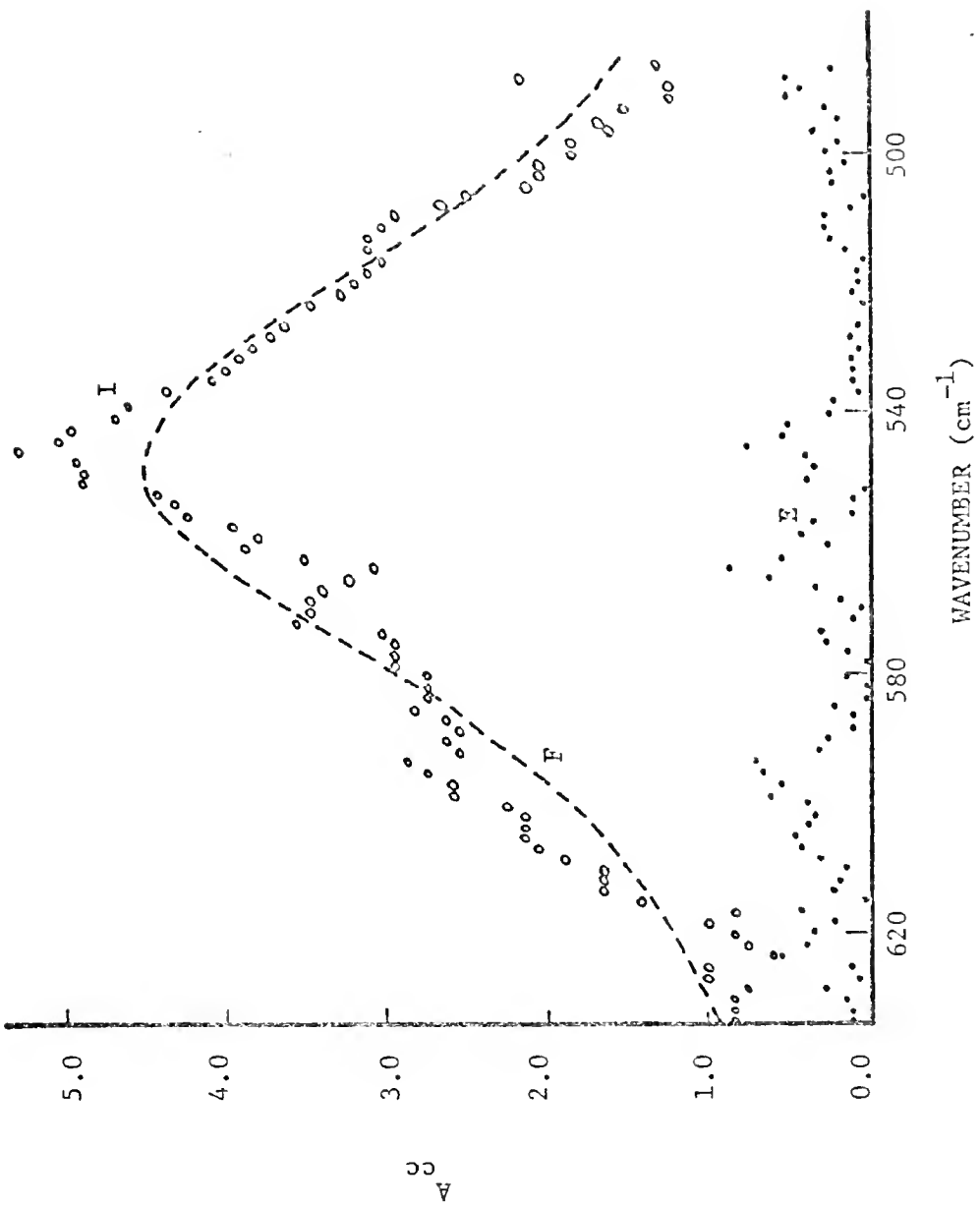
5.0
4.0
3.0
2.0
1.0
0.0
A cc
620
580
540
500
WAVENUMBER (cm^{-1})
I
F
Σ

for scaling was because it was easier then to see how good the curve fitting was. In Fig. 25, the Lorentzian curve fits quite well to the observed spectrum of chlorine in benzene near the maximum absorbance, but the fit in the wings is not so good. Similar results are found for Figs. 26 and 27. As it can be seen from these figures, the band area from the Lorentzian curve is always an underestimate of the true band area except for chlorine in carbon tetrachloride, since the wings of the Lorentzian curve are lower than the observed ones. The underestimate in band area by this method was around 8-10% as estimated from the integrated area of the difference between the calculated Lorentzian curve and the observed spectrum shown as curve E in Figs. 25 and 26.

Since the agreement between the Lorentzian curves and the observed ones is quite good for all the chlorine solutions we measured, we could then estimate the absolute intensities of chlorine in different benzene solutions from the values of the total absorption intensity S from the following equation:

$$A = S/n_{Cl_2}\ell \quad . \tag{5-6}$$

Here A (as defined in Eq. 1-5) is the absolute integrated molar absorption coefficient in cm mmole^{-1} of chlorine, n_{Cl_2} is the total molar concentration of chlorine (n_{Cl_2} = 0.5 M here), ℓ is the path-length of the liquid cell. The absolute integrated intensities of the Cl-Cl stretching vibration for chlorine in benzene solutions are shown in Table VI. The uncertainty in n_{Cl_2} was around $\pm$ 8%, the uncertainty in ℓ was less than $\pm$ 2%, and the uncertainty in S has been discussed earlier; from these, the overall uncertainty for A was estimated to be + 13% or - 8%.

The intensity (A) of the chlorine absorption band increases by a factor of five from the solution in pure carbon tetrachloride to the solution in pure benzene. The enhancement in intensity for the chlorine vibration for solutions in benzene has been interpreted on the basis of two extreme theories -- one is the vibronic coupling effect (26) from the theory of charge-transfer complexes, and the other is the quadrupole-induced dipole effect (30-31) of classical electrostatic interaction theory. We shall discuss the relative contributions of these two possible effects to the enhancement of the intensity of chlorine in benzene after we present our investigation of this electrostatic effect in Chap. VI.

Comparing the frequencies of the maxima of the infrared absorption of chlorine solutions given in Table VII with the maxima of the Raman band shifts reported in Table V (Chap. IV), we see clearly that there is a significant difference in the frequency shift between infrared and Raman spectra of chlorine solutions as the solvent is gradually changed from benzene to carbon tetrachloride. The frequency maximum of the infrared spectrum shifts slightly from 527 cm^{-1} for chlorine in 11.3 M (pure) benzene to 532 cm^{-1} for chlorine in 2.26 M benzene in CCl_4; then suddenly there is a big jump to 545 cm^{-1} for chlorine in pure carbon tetrachloride. On the other hand, the Raman frequency maximum of chlorine apparently shifts smoothly from 530 cm^{-1} in pure benzene to 543 cm^{-1} in pure carbon tetrachloride. These results may indicate that the infrared absorption band of the chlorine solutions in benzene is composed of only one band (from the complexed chlorine) while the Raman band of the chlorine solutions in benzene is a composite of two unresolved bands, one for the complexed chlorine and the other

TABLE VII

INTEGRATED INFRARED MOLAR ABSORPTION COEFFICIENTS (A) AND THE PARAMETERS OF THE LORENTZIAN FUNCTIONS FOR THE Cl-Cl VIBRATION OF CHLORINE IN BENZENE SOLUTIONS

Concentration of Benzene (M)	Integrated Infrared[a] Absorption Intensity of Chlorine (A) (cm/(mmole)	Parameters[b] of the Lorentzian Curve		
		S[c]	$\tilde{\nu}_0(cm^{-1})$[d]	$\Delta\tilde{\nu}_{1/2}(cm^{-1})$[e]
11.3	333.0	49.95	527.1	40.9
9.04	325.6	48.84	528.4	37.1
6.78	274.0	41.10	530.0	35.3
4.52	185.0	27.74	531.0	30.9
2.26	122.0	18.29	532.3	33.2
0.0[f]	78.1	11.72	545.0	87.6

a. The values are believed to be reliable to + 13% or - 8% (see text).
b. All parameters were obtained from curves normalized to 0.5 M (see text).
c. The values (except for chlorine in carbon tetrachloride) are believed to be underestimated by 8-10%.
d. The reliability of the frequency maximum ($\tilde{\nu}_0$) is believed to be $\pm$ 0.5 cm^{-1}.
e. The half-band widths ($\Delta\tilde{\nu}_{1/2}$) are believed to be reliable to $\pm$ 2 cm^{-1}.
f. In carbon tetrachloride.

for free chlorine in CCl_4. This may occur since the infrared spectrum for a free homonuclear diatomic molecule like chlorine is forbidden, but its Raman spectrum is allowed.

The half-band width of the infrared spectrum in benzene is twice as small as that for chlorine in carbon tetrachloride as is shown in column 5 of Table VII. We may estimate the lifetime of the "complex" of chlorine with benzene (or with carbon tetrachloride), based on the Heisenberg uncertainty principle:

$$\Delta E \cdot \Delta t \leq h \quad ,$$

or (5-7)

$$c\Delta\tilde{\nu}_{1/2} \cdot \Delta t \leq 1 \quad .$$

Here h and c are universal constants, $\Delta\tilde{\nu}_{1/2}$ is the true half-band width, ΔE and Δt are uncertainties in energy and time, respectively. We find from our data that the lifetime of the complex of chlorine with benzene may be about 0.83×10^{-12} sec and that of the complex of chlorine with carbon tetrachloride about 0.41×10^{-12} sec. Even though the lifetimes in both cases are in the same order of magnitude (10^{-12}) as was found for the lifetime of the complex of iodine with benzene by Kettle and Price (see Ref. 33 and the footnotes cited), they are clearly different from each other, suggesting a difference in the intermolecular interactions for the two cases. Furthermore, the half-band width of the infrared spectrum of chlorine in benzene is twice that found for the Raman band of chlorine in benzene (see Table V). This may relate to the difference in the time-correlation functions (72) between the infrared absorption band and the Raman band. Since the analysis of these data to obtain the time correlation functions requires

fairly complete measurements over the entire absorption band, we did not attempt the analysis because of the incompleteness of the chlorine spectra in both our Raman and infrared measurements, as described earlier.

In principle, we could also analyze the complex formation of chlorine with benzene from the infrared integrated intensity data, using either the Benesi-Hildebrand method (2) or Scott method (14). In order to use the same method as for the ultraviolet data and the Raman data, we applied the Scott method here. We rewrote Eq. 3-1 for the analysis of the infrared intensity data,

$$\ell\, C_D^\circ\, C_A^\circ / A_c = (1/\varepsilon) C_D^\circ + 1/K\varepsilon \quad . \tag{5-8}$$

Here $A_c/\ell C_A^\circ$ is the absolute integrated infrared intensity of the chlorine in each chlorine solution (based on the total chlorine concentration), ε is the absolute integrated infrared intensity ($\varepsilon = A$) for the completely complexed chlorine. Actually $A_c/\ell C_A^\circ$ is not A of Eq. 5-6. We have to subtract the absorption intensity of "free" chlorine in the presence of carbon tetrachloride. However, it is difficult to make the correction properly because the wings of the absorption of chlorine were not complete (see Figs. 25 and 26).

Therefore, we analyzed the data in two ways, one without any correction and the other with an estimated semi-quantitative correction. In the first case, we assumed that $A_c/\ell C_A^\circ$ is just the value of A from Eq. 5-6, and plotted C_D°/A vs. C_D° as shown in Fig. 28. From the best least-squares fit, we obtained the product of $K\varepsilon$ from the intercept to be 64 ± 8 [liter · cm(mmole)$^{-1}$ mole^{-1})], ε to be $(6.608 \pm 1.2) \times 10^3$ cm(mmole)$^{-1}$ from the slope, and K to be 0.09 ± 0.04 liter

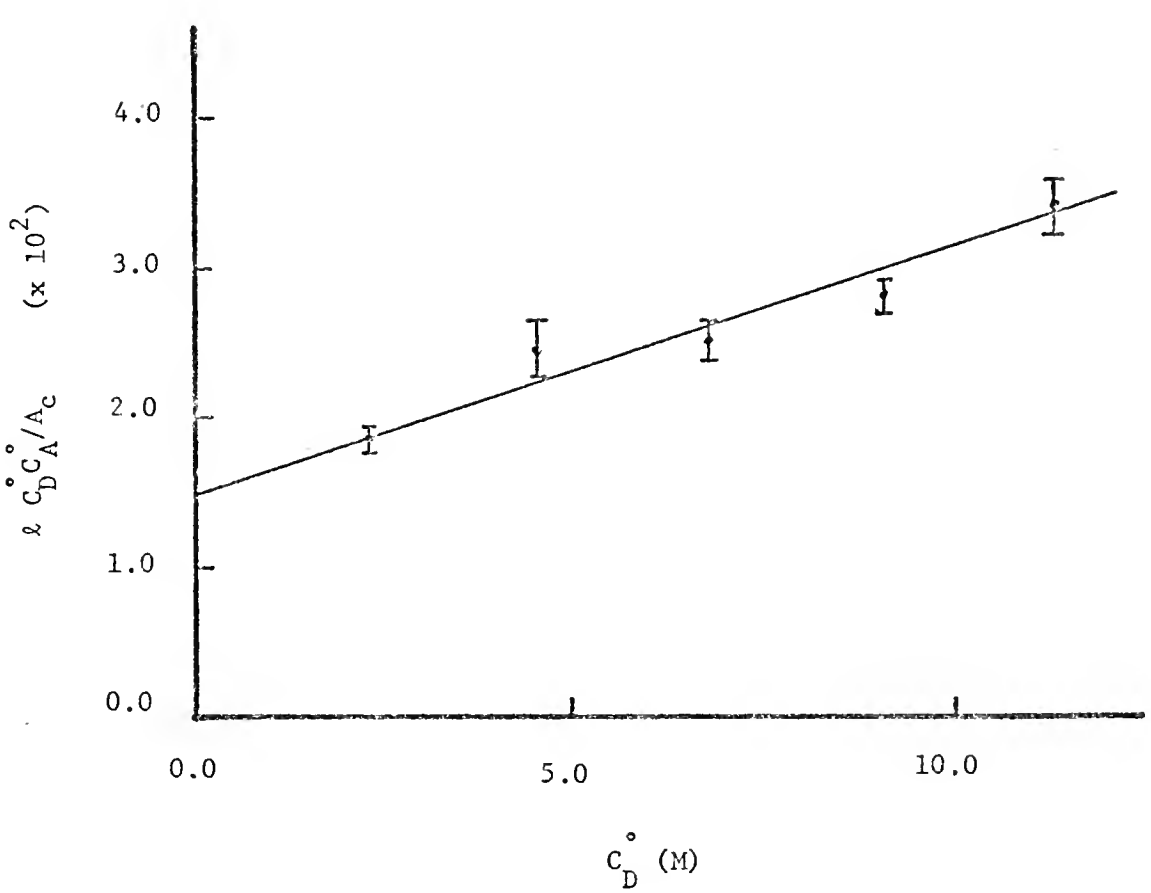

Fig. 28. -- Scott plot of the infrared data for the complex of chlorine with benzene (neglecting the intensity of "free" chlorine in the presence of carbon tetrachloride).

mole^{-1}. Here the uncertainties are the standard deviations. In the second case, we made a trial-and-error estimate of how much absorption intensity for free chlorine in carbon tetrachloride should be subtracted from A in order to obtain an equilibrium constant closer to those we obtained from analysis of the ultraviolet and Raman data and still give a reasonably good linear plot for Eq. 5-8. We found a fairly good linear plot of Eq. 5-8 by subtracting one-half of the absorption intensity for chlorine dissolved in pure carbon tetrachloride from the value of A from Eq. 5-6. Thus we made the correction by:

$$A_c/\ell\, C_A^\circ = A - (1/2)X_{CCl4}\, A^{Cl_2}_{CCl_4} \quad . \qquad (5\text{-}9)$$

Here X_{CCl_4} is the mole fraction of the carbon tetrachloride in benzene-carbon tetrachloride mixture, and $A^{Cl_2}_{CCl_4}$ is the absolute intensity of chlorine in carbon tetrachloride from Table VII. The factor of 2 is not so unreasonable if we consider the amount of our underestimate for the intensity (A) of chlorine in benzene solutions discussed above. After making the correction with Eq. 5-9, we replotted Eq. 5-8 to obtain Fig. 29. The best least-squares fit of it gave $K\varepsilon$ to be 44 ± 10 (liter cm mmole^{-2}), ε to be $(1.2 \pm 0.3) \times 10^3$ (cm mmole^{-1}), and K to be 0.036 ± 0.025 liter mole^{-1}.

From the above Scott analysis, we cannot say how well the equilibrium constant for the complex of chlorine with benzene has been determined from the infrared data, but we can say with some confidence that the absolute integrated molar absorption coefficient (ε) for the complex of chlorine with benzene (presumably a one-to-one complex) lies between 660 and 1200 cm mmole^{-1}. This value is to be compared with

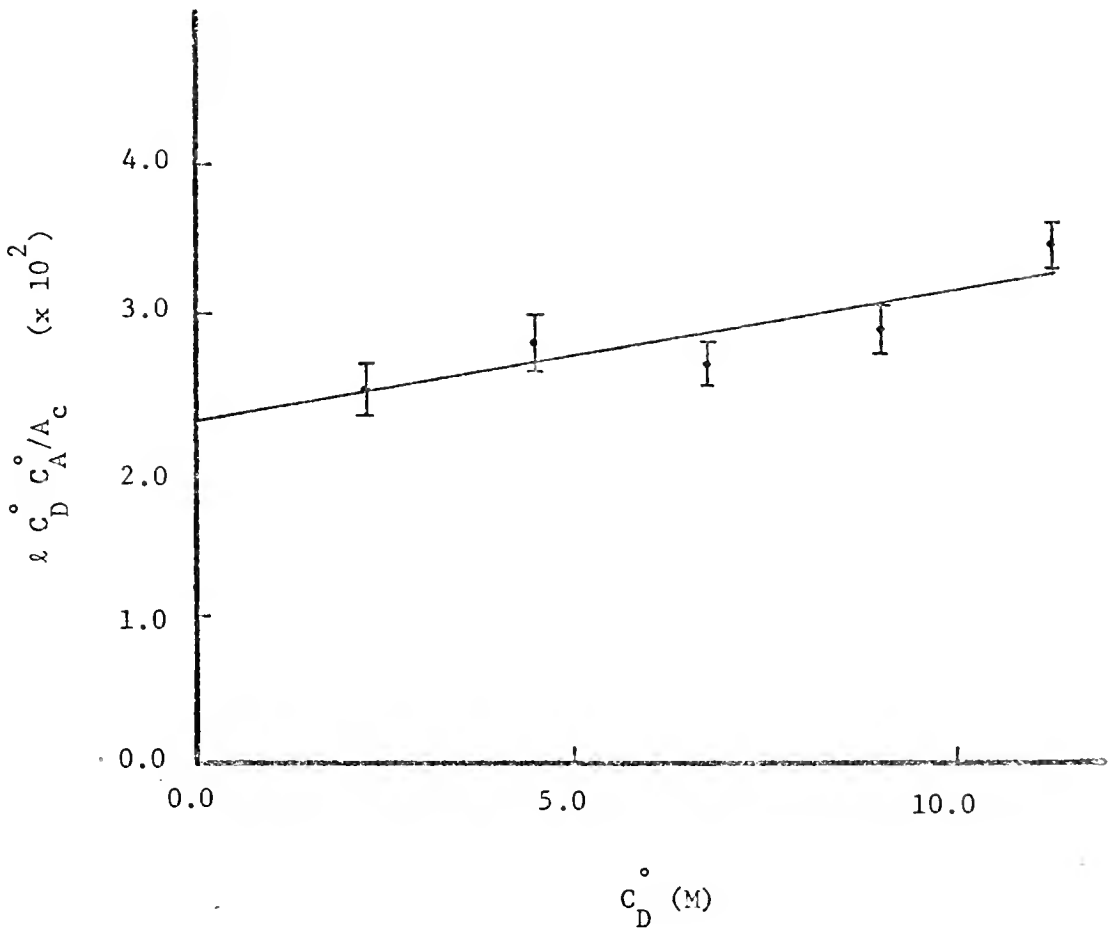

Fig. 29. -- Scott plot of chlorine complex with benzene, using a recalculated intensity of chlorine, as given by Eq. 5-9, and described in the text.

the less accurately measured estimate of 153 cm $mmole^{-1}$ (based on total Cl_2 concentration) for the intensity of this absorption band, given by Person, Erickson and Buckles (21). The dramatically increased value of this intensity suggests that it would be desirable to repeat accurately the other intensity estimates given earlier (21) for the halogen complexes, with carefully determined equilibrium constants.

CHAPTER VI

COLLISION-INDUCED INFRARED INTENSITY OF CHLORINE IN BENZENE AND IN CARBON TETRACHLORIDE SOLUTIONS

Introduction

We have mentioned in Chap. I that there are two different interpretations for the observed infrared spectra of halogens in benzene solution, and we have reported the observed infrared spectrum of chlorine in both benzene and carbon tetrachloride solutions in the preceeding chapters. The intermolecular interaction between chlorine and carbon tetrachloride is not expected by the charge transfer theory to result in any infrared absorption by the Cl_2 so that the observed band is more likely due to electrostatic effects. In order to estimate the contribution of ordinary electrostatic effects to the infrared absorption intensities of chlorine in benzene and in carbon tetrachloride solutions, we carried out theoretical calculations of the collision induced infrared absorption intensity, based on the theory developed by Van Kranendonk (43) and Fahrenfort (44), and on the related thoery of collision-induced far infrared absorption intensity mentioned in Chap. I. At first, we shall present calculations of the induced infrared intensity of chlorine-benzene pairs or chlorine-carbon tetrachloride pairs for definite, specific fixed orientations of the molecules, and then find a suitable way to obtain the value averaged over all orientations.

General Expression for the Integrated Collision-Induced Absorption Intensity

The integrated absorption coefficient is defined generally as

$$A = (1/n_{Cl_2}) \int \kappa(\tilde{\nu}) d\tilde{\nu} = (8\pi^3 N'_{12} \tilde{\nu}/3hcn_{Cl_2}) \left| \int \Psi_{12} \cdot \vec{\mu} \cdot \Psi'_{12} \, d\tau \right|^2 \quad . \tag{6-1}$$

Here A and n_{Cl_2} are the same as Eq. 5-6; $\kappa(\tilde{\nu})$ is the absorption coefficient, related to the incident light I_0 and the emerging light I through a medium of pathlength ℓ by the equation $I = I_0 e^{-\kappa(\tilde{\nu})\ell}$; $\tilde{\nu}$ is the wavenumber (cm^{-1}) of the measured light; N'_{12} is the number of collision pairs per cm^3; Ψ_{12} and Ψ'_{12} are the wavefunctions associated with the ground and excited states of the collision pair; $\vec{\mu}$ is the (induced) dipole moment operator for the collision pair; h is Planck's constant; c is the velocity of light; and $\left| \int \Psi_{12} \cdot \vec{\mu} \cdot \Psi'_{12} \, d\tau \right|^2$ is the squared matrix element from the induced dipole moment matrix. For a dilute gas with dipole moment operator $\vec{\mu}$, the expression for the integrated absorption coefficient A has the same form as Eq. 6-1, except that N'_{12} is the density of the pure gas and Ψ_{12} in $\left| \int \Psi_{12} \cdot \vec{\mu} \cdot \Psi'_{12} \, d\tau \right|^2$ is replaced by Ψ, the wavefunction of the isolated molecule. We will discuss more precisely these two important quantities (N'_{12} and $\left| \int \Psi_{12} \cdot \vec{\mu} \cdot \Psi'_{12} \, d\tau \right|^2$) as we proceed now to their calculation.

N'_{12}, the Number of Collision Pairs

The number of collision pairs occurring with one particular orientation of chlorine with respect to the solvent (either benzene or carbon tetrachloride) in the solution may be estimated from the pair-correlation function $G(\vec{R}_{12}, \omega_1, \omega_2)$ for the system. (See Reed and Gubbins, Ref. 73, for a detailed discussion of pair correlation functions.) We have adapted Fahrenfort's method (44) for calculating

N'_{12} for a gas mixture with a slight modification in order to calculate N'_{12} in our liquid mixture. In our case, the pair-correlation function $G(\vec{R}_{12}, \omega_1, \omega_2)$ is a function of both isotropic and anisotropic potentials. The isotropic part is assumed to be a Lennard-Jones (6-12) potential, while the anisotropic part is assumed to be just the electrostatic interaction energy; for the case of the chlorine and benzene pair this electrostatic interaction energy will be the quadrupole-quadrupole interaction energy, and it will be the quadrupole-octapole interaction energy for the chlorine and carbon tetrachloride pair, since the first electric moment for carbon tetrachloride is the octapole moment. For different solute-solvent orientations, the expressions for $G(\vec{R}_{12}, \omega_1, \omega_2)$ have been derived and the results are shown in the Appendix.

The differential probability of dP of finding a molecule of type B (we shall label this molecule "2") in a given volume element $d\tau_B$ near a given molecule of type A (we shall label it molecule "1") anywhere within the volume V is given by:

$$dP(\vec{R}_{12}, \omega_1, \omega_2) = (1/V)\, G(\vec{R}_{12}, \omega_1, \omega_2)\, d\tau_B \quad . \tag{6-2}$$

Here the magnitude of $\vec{R}_{12}$ is the distance between the type B molecule and the type A molecule; ω_1 and ω_2 represent the orientations of molecules 1 and 2 [$\omega_1 = (\theta_1, \phi_1)$ and $\omega_2 = (\theta_2, \phi_2)$]; θ_i and ϕ_i for the ith linear molecule are defined according to Fig. 30. Alternatively, Fahrenfort (44) wrote

$$dP(\vec{R}_{12}, \omega_1, \omega_2) = (1/V) e^{-\beta u_{12}(\vec{R}_1, \vec{R}_2)}\, d\tau_B \quad . \tag{6-3}$$

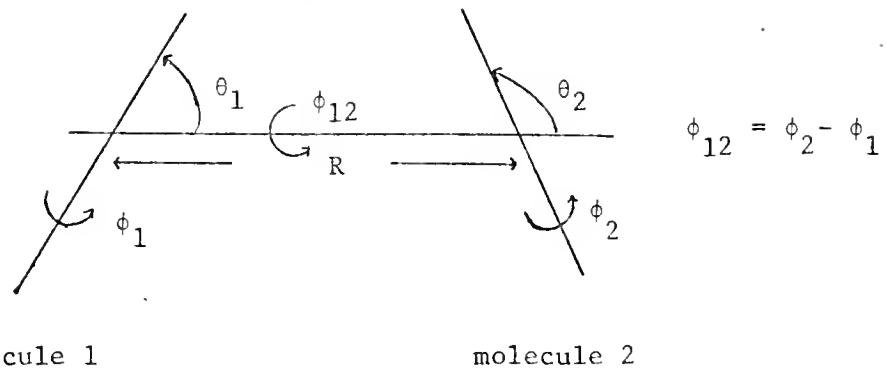

Fig. 30. -- Coordinate system used in defining the orientation of linear molecules

---

Here β is $1/kT$, $\vec{R}_1$ and $\vec{R}_2$ are the position coordinates of molecules 1 and 2, respectively, and $u_{12}(\vec{R}_1, \vec{R}_2)$ is the pair potential energy.

The differential probability of finding the type B molecule within a sphere around A defined by radius R_a and at a given solid angle $d\Phi = \sin\theta\, d\theta\, d\phi$) is given by

$$dP'(\omega_1, \omega_2) = [(1/V) \int_{R_0}^{R_a} G(\vec{R}_{12}, \omega_1, \omega_2)\, R^2 dR]\, d\Phi \quad . \qquad (6\text{-}4)$$

Here R_0 is the shortest allowed distance (the contact distance) between the type B molecule and the type A molecule, and R_a is the radius of a sphere centered at the type A molecule containing the type B molecule, and with volume V.

The probability per unit solid angle of finding the type B molecule in a sphere of radius R_a is given by

$$dP'/d\Phi = (1/V) \int_{R_0}^{R_a} G(\vec{R}_{12}, \omega_1, \omega_2)\, R^2\, dR \quad . \qquad (6\text{-}5)$$

Finally, the total number of pairs formed at a particular orientation (ω_1, ω_2) within the sphere of radius R_a is given by

$$N'_{12} = N_A N_B\, (dP'/d\Phi) = (N_A N_B/V) \int_{R_0}^{R_a} G(\vec{R}_{12}, \omega_1, \omega_2)\, R^2\, dR \; . \qquad (6\text{-}6)$$

In order to illustrate the use of Eq. 6-6, let us calculate N'_{12} for collision pairs of chlorine and benzene in an orientation with the symmetry axis of chlorine aligned along the six-fold symmetry axis of benzene [the "axial" orientation (37)] at certain distance R apart. Denote the chlorine molecule to be the type A molecule, and the benzene molecule to be the type B molecule. Here the value of ω_2 gives the orientation of the six-fold symmetry axis. If we consider the case where the molar concentration (n_{Cl_2}) of chlorine in the benzene solution is 0.4 M, and the concentration $(n_{C_6H_6})$ of benzene is 11.3 M (as in pure liquid benzene), then

$$N_A = n_{Cl_2} N_0/1000 = 2.48 \times 10^{20} \text{ molecules/cm}^3 \; ,$$

and

$$N_B = n_{C_6H_6} N_0/1000 = 68.026 \times 10^{20} \text{ molecules/cm}^3 .$$

Here N_0 is Avogadro's number. From Eq. 6-6, we see that we have to evaluate the integral $\int_{R_0}^{R_a} G(\vec{R}_{12}, \omega_1, \omega_2)\, R^2\, dR$, where $G(\vec{R}_{12}, \omega_1, \omega_2)$ is now the pair-correlation function for chlorine-benzene pairs in this "axial" orientation. In order to evaluate the integral numerically, we write:

$$\int_{R_0}^{R_a} G(\vec{R}_{12}, \omega_1, \omega_2)\, R^2\, dR = \sigma_{12}^3 \left[\int_{R_0^*}^{R_a^*} G(\vec{R}^*_{12}, \omega_1, \omega_2)\, R^{*2}\, dR^*\right] . \tag{6-7}$$

Here we have defined a set of "reduced coordinates," R^* to be R/σ_{12} and σ_{12} to be $(\sigma_1 + \sigma_2)/2$, where σ_1 and σ_2 are the parameters of the Lennard-Jones potential for chlorine ($\sigma_1 = 4.40$ Å) and for benzene ($\sigma_2 = 5.27$ Å) (74). We chose R_0^* to be 0.84 and R_a^* to be 2.40 because the factor $1/R^8$, which appears in the squared-matrix element $\left|\int \psi_{12} \cdot \vec{\mu}_{ind} \cdot \psi_{12}\, d\tau\right|^2$, falls off very rapidly for R_a^* greater than 2.40. The integral $\int_{R_0^*}^{R_a^*} G(\vec{R}^*_{12}, \omega_1, \omega_2)\, R^{*2}\, dR^*$ was evaluated numerically by a computer program written for Simpson's numerical integration method, with the interval between any two successive values of R^*s taken to be 0.04. From Eq. 6-7 and the parameters given above, we found for the "axial" orientation that:

$$\int_{R_0}^{R_a} G(\vec{R}_{12}, \omega_1, \omega_2)\, R^2\, dR = 9.231 \times 10^{-22} \text{ cm}^3 .$$

Finally, the number of pairs N'_{12} for chlorine and benzene pairs in this "axial" orientation is

$$N'_{12} = (N_A N_B/V) \int_{R_0}^{R_a} G(\vec{R}_{12}, \omega_1, \omega_2)\, R^2\, dR = 1.56 \times 10^{21} \text{ pairs/cm}^3 ,$$

or

$$N'_{12}/N_A = 6.28 .$$

Here N'_{12}/N_A given the average number of the axially oriented chlorine-benzene pairs per cm^3 per chlorine molecule. Since a pair is formed by two molecules, the unit "molecule^2 cm^{-6}" is equivalent to "pairs per cm^3" . Note that the number of pairs (N'_{12}) here is physically different from the "contact pairs" defined by Orgel and Mulliken (34).

The "contact pairs" are pairs in which the solvent molecules (benzene) are in immediate contact with the solute molecule (chlorine), while the N'_{12} defined here is the number of solvent molecules which are at a particular orientation with respect to the chlorine within the electrostatic interaction distance ($R^*_a < 2.40$), but which are not necessarily in physical contact.

Evaluation of $\left|\int \Psi_{12} \cdot \vec{\mu} \cdot \Psi'_{12}\, d\tau\right|^2$

To be exact, the wavefunction for the collision pair should be written as a function of all normal coordinates of both molecule 1 and molecule 2: $\Psi_{12}(\xi_{1s}, \xi_{1a}, \ldots, \xi_{2s}, \xi_{2a}, \ldots)$. However, for a weak intermolecular interaction the normal coordinates of each constituent molecule are probably not appreciably perturbed; such is expected to be the case for the pairs between chlorine and benzene (or chlorine and carbon tetrachloride). We can approximate Ψ_{12} by:

$$\Psi_{12}(\xi_{1s}, \xi_{1a}, \ldots, \xi_{2s}, \xi_{2a}, \ldots) = \Psi_1(\xi_{1s}, \xi_{1s}, \ldots)\, \Psi_2(\xi_{2s}, \xi_{2a}, \ldots). \tag{6-8}$$

Here $\xi_{1s}, \xi_{1a}, \ldots$ are the normal coordinates of molecule 1; $\xi_{2s}, \xi_{2a}, \ldots$ are the normal coordinates of molecule 2; $\Psi_1(\xi_{1s}, \xi_{1a}, \ldots)$ is the wavefunction for an isolated molecule 1; and $\Psi_2(\xi_{2s}, \xi_{2a}, \ldots)$ is the wavefunction for an isolated molecule 2. Then the squared induced dipole matrix element can be rewritten as

$$\left|\int \Psi_{12} \cdot \vec{\mu} \cdot \Psi'_{12}\, d\tau\right|^2 = \left|\int \Psi_1 \Psi_2 \cdot \vec{\mu} \cdot \Psi'_1 \Psi'_2\, d\tau\right|^2 \quad . \tag{6-9}$$

We are dealing with the case where only one of the molecules in the pair undergoes a vibrational transition (the Cl-Cl vibration of chlorine in benzene solution) and not the absorption by both chlorine

and benzene simultaneously. For this case, Ψ_2 and Ψ_2' are approximately the same, so that

$$\left|\int \Psi_1 \Psi_2 \cdot \vec{\mu} \cdot \Psi_1' \Psi_2' \, d\tau\right| \simeq \left|\int \Psi_1 \cdot \vec{\mu} \cdot \Psi_1' \, d\tau_1\right|^2 \left|\int \Psi_2 \Psi_2' \, d\tau_2\right|^2$$

$$= \left|\int \Psi_1 \cdot \vec{\mu} \cdot \Psi_1 \, d\tau_2\right|^2 \quad . \tag{6-10}$$

The induced dipole $\vec{\mu}$ arising from the electrostatic fields of the molecules in the collision pair was defined (43, 44) as

$$\vec{\mu} = \alpha_1 \vec{F}_2 + \alpha_2 \vec{F}_1 \quad . \tag{6-11}$$

Here α_1, α_2 are the polarizability tensors of molecule 1 and molecule 2, respectively; $\vec{F}_1$ is the electrostatic field generated by molecule 1 at the center of mass of molecule 2, and $\vec{F}_2$ is the electrostatic field generated by molecule 2 at the center of mass of molecule 1. We can also expand the induced dipole moment $\vec{\mu}$ in a Taylor series:

$$\vec{\mu} = \vec{\mu}_0 + (\partial\vec{\mu}/\partial\xi_{1s})_0 \, \xi_{1s} + (\partial\vec{\mu}/\partial\xi_{1a})_0 \, \xi_{1a} + (\partial\vec{\mu}/\partial\xi_{2s})_0 \, \xi_{2s} +$$

$$(\partial\vec{\mu}/\partial\xi_{2a})_0 \, \xi_{2a} + \ldots. + \text{higher order terms.} \tag{6-12}$$

Since there is no permanent dipole moment either for the chlorine or for the benzene molecule, $\vec{\mu}_0 = 0$. From the expansion of Eq. 6-12, the term which contributes to the variation of $\vec{\mu}$ with the frequency of the normal vibration ν_{1s} of molecule 1 is $(\partial\vec{\mu}/\partial\xi_{1s})_0 \, \xi_{1s}$. To simplify the notation, from now on we write ξ_{1s} as ξ_1, so

$$\vec{\mu} = (\partial\mu/\partial\xi_1)_0 \, \xi_1 \quad . \tag{6-13}$$

More explicitly, we rewrite Eq. 6-13 as

$$\vec{\mu} = [(\partial\alpha_1/\partial\xi_1)_0 \vec{F}_2 + \alpha_2(\partial\vec{F}_1/\partial\xi_1)_0] \xi_1 \quad . \tag{6-14}$$

When we substitute $\vec{\mu}$ from Eq. 6-14 into Eq. 6-10:

$$\begin{aligned} &\left|\int \Psi_{12} \cdot \vec{\mu} \cdot \Psi'_{12} \, d\tau\right|^2 \\ &\quad = \left|\int \Psi_1 [(\partial\alpha_1/\partial\xi_1)_0 \vec{F}_2 + \alpha_2 (\partial\vec{F}_1/\partial\xi_1)_0] \xi_1 \Psi_1 \, d\tau_1\right|^2 \\ &\quad = [(\partial\alpha_1/\partial\xi_1)_0 \vec{F}_2 + \alpha_2 (\partial\vec{F}_1/\partial\xi_1)_0] \left|\int \Psi_1 \cdot \xi_1 \cdot \Psi'_1 \, d\tau_1\right|^2 \quad . \end{aligned} \tag{6-15}$$

Since $\int \Psi_1 \xi_1 \Psi'_1 \, \tau_1 = [(v + 1)/2\gamma]^{1/2}$, where v is the vibrational quantum number, and $\gamma = 4\pi^2 \nu/h$ (see Appendix III of reference 75), and since $v = 0$ for the fundamental vibration transition, $\int \Psi_1 \xi_1 \Psi'_1 d\tau_1 = (h/8\pi^2\nu)^{1/2}$.

Finally,

$$\begin{aligned} &\left|\int \Psi_{12} \cdot \vec{\mu} \cdot \Psi'_{12} \, d\tau\right|^2 \\ &\quad = [(\partial\alpha_1/\partial\xi_1)_0 \vec{F}_2 + \alpha_2 (\partial\vec{F}_1/\partial\xi_1)_0]^2 (h/8\pi^2\nu) \quad . \end{aligned} \tag{6-16}$$

In order to obtain an appropriate average value (designated by < >) over the radial distribution function $G(\vec{R}_{12}, \omega_1, \omega_2)$, the value of $[(\partial\alpha_1/\partial\xi_1)_0 \vec{F}_2 + \alpha_2 (\partial\vec{F}_1/\partial\xi_1)_0]^2$ at a single R_{12} value should be replaced by

$$\begin{aligned} &\left\langle [(\partial\alpha_1/\partial\xi_1)_0 F_2 + \alpha_2 (\partial F_1/\partial\xi_1)_0]^2 \right\rangle_R \\ &= \frac{\int G(\vec{R}_{12}, \omega_1, \omega_2)[(\partial\alpha_1/\alpha\xi_1)_0 \vec{F}_2 + \alpha_2(\partial\vec{F}_1/\partial\xi_1)_0]^2 R^2 \, dR}{\int G(R_{12}, \omega_1, \omega_2) R^2 \, dR} \end{aligned} \tag{6-17}$$

Then Eq. 6-16 will be rewritten as

$$\left|\int \Psi_{12} \cdot \vec{\mu} \cdot \Psi'_{12}\, d\tau\right|^2 = \left\langle \left[(\partial\alpha_1/\partial\xi_1)_0 \vec{F}_2 + \frac{\alpha}{2} (\partial\vec{F}_1/\partial\xi_1)_0\right]^2 \right\rangle_R (h/8\pi^2\nu). \tag{6-18}$$

(Actually, the average should also be carried out over all orientations, too, as we discuss later.)

Explicit Expression for the Integrated Collision-Induced Absorption Intensity

Substituting Eq. 6-18 into Eq. 6-1,

$$A = 1/n_{Cl_2} \int \kappa(\tilde{\nu}) d\tilde{\nu}$$

$$= (\pi N'_{12}/3c^2 n_{Cl_2}) \left\langle \left[(\partial\alpha_1/\partial\xi_1)_0 \vec{F}_2 + \alpha_2 (\partial\vec{F}_1/\partial\xi_1)_0\right]^2 \right\rangle_R , \tag{6-19a}$$

or

$$A = (\pi N'_{12}/3c^2 n_{Cl_2}) \left\langle (\partial\vec{\mu}/\partial\xi_1)^2 \right\rangle_R . \tag{6-19b}$$

Note that Eq. 6-19b is equivalent to the usual expression for the intensity of infrared absorption (76), but with N'_{12}/n_{Cl_2} corresponding to N, the Avogadro's number, and $\left\langle (\partial\vec{\mu}/\partial\xi_1)^2 \right\rangle_R$ corresponding to $(\partial\vec{\mu}/\partial\xi)_0^2$, the square of the dipole moment derivative with respect to a particular normal mode vibration.

Evaluation of $\left\langle \left[(\partial\alpha_1/\partial\xi_1)_0 F_2 + \alpha_2 (\partial F_1/\partial\xi_1)_0\right]^2 \right\rangle_R$ for the "Axial" Chlorine-Benzene Pair

The polarizability tensor or the polarizability derivative tensor can be expressed in terms of its principal components (α_{xx}, α_{yy}, α_{zz} or α'_{xx}, α'_{yy}, α'_{zz}) if the induced dipole is parallel to the interacting electrostatic field direction, which is the case for the particular coordinate system for this study. Now it is necessary to evaluate the quantities $(\partial F_1/\partial\xi_1)_0$ and $\vec{F}_2$ for two axially symmetric

molecules such as chlorine and benzene. The electrostatic field generated by molecule $\underline{i}$ at the center of mass of other molecule is given by Buckingham (77) as

$$\vec{F}_i = F_{ir}\,\vec{e}_r + F_{i\theta}\,\vec{e}_\theta + F_{i\phi}\,\vec{e} \quad ,$$

where the components are

$$F_{ir} = (3/2R^4)\, Q_i\, (3\cos^2\theta_i - 1) \quad , \tag{6-20a}$$

$$F_{i\theta} = (3/R^4)\, Q_i\, (\cos\theta_i \sin\theta_i) \quad , \tag{6-20b}$$

and

$$F_{i\phi} = 0 \quad . \tag{6-20c}$$

Here Q_i is the quadrupole moment of molecule $\underline{i}$, R is the distance between the two centers of mass (the same as R_{12}), with θ_i and R as defined in Fig. 30. The electrostatic field expressed in the cartesian coordinates defined in Fig. 30 is found after a transformation of coordinates from $(F_{ir}, F_{i\theta}, F_{i\phi})$ to (F_{ix}, F_{iy}, F_{iz}). (For details of this transformation see Ref. 78.) The results of the transformation are:

$$F_{ix} = (3/R^4)\, Q_i \cos\theta_i \sin\theta_i \cos\phi_i \quad , \tag{6-21a}$$

$$F_{iy} = (3/R^4)\, Q_i \cos\theta_i \sin\theta_i \cos\phi_i \quad , \tag{6-21b}$$

$$F_{iz} = (3/2R^4)\, Q_i\, (3\cos^2\theta_i - 1) \quad . \tag{6-21c}$$

In the expression for F_{ix}, F_{iy}, F_{iz} the only quantity which depends on the normal coordinate of molecule $\underline{i}$ is the quadrupole moment Q_i, so that the derivative of F_i with respect to the normal

coordinate ξ_i is:

$$(\partial F_{ix}/\partial \xi_i)_0 = F'_{ix} = (3/R^4)(\partial Q_i/\partial \xi_i)_0 \cos\theta_i \sin\theta_i \cos\phi_i, \quad (6\text{-}22a)$$

$$(\partial F_{iy}/\partial \xi_i)_0 = F'_{iy} = (3/F^4)(\partial Q_i/\partial \xi_i)_0 \cos\theta_i \sin\theta_i \sin\phi_i, \quad (6\text{-}22b)$$

$$(\partial F_{iz}/\partial \xi_i)_0 = F'_{iz} = (3/2R^4)(\partial Q_i/\partial \xi_i)_0 (3\cos^2\theta_i - 1) . \quad (6\text{-}22c)$$

In particular for the "axial" chlorine-benzene pairs, θ_1 and θ_2 and 0°, so the only non-zero components of $\vec{F}_1$ (and also $\vec{F}_2$) and of the derivative of $\vec{F}_1$ are F_{1z} (and also F_{2z}) and F'_{1z} with $F_{1z} = 3Q_1/R^4$, $F_{2z} = 3Q_2/R^4$ and $F'_{1z} = (3/R^4)(\partial Q_1/\partial \xi_1)_0$. Thus, substitution of these values into Eq. 6-14 gives

$$[(\partial \alpha_1/\partial \xi_1)_0 \vec{F}_2 + \alpha_2 (\partial \vec{F}_1/\partial \xi_1)_0] = \alpha'_1 \vec{F}_2 + \alpha_2 \vec{F}'_1$$

$$= \begin{pmatrix} \alpha'_{1xx} & 0 & 0 \\ 0 & \alpha'_{1yy} & 0 \\ 0 & 0 & \alpha'_{1zz} \end{pmatrix} \begin{pmatrix} F_{2x} \\ F_{2y} \\ F_{2z} \end{pmatrix}$$

$$+ \begin{pmatrix} \alpha_{2xx} & 0 & 0 \\ 0 & \alpha_{2yy} & 0 \\ 0 & 0 & \alpha_{2zz} \end{pmatrix} \begin{pmatrix} F'_{1x} \\ F'_{1y} \\ F'_{1z} \end{pmatrix}$$

$$= \alpha'_{1zz} F_{2z} + \alpha_{2zz} F'_{1z} . \quad (6\text{-}23)$$

Here we introduce the compact notation α'_1 to stand for $(\partial \alpha_1/\partial \xi_1)_0$, etc.

More explicitly,

$$[(\partial\alpha_1/\partial\xi_1)_0 \vec{F}_2 + \alpha_2 (\partial\vec{F}_1/\partial\xi_1)_0]$$

$$= (3/R^4)[(\alpha'_{1zz})_0 Q_2 + \alpha_{2zz}(Q'_1)_0] \qquad (6\text{-}24)$$

so

$$[\alpha'_1 \vec{F}_2 + \alpha_2 \vec{F}'_1] = [\alpha'_{1zz} Q_2 + \alpha_{2zz}(Q'_1)_0]^2 . \qquad (6\text{-}25)$$

Therefore, the statistical average for $[\alpha'_1 \vec{F}_2 + \alpha_2 \vec{F}'_1]^2$ over a radial distribution for this particular orientation (eq. 6-17) is

$$\left\langle [\alpha'_1 \vec{F}_2 + \alpha_2 \vec{F}'_1]^2 \right\rangle_R = 9[\alpha'_{1zz} Q_2 + \alpha_{2zz} Q'_1]^2 \left\langle 1/R^8 \right\rangle . \qquad (6\text{-}26)$$

Here

$$\left\langle 1/R^8 \right\rangle_R = \frac{\int_{R_0}^{R_a} G(\vec{R}_{12}, \omega_1, \omega_2)\,(R^2/R^8)\,dR}{\int_{R_0}^{R_a} G(\vec{R}_{12}, \omega_1, \omega_2)\,R^2 dR} \quad , \text{ and the}$$

expression in Eq. 6-26 was so obtained because α' (etc) is independent of R. The value of $\left\langle 1/R^8 \right\rangle_R$ was obtained numerically as in Eq. 6-7. Substituting Eq. 6-26 into Eq. 6-19a, the integrated absorption coefficient can then be expressed for axially oriented chlorine-benzene pairs as:

$$A = (1/n_{Cl_2}) \int \kappa(\tilde{\nu})\,d\tilde{\nu}$$

$$= (\pi N'_{12}/3c^2 n_{Cl_2}) \left\langle (\partial\vec{\mu}/\partial\xi_1)^2 \right\rangle_R$$

$$= (\pi N'_{12}/3c^2 n_{Cl_2}) \cdot 9[(\alpha'_{1zz})_0 Q_2 + \alpha_{2zz}(Q'_1)_0]^2 \left\langle 1/R^8 \right\rangle_R . \qquad (6\text{-}27)$$

The expression for the contribution to the integrated intensity A from other chlorine-benzene pairs with different orientation can be similarly derived.

Actual Calculation of the Infrared Intensity of Chlorine in Benzene Solution for Collision Pairs in Different Orientations

The parameters used for this calculation are listed in Table VIII (and also in Table A-1) (79-80). To obtain the polarizability derivative $(\partial\alpha_1/\partial\xi_1)_0$ or quadrupole moment derivative $(\partial Q_1/\partial\xi_1)_0$ of chlorine from Table VIII, we simply multiply $(\partial\alpha_1/\partial r_1)_0$ or $(\partial Q_1/\partial r_1)_0$ by $\mu^{1/2}$, the square root of the reduced mass of chlorine (μ = 29.43 x 10^{-24} g) since $\xi_1 = \mu^{-1/2} r_1$. Since there are three different estimates of $(\partial\alpha_1''/\partial r_1)_0$ and $(\partial\alpha_1^{\perp}/\partial r_1)_0$ given in Table VIII we will use the values from our measurement of the Raman intensities for this calculation, since we believe that the measured values are probably the more reliable estimates, with the other estimates in Table VIII indicating the potential range of uncertainty.

We have calculated the collision-induced infrared intensity for four different chlorine-benzene orientations; the results are shown in Table IX. In the axial chlorine-benzene orientation, the values of $(\partial\alpha_1''/\partial\xi_1)_0\ Q_2$ is found to be the dominant term in the expression for $\left\langle(\partial\vec{\mu}/\partial\xi_1)_0\right\rangle_R$, although this is not necessarily true for other orientations. We see from Table VIII that the induced intensity for chlorine-benzene pairs comes predominantly from one orientation; namely, the axial one. The other orientations predict only a very small collision-induced infrared intensity for these pairs.

Now the question is how to obtain the total collision-induced infrared intensity expected for chlorine dissolved in benzene, averaging over all the contributions for different orientations. From Eq. 6-6, we see that we should now integrate over the entire

TABLE VIII

PARAMETERS USED FOR THE CALCULATION OF THE COLLISION-INDUCED INFRARED INTENSITY OF CHLORINE IN BENZENE OR CARBON TETRACHLORIDE SOLUTIONS

Parameter		Value	Source of the value
polarizability derivative of chlorine (x 10^{16} cm^2)	$(\partial\alpha_1''/\partial r_1)_0$[a]	(1) 11.2	(1) Ref. 31
		(2) 8.04	(2) our measurement[b]
		(3) 3.6	(3) Ref. 79
	$(\partial\alpha_1^{\perp}/\partial r_1)_0$[a]	(1) 0.0	(1) Ref. 42
		(2) 1.804	(2) our measurement[b]
		(3) - 0.045	(3) Ref. 79
polarizability of benzene (x 10^{25} cm^3)	α''[a]	635	Ref. 80
	$\alpha^{\perp}$[a]	123.1	Ref. 80
quadrupole moment derivative of chlorine (x 10^{18} esu cm)	$(\partial Q_1/\partial r_1)_0$	6.0	Ref. 79
polarizability of carbon tetrachloride (x 10^{25} cm^3)	α	105.0	Ref. 80

a. The parallel component (α'') is along the axial symmetry axis; the perpendicular component ($\alpha^{\perp}$) is thus perpendicular to this axis.

b. We converted the average and anisotropy polarizability derivatives (Chap. IV) to these values.

TABLE IX

CALCULATED COLLISION-INDUCED INFRARED INTENSITY
FOR CHLORINE-BENZENE PAIRS IN DIFFERENT ORIENTATIONS

	(I)	(II)	(III)	(IV)
Clorine-benzene orientation[a]	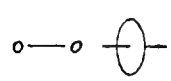	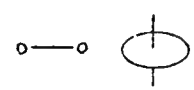	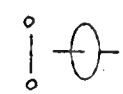	
Coefficient of $\left\langle 1/R^8 \right\rangle$ in $\left\langle (\partial\vec{\mu}/\partial\xi_1)_0^2 \right\rangle$ (Eq. 6-27)[b]	$9[(\alpha_1'')'_0 Q_2 + \alpha_2''(Q_1')_0]^2$	$9[-1/2(\alpha_1'')'_0 Q_2 + \alpha_2^{\perp}(Q_1')_0]^2$	$[3(\alpha_1^{\perp})'_0 Q_2 - 3/2\ \alpha_2''(Q_1')_0]^2$	$9/4\ [(\alpha_1^{\perp})'_0 Q_2 + \alpha_1^{\perp}(Q_1')_0]^2$
Calculated value for $\left\langle 1/R^8 \right\rangle$ ($\times 10^{57}$ cm^8)	9.20	0.274	0.274	6.55
Calculated value for[b] N'_{12} ($\times 10^{-20}$ pairs/cm^3)	15.57	5.98	5.98	11.1

TABLE IX (continued)

Collision-induced intensity cm mmole^{-1} (from Eq. 6-27	97.5[c]	2.72	0.33	3.40

---

a. Orientation I is "axial"; III is "resting" and II, IV, and V are different edgewise interactions. In these figures o—o is the chlorine molecule and ⊖ is benzene. The line represents the six-fold axis.

b. These values have been derived as illustrated in the text for the axial orientation.

c. When we used the value of 11.2 x 10^{-16} for $(\partial\alpha_1''/\partial r_1)_0$, the intensity is 237 cm mmole^{-1}, and when we used the value of 3.6 x 10^{-16} for $(\partial\alpha_1''/\partial r_1)_0$, we found the intensity to be 4.16 cm mmole^{-1}.

solid angle (4π) in order to obtain the total number of collision pairs and hence the total induced intensity. This cannot be done as illustrated above in the example given for the axial chlorine-benzene pair, since the radial distribution is not the same for all orientations. However, from our calculations the contribution to the total collision-induced infrared intensity from any chlorine-benzene orientation other than the "axial" one is expected to be negligible. We may take the largest intensity contribution from one of these alternate orientations (3.40 cm mmole^{-1} from case IV in Table IX) and multiply it by 4π to obtain the upper limit of the total collision-induced infrared intensity expected from all chlorine-benzene orientations except the axial one, then add the contribution from the axially oriented pair to estimate the overall total intensity from the collision-induced absorption. When this was done, we found that the upper limit of the total collision-induced infrared absorption intensity for chlorine in benzene solution is 140 cm mmole^{-1}. The lower limit for this estimated intensity would be 97.5 cm mmole^{-1} (assuming that all benzene-chlorine pairs have the axial orientation). Since these values are much smaller than the observed intensity (333 cm mmole^{-1}, based on total Cl_2 concentration) from Table VII, we conclude that the neglected charge transfer vibronic effect probably accounts for the remainder. This conclusion differs from that reached by Hanna and Williams (31) because of two things: first, the re-measured intensity (see Chap. V) was found to be greater by a factor of two than had been previously estimated (21), and second, the values of $(\partial\alpha''/\partial r_1)$ estimated from Lippincott's model by Hanna and Williams (31) are believed to be too large by a factor of two (Table VIII).

We believe that the refined measurements and calculations presented here are accurate enough so that we may conclude definitely that the predicted collision-induced intensity is indeed less than the experimental value.

Evaluation of $\left\langle [\alpha_1' F_2 + \alpha_2 F_1']^2 \right\rangle_R$ for Chlorine-Carbon Tetrachloride Collision Pairs

As a test of the reliability of the theory in predicting collision-induced infrared intensities, we have repeated the calculations for chlorine-carbon tetrachloride collision pairs in order to compare the predicted intensity with the observed result reported in Table VII.

Since the carbon tetrachloride molecule has tetrahedral symmetry, the electrostatic field it generates is different from that from an axially symmetric molecule. Therefore, a brief description of the coordinate system for these two interacting molecules (CCl_4 and Cl_2) is given below. We expect that the collision-induced infrared absorption intensity of chlorine should not depend drastically upon the relative orientation of the carbon tetrachloride molecule with respect to the chlorine molecule. For this reason, we selected only two different chlorine-carbon tetrachloride orientations for study.

For one case, we chose the relative orientation of chlorine and carbon tetrachloride shown in Fig. 31. (The other orientation is indicated in Table X.)

The molecule fixed axes for carbon tetrachloride were chosen to be parallel to the sides of a cube, as was done by Garg, et al. (50). A simple coordinate transformation was carried out from molecule fixed axes to obtain the expression in the laboratory fixed

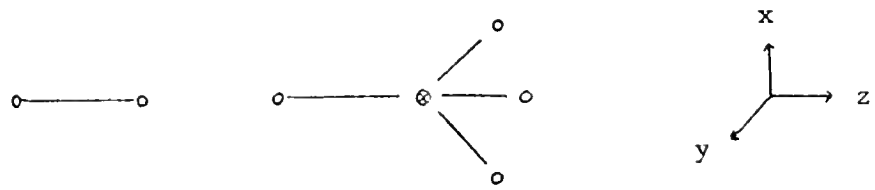

Fig. 31. -- Coordinate system used in defining the orientation of chlorine and carbon tetrachloride. o is a chlorine atom; ⊗ is a carbon atom.

---

axes shown in Fig. 31 for the electrostatic field generated by the carbon tetrachloride molecule at the center of mass of the Cl_2 molecule (for details, see Ref. 80). The components of the electrostatic field transformed from Garg *et al.* (50) to the coordinate system defined in Fig. 31 are

$$F_{2x} = F_{2y} = 0. \tag{6-28a}$$

$$F_{2z} = 0.77\ \Omega/R^5 \quad . \tag{6-28b}$$

Here Ω is defined slightly differently from that defined by Garg *et al.* (50) in that Ω of Eq. 6-28b is the total octapole moment.

The expression for the collision-induced infrared absorption intensity (A) for the chlorine-carbon tetrachloride pairs was derived by the same method given above for the chlorine-benzene system. The calculated results for two different orientations are shown in Table X.

TABLE X

CALCULATED COLLISION-INDUCED INFRARED INTENSITY OF
CHLORINE-CARBON TETRACHLORIDE PAIRS IN TWO DIFFERENT ORIENTATIONS

Chlorine-carbon tetrachloride orientation	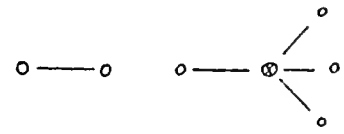	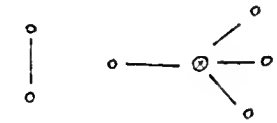
Expression for $\left\langle (\partial\mu/\partial\xi_1)_0^2 \right\rangle$ [a]	$\{9\alpha_2^2 (Q_1')_0^2 \left\langle 1/R^8 \right\rangle_R$	$\{2.25\ \alpha_2^2 (Q_1')_0^2 \left\langle 1/R^8 \right\rangle_R$
	$+ 4.62\ \Omega_2 \alpha_2 (\alpha_\perp'')_0' (Q_1')_0 \left\langle 1/R^9 \right\rangle_R$	$- 2.312\ \Omega_2 \alpha_2 (\alpha_1^\perp)_0' (Q_1')_0 \left\langle 1/R^9 \right\rangle_R$
	$+ 0.77\ \Omega_2^2 (\alpha'')_{1\,0}'^2 \left\langle 1/R^{10} \right\rangle_R\}$	$+ 0.594\ \Omega_2^2 (\alpha_1^\perp)_{1\,0}'^2 \left\langle 1/R^{10} \right\rangle_R\}$
Calculated values of: $\left\langle 1/R^8 \right\rangle$	1.96×10^{57} cm^{-8}	4.9×10^{57} cm^{-8}
$\left\langle 1/R^9 \right\rangle$	3.48×10^{64} cm^{-9}	9.6×10^{64} cm^{-9}
$\left\langle 1/R^{10} \right\rangle$	6.28×10^{71} cm^{-10}	1.91×10^{77} cm^{-10}

TABLE X (continued)

Value for N'_{12} ($\times 10^{-20}$ pairs cm^{-3})	6.16		7.25	
Collision-induced intensity (A) ($cm\ mmole^{-1}$)	5.70^{b}	4.27^{c}	3.12^{b}	3.5^{e}
		1.294^{d}		-0.4^{d}
		0.130^{e}		0.018^{e}

a. Derived for the particular chlorine-carbon tetrachloride pair indicated.

b. Total intensity for this orientation. See text for the result averaged over all angles.

c. Contribution from the $\langle 1/R^{8} \rangle_{R}$ term.

d. Contribution from the $\langle 1/R^{9} \rangle_{R}$ term.

e. Contribution from the $\langle 1/R^{10} \rangle_{R}$ term.

It is worthwhile to point out that the dominant term in $(\partial\vec{\mu}/\partial\xi_1)_0^2$ is the term in $\alpha_2^2 (\partial Q_1/\partial\xi_1)_0^2 \langle 1/R^8 \rangle_R$. As we expected, the collision-induced infrared intensities for the two different chlorine-carbon tetrachloride orientations are not much different. It is believed that the average of these two values multiplied by 4π (the total solid angle) as required by Eq. 6-6 will yield an accurate prediction of the total collision-induced infrared intensity for chlorine in a carbon tetrachloride solution. The total collision-induced infrared intensity of chlorine in carbon tetrachloride solution calculated in this way is expected to be about 55.5 cm mmole^{-1}.

When we compare this calculated total collision-induced infrared absorption intensity of chlorine in carbon tetrachloride (55.5 cm mmole^{-1}) with the observed absolute infrared intensity for this system (78 cm mmole^{-1} from Table VI), the agreement is very good indeed. Thus, the ordinary electrostatic effect does account for most of the observed infrared absorption for chlorine in the carbon tetrachloride solution. We conclude that this theory of collision-induced infrared intensity is good, and that the parameter values used in the calculation (from Table VIII) are probably correct. The success in predicting the collision-induced intensity of Cl_2 in CCl_4 reinforces our conclusion that the failure of this theory to account for the intensity observed for Cl_2 in benzene must be because some other important contribution (probably the charge-transfer effect) has been ignored.

CHAPTER VII

CALCULATIONS OF THE RAMAN INTENSITY ENHANCEMENT FOR CHLORINE IN BENZENE AND IN CARBON TETRACHLORIDE SOLUTIONS

Introduction

From both the ultraviolet and Raman spectroscopic studies discussed in Chaps. III and IV, we see that the complex of chlorine with benzene is indeed very weak. On the other hand, we observed a large intensification in the relative Raman intensity of chlorine when we changed the solvent from pure carbon tetrachloride to pure benzene (see Table V). We have proposed two possible reasons for this drastic change in intensity; one due to the non-specific solvent effects, the other due to a charge-transfer vibronic effect from a definite one-to-one complex. To test which of these two possible mechanisms may be responsible for our observation, we carried out two theoretical calculations of possible non-charge-transfer mechanisms; one based on the collision complex theory of Bernstein (81), the other based on the pre-resonance Raman effect (82-84). The former theory was derived by considering the ordinary electrostatic interaction (such as induced-dipole-induced-dipole interaction) between solute and solvent; the latter describes the dependence of Raman intensity on the frequency difference between the Raman exciting line and the electronic transition of the molecule. However, Bernstein (81) assumed that the collision complexes were in contact, with only one

dominant configuration. In our application of his theory given below, we calculate the contribution to the Raman intensity enhancement for all the chlorine-benzene pairs (or chlorine-carbon tetrachloride pairs) that have the same orientation, averaged over all values of R, the distance between chlorine and benzene (or chlorine and carbon tetrachloride) molecules. Thus, our treatment is parallel to the calculation given in Chap. VI for the collision-induced infrared intensity.

As in that chapter, our aim here is to make the best possible quantitative attempt to explain the observed intensification of the Raman shift (here; the infrared spectrum in Chap. VI) of chlorine in benzene without involving any charge-transfer vibronic effects. Any unexplained intensification may be the result of charge-transfer vibronic effects, since we believe there are no other possible mechanisms to explain this intensification that do not involve charge-transfer.

Theory of the Raman Intensity Enhancement Caused by Electrostatic Interaction (Bernstein's Collision-Complex Theory)

The theory was formulated to estimate the magnitude of Raman intensity changes from gas phase to liquid phase (or solution) when a nonpolar solute is condensed (or dissolved). The direct electrostatic interaction becomes significant in solution, since the intermolecular distances between molecules are much smaller there than they are in the gas phase at low pressure.

Physically, the potential at point B(R, θ, ϕ) due to a real dipole at origin A can be expressed (74) (for $R > \ell/2$) by:

$$V(R, \theta, \phi) = e/R \sum_{n=0}^{\infty} [1 - (-1)^n] (\ell/2R)^n P_n (\cos \theta)$$

$$= \mu \cos \theta / R^2 \left[1 + (\ell^2/8R^2)(5 \cos^2 \theta - 3) + \ldots \right] . \quad (7\text{-}1)$$

Here e is the point charge, $P_n (\cos \theta)$ is the nth Legendre polynomial and μ is the real dipole $\mu = e\ell$. Although Eq. 7-1 is derived for a real dipole, it can also be applied for an induced dipole. The coordinates used for Eq. 7-1 are defined in Fig. 32.

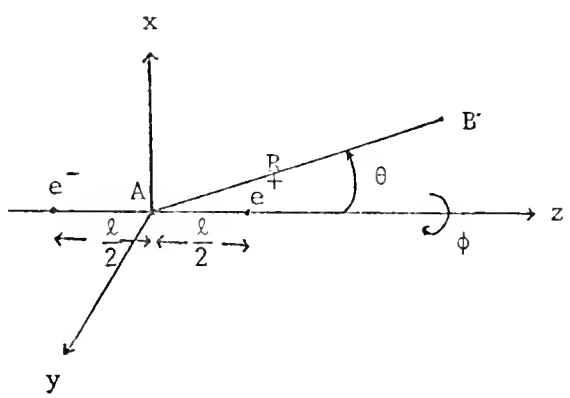

Fig. 32. -- Coordinate system and symbols used for deriving the electrostatic potential due to a dipole.

When $R >> \ell/2$ (as is usually true), we retain only the first term of the expression so that Eq. 7-1 becomes:

$$V(R, \theta, \phi) = \mu \cos \theta / R^2 . \quad (7\text{-}2)$$

The components of the field produced by this potential are then given by:

$$F_R = -\partial V/\partial R = (2\mu/R^3)\cos\theta \quad , \tag{7-3a}$$

$$F_\theta = -\partial V/R\partial\theta = (\mu/R^3)\sin\theta \quad , \tag{7-3b}$$

$$F_\phi = -\partial V/(R\sin\theta)\partial\phi = 0 \quad . \tag{7-3c}$$

Thus, the field $\vec{F}$ is

$$\vec{F} = \vec{e}_R\,(2\mu/R^3)\cos\theta + \vec{e}_\theta\,(\mu/R^3)\sin\theta \quad . \tag{7-4}$$

Here $\vec{e}_R$ and $\vec{e}_\theta$ are the polar coordinate unit vectors.

We denote by $\vec{P}^z_A$, $\vec{P}^x_A$, and $\vec{P}^y_A$ the induced dipoles of molecule A at point A along the z, x, and y axes, respectively. Let us consider the special case where the polar coordinate unit vectors $\vec{e}_R$, $\vec{e}_\theta$, and $\vec{e}_\phi$ are parallel to the z, x, and y axes, as shown in Fig. 33.

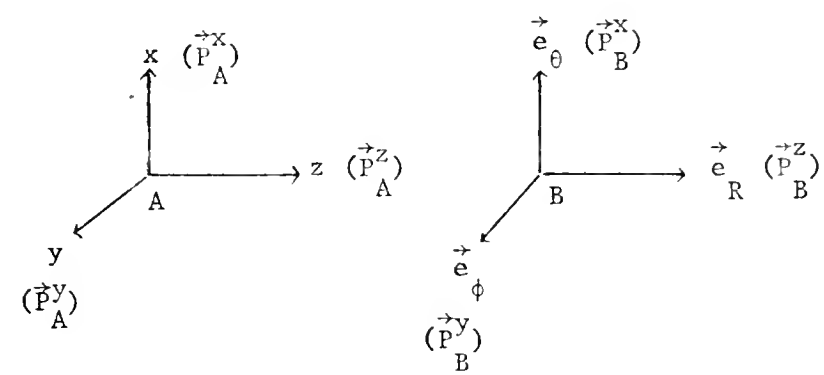

Fig. 33. -- The relative orientation between cartesian coordinates (x, y, z) and the polar coordinate unit vectors $(\vec{e}_R, \vec{e}_\theta, \vec{e}_\phi)$.

Then from Eq. 7-4, we see that $\vec{P}^{z}_{A}$ will produce a field at B given by:

$$\vec{F}^{z}_{A} = \vec{e}_{R} (2|\vec{P}^{z}_{A}| / R^{3}) \quad , \tag{7-5}$$

since θ for this case is 0°. $\vec{F}^{z}_{A}$ will then interact with the polarizability α^{z}_{B} of molecule B at B and produce an induced dipole moment $\alpha^{z}_{B}\,\vec{F}^{z}_{A}$ in the same direction as $\vec{P}^{z}_{A}$; i.e.,

$$\alpha^{z}_{B}\,\vec{F}^{z}_{A} = \vec{e}_{R}(2\,\alpha^{z}_{B}\,|\vec{P}^{z}_{A}|\,/R^{3}) = 2\,\alpha^{z}_{B}\,\vec{P}^{z}_{A}/R^{3} \quad , \tag{7-6a}$$

since $\vec{P}^{z}_{B}$ and $\vec{e}_{R}$ are in the same direction (see Fig. 33). Similarly, $\vec{P}^{x}_{A}$ and $\vec{P}^{y}_{A}$ will produce induced dipoles at B given by

$$\alpha^{x}_{B}\,\vec{F}^{x}_{A} = -\,\alpha^{x}_{B}\,\vec{P}^{x}_{A}/R^{3} \quad , \tag{7-6b}$$

$$\alpha^{x}_{B}\,\vec{F}^{y}_{A} = -\,\alpha^{y}_{B}\,\vec{P}^{y}_{A}/R^{3} \quad . \tag{7-6c}$$

Here α^{x}_{B}, α^{y}_{B} are the principal polarizability components of molecule B because of the way we have chosen the coordinate system (with x, y, and z axes parallel to the principal axes of the polarizability tensor of B), $\vec{F}^{x}_{A}$ and $\vec{F}^{y}_{A}$ are the fields produced by $\vec{P}^{x}_{A}$ and $\vec{P}^{y}_{A}$, respectively. The reason for the negative signs in Eqs. 7-6b and 7-6c is because in both cases θ is 270°.

On the other hand, the polarizability α_{B} of molecule B will interact with the electric field $\vec{E}$ of the exciting light and produce an induced dipole moment $\alpha_{B}\,\vec{E}$, which has 3 components $\alpha^{z}_{B}\,\vec{E}$, $\alpha^{x}_{B}\,\vec{E}$, and $\alpha^{y}_{B}\,\vec{E}$. Therefore, there are two contributions for the induced dipole moment of molecule B, i.e.:

$$\vec{P}^{z}_{B} = \alpha^{z}_{B} \vec{E} + 2\alpha^{z}_{B} \vec{P}^{z}_{A}/R^{3} \quad , \tag{7-7a}$$

$$\vec{P}^{x}_{B} = \alpha^{x}_{B} \vec{E} - \alpha^{x}_{B} \vec{P}^{x}_{A}/R^{3} \quad , \tag{7-7b}$$

$$\vec{P}^{y}_{B} = \alpha^{y}_{B} \vec{E} - \alpha^{y}_{B} \vec{P}^{y}_{A}/R^{3} \quad . \tag{7-7c}$$

And similarly,

$$\vec{P}^{z}_{A} = \alpha^{z}_{A} \vec{E} + 2\alpha^{z}_{A} \vec{P}^{z}_{B}/R^{3} \quad , \tag{7-8a}$$

$$\vec{P}^{x}_{A} = \alpha^{x}_{A} \vec{E} - \alpha^{x}_{A} \vec{P}^{x}_{B}/R^{3} \quad , \tag{7-8b}$$

$$\vec{P}^{y}_{A} = \alpha^{y}_{A} \vec{E} - \alpha^{y}_{A} \vec{P}^{y}_{B}/R^{3} \quad . \tag{7-8c}$$

(We note that Bernstein started his formulation (81) for the collision complex theory from Eqs. 7-7 and 7-8.) By stustituting $\vec{P}^{z}_{B}$ in Eq. 7-8a, we get

$$\vec{P}^{z}_{A} = \frac{[\alpha^{z}_{A} + (2\,\alpha^{z}_{A}\,\alpha^{z}_{B}/R^{3})]}{[1 - (4\,\alpha^{z}_{A}\,\alpha^{z}_{B}/R^{6})]} \vec{E} \quad . \tag{7-9a}$$

In the same way, we get the expression for the other two quantities:

$$\vec{P}^{x}_{A} = \frac{[\alpha^{x}_{A} - (\alpha^{x}_{A}\,\alpha^{x}_{B}/R^{3})]}{[1 - (\alpha^{x}_{A}\,\alpha^{x}_{B}/R^{6})]} \vec{E} \quad . \tag{7-9b}$$

$$\vec{P}^{y}_{A} = \frac{[\alpha^{y}_{A} - (\alpha^{y}_{A}\,\alpha^{y}_{B}/R^{3})]}{[1 - (\alpha^{y}_{A}\,\alpha^{y}_{B}/R^{6})]} \vec{E} \quad . \tag{7-9c}$$

And similarly

$$\vec{P}^{z}_{B} = \frac{[\alpha^{z}_{B} + (2\,\alpha^{z}_{B}\,\alpha^{z}_{A}/R^{3})]}{[\,1 - (4\,\alpha^{z}_{B}\,\alpha^{z}_{A}/R^{6})]}\,\vec{E} \quad , \tag{7-10a}$$

$$\vec{P}^{x}_{B} = \frac{[\alpha^{x}_{B} - (\alpha^{x}_{B}\,\alpha^{x}_{A}/R^{3})]}{[\,1 - (\alpha^{x}_{B}\,\alpha^{x}_{A}/R^{6})]}\,\vec{E} \quad , \tag{7-10b}$$

$$\vec{P}^{y}_{B} = \frac{[\alpha^{y}_{B} - (\alpha^{y}_{B}\,\alpha^{y}_{A}/R^{3})]}{[\,1 - (\alpha^{y}_{B}\,\alpha^{y}_{A}/R^{6})]}\,\vec{E} \quad . \tag{7-10c}$$

Now we can express the total induced dipole moment as a function of the two polarizabilities α_A and α_B, the electric field of the exciting light $\vec{E}$, and the intermolecular distance R. Bernstein defined the principal polarizabilities of a binary collision pair AB as follows:

$$\vec{P}^{i}_{A} + \vec{P}^{i}_{B} = \alpha^{i}_{AB} \cdot \vec{E}, \text{ where } i = x, y \text{ or } z,$$

or

$$\alpha^{i}_{AB} = (\vec{P}^{i}_{A} + \vec{P}^{i}_{B})/E \quad . \tag{7-11}$$

From Eqs. 7-9a, 7-10a and 7-11, we obtain

$$\alpha^{z}_{AB} = \alpha^{z}_{A} + \alpha^{z}_{B} + 4\alpha^{z}_{A}\,\alpha^{z}_{B}/R^{3} + 4\alpha^{z}_{A}\,\alpha^{z}_{B}(\alpha^{z}_{A} + \alpha^{z}_{B})/R^{6} + 0\,(1/R^{9}). \tag{7-12a}$$

Here $0\,(1/R^{9})$ refers to terms depending on $1/R^{9}$.

Similarly,

$$\alpha^{x}_{AB} = \alpha^{x}_{A} + \alpha^{x}_{B} - 2\alpha^{x}_{A}\,\alpha^{x}_{B}/R^{3} + \alpha^{x}_{A}\,\alpha^{x}_{B}\,(\alpha^{x}_{A} + \alpha^{x}_{B})/R^{6} + 0\,(1/R^{9})$$

and (7-12b)

$$\alpha^{y}_{AB} = \alpha^{y}_{A} + \alpha^{y}_{B} - 2\alpha^{y}_{A}\alpha^{y}_{B}/R^{3} + \alpha^{y}_{A}\alpha^{y}_{B}\,(\alpha^{y}_{A} + \alpha^{y}_{B})/R^{6} + 0\,(1/R^{9}). \quad (7\text{-}12c)$$

Eqs. 7-12a, 7-12b and 7-12c indicate that we can express the polarizability of the complex AB in terms of the polarizabilities of the parent molecules A and B.

The average and the anisotropic polarizabilities of the AB pair can now be obtained from these principal polarizability components. The average polarizability is given by

$$\alpha_{AB} = (1/3)\,(\alpha^{x}_{AB} + \alpha^{y}_{AB} + \alpha^{z}_{AB}) \quad , \quad (7\text{-}13)$$

and the anisotropic polarizability is given by

$$\gamma^{xy}_{AB} = \alpha^{x}_{AB} - \alpha^{y}_{AB}, \quad \gamma^{yz}_{AB} = \alpha^{y}_{AB} - \alpha^{z}_{AB}, \quad \gamma^{zx}_{AB} = \alpha^{z}_{AB} - \alpha^{x}_{AB} \quad . \quad (7\text{-}14)$$

Correspondingly, the derivatives of the average and of the anisotropy polarizability of the complex AB with respect to one of the normal coordinates (ξ_A) of molecule A is given by

$$(\alpha'_{AB})^{2} = 1/9[(\alpha^{x}_{AB})' + (\alpha^{y}_{AB})' + (\alpha^{z}_{AB})']^{2} \quad , \quad (7\text{-}15)$$

and

$$(\gamma'_{AB})^{2} = 1/2\,\{[(\alpha^{x}_{AB})' - (\alpha^{y}_{AB})']^{2} + [(\alpha^{y}_{AB})' - (\alpha^{z}_{AB})']^{2} + [(\alpha^{z}_{AB})' - (\alpha^{x}_{AB})']^{2}\}^{1/2} \quad . \quad (7\text{-}16)$$

Here the prime denotes the derivative with respect to ξ_A; e.g., $\alpha'_{AB} = \partial\alpha_{AB}/\partial\xi_A$.

In principle, one can take the derivatives of α_{AB} in Eq. 7-13 and of γ^{xy}_{AB}, γ^{yz}_{AB}, and γ^{zx}_{AB} in Eq. 7-14 with respect to ξ_A, and then

substitute them into Eqs. 7-15 and 7-16 to obtain a general expression for either $(\alpha'_{AB})^2$ or $(\gamma'_{AB})^2$ in terms of the derivatives of the principal polarizability components of the parent molecules. For pairs formed between two axially symmetric molecules or between an axially symmetric molecule and a tetrahedrally symmetric molecule, so that the AB pair has at least two equal principal polarizability components, the expression for $(\alpha'_{AB})^2$ and $(\gamma'_{AB})^2$ can be very much simplified. Formulae for special cases like those mentioned above have been derived by Bernstein (81).

Calculation of the Raman Intensity Enhancement for Chlorine-Benzene and Chlorine-Carbon Tetrachloride Pairs in Different Solute-Solvent Orientations

In these calculations what we must actually do is to estimate the magnitude of the intensity enhancement, so that we want to calculate the differences $\Delta(\alpha'_{AB})^2$ and $\Delta(\gamma'_{AN})^2$, which are defined as

$$\Delta(\alpha'_{AB})^2 = (\alpha'_{AB})^2 - (\alpha'_{A})^2 \quad , \tag{7-17a}$$

and

$$\Delta(\gamma'_{AB})^2 = (\gamma'_{AB})^2 - (\gamma'_{A})^2 \quad . \tag{7-17b}$$

There are at least two ways to evaluate $\Delta(\alpha'_{AB})^2$ and $\Delta(\gamma'_{AB})^2$. One is to make the evaluation at only one particular value for R, the intermolecular distance between a pair of solute and solvent molecules in contact; the other is to evaluate $\Delta(\alpha'_{AB})^2$ and $\Delta(\gamma'_{AB})^2$ as an appropriate statistical average for all pairs of appropriately oriented molecular pairs over all possible distances as defined in Eqs. 7-18a and 7-18b, and then multiply each average value by (N'_{12}/N_A) as defined in Chap. VI, and make another statistical average

over all possible angular orientations. For comparison, we have evaluated $\Delta(\alpha'_{AB})^2$ and $\Delta(\gamma'_{AB})^2$ for the chlorine-benzene pair at one particular distance (the van der Waals distance) for one particular orientation (axial model). For the most part we will estimate these quantities by the second method, since the liquid structure (unlike a solid) is distorted even though there may be one preferred orientation of the solute-solvent pair. To obtain an appropriate statistical average of $\Delta(\alpha'_{AB})^2$ and $\Delta(\gamma'_{AB})^2$ over all distances for the AB complex at one particular orientation, we define

$$\left\langle \Delta(\alpha'_{AB})^2 \right\rangle_R = \frac{\int_{R_0}^{R_a} \Delta(\alpha'_{AB})^2 \, G(\vec{R}_{12}, \omega_1, \omega_2) \, R^2 dR}{\int_{R_0}^{R_a} G(\vec{R}_{12}, \omega_1, \omega_2) \, R^2 dR} , \qquad (7\text{-}18a)$$

and

$$\left\langle \Delta(\gamma'_{AB})^2 \right\rangle_R = \frac{\int_{R_0}^{R_a} \Delta(\gamma'_{AB})^2 \, G(\vec{R}_{12}, \omega_1, \omega_2) \, R^2 dR}{\int_{R_0}^{R_a} G(\vec{R}_{12}, \omega_1, \omega_2) \, R^2 dR} . \qquad (7\text{-}18b)$$

Here $G(\vec{R}_{12}, \omega_1, \omega_2)$ is the same pair correlation function for chlorine in benzene solution or chlorine in carbon tetrachloride solution as that used in Chap. VI and given also in the Appendix. Before the integrals in Eqs. 7-18a and 7-18b were evaluated, we inserted all the parameters into the expressions for $(\alpha'_{AB})^2$ and $(\gamma'_{AB})^2$ (such as the ones given by Eqs. 7-19a and 7-19b) and simplified the expressions into 4 terms. The first one is a constant, the second one involved $1/R^3$, and the third and fourth ones involved $1/R^6$. [Note: In our re-derivation of these expressions we believe that some errors in some of the coefficients of the $1/R^6$ terms originally given by Bernstein (81) have been detected. For this reason we write the

$1/R^6$ term as a sum of two terms (the third and fourth); we believe the coefficients of the third term (containing $\alpha_A\alpha_B$, $\alpha_A\gamma_B$, $\alpha_B\gamma_A$ and $\gamma_A\gamma_B$) given by Bernstein (81) are correct, but that the coefficients of the fourth term (containing α_B^2, $\alpha_B\gamma_B$, and γ_B^2) given by Bernstein (81) are not correct. Since both $1/R^6$ terms make only a small contribution to the intensity enhancement, we used Bernstein's terms without any correction. (The term in question is the coefficient C_3 in Table XI.) Since the first term is exactly $(\alpha'_A)^2$ [or $(\gamma'_A)^2$], the expressions for $\Delta(\alpha'_{AB})^2$ and $\Delta(\gamma'_{AB})^2$ contain only the second $(1/R^3)$ and the third and fourth $(1/R^6)$ terms. The numerator of Eq. 7-18 was then broken into three separate integrals, which were calculated numerically as described in Chap. VI. The process will become clear below where we present a sample calculation in some detail. The limits of the integral (in Eqs. 7-18a and 7-18b) were chosen to be from $R_0^* = 0.84$ to $R_a^* = 5.0$, in reduced units. The reason for choosing these limits of integration instead of $R_0^* = 0.84$ to $R_a^* = 2.40$ as in Chap. VI for the collision-induced infrared intensity calculations is because the expressions for $\Delta(\alpha'_{AB})^2$ and $\Delta(\gamma'_{AB})^2$ involve $1/R^3$ terms. which do not fall off as rapidly as does the $1/R^8$ (or $1/R^9$, $1/R^{10}$) term in the expression for the collision-induced infrared intensity.

The expressions for $(\alpha'_{AB})^2$ and $(\gamma'_{AB})^2$ which were derived by Bernstein (81) for chlorine (label A) and benzene (label B) in the axial orientation are given below:

$$(\alpha'_{AB})^2 = (\alpha'_A)^2 \{1 + 8\gamma_B/3R^3 + (1/3R^3)[24\alpha_A\alpha_B + 8\alpha_A\gamma_B + 8\alpha_B\gamma_A + 8\gamma_A\gamma_B + 12\alpha_B^2 + 8\alpha_B\gamma_B + 16\gamma_B^2/3]\} + (\gamma'_A)^2 (12\alpha_B + 4\gamma_B)^2/81R^6 + (\gamma'_A\alpha'_A)\{(24\alpha_B + 8\gamma_B)/9R^3 + (1/9R^6)[24\alpha_A\alpha_B + 24\alpha_A\gamma_B + 24\alpha_B\gamma_A + 40\gamma_A\gamma_A/3 + 12\alpha_B^2 + 56\alpha_A\gamma_B + 52\gamma_B^2/3]\} , \quad (7\text{-}19a)$$

$$(\gamma'_{AB})^2 = (\gamma'_A)^2 \{1 + 4(\alpha_B + \gamma_B)/R^3 + (1/3R^6)[36\alpha_A\alpha_B + 20\alpha_A\gamma_B + 20\alpha_B\gamma_A + 43\gamma_A\gamma_B/3 + 30\alpha_B^2 + 44\alpha_B\gamma_B + 58\gamma_B^2/3]\} + (\alpha'_A)^2 (6\alpha_B + 2\gamma_B)^2/R^6 + (\gamma'_A\alpha'_A)\{2(6\alpha_B + 2\gamma_B)/R^3 + (1/R^6)[12\alpha_A\alpha_B + 12\alpha_A\gamma_B + 12\alpha_B\gamma_A + 20\gamma_A\gamma_B/3 + 30\alpha_B^2 + 44\alpha_B\gamma_B + 28\gamma_B^2/3]\} . \quad (7\text{-}19b)$$

The polarizabilities (α_A and α_B, respectively) of chlorine and benzene and these estimates for the polarizability derivatives of chlorine [isotropic (α'_A) and anisotropic (γ'_A)] were calculated from Table VIII. For the calculations in this chapter we will use the experimental values of the polarizability derivatives [set (2) in Table VIII]. With these parameters, we obtain from Eqs. 7-19a and 7-19b,

$$(\alpha'_{AB})^2 = [0.1508 + (0.0264/R^{*3}) + (0.0061/R^{*6}) + (0.0043/R^{*6})] \times 10^{-30}\ \text{cm}^4 , \quad (7\text{-}20a)$$

and

$$(\gamma'_{AB})^2 = [0.389 + (0.2743/R^{*3}) + (0.0248/R^{*6}) + (0.0569/R^{*6})] \times 10^{-30} \text{ cm}^4 \quad . \tag{7-20b}$$

So from Eqs. 7-17a and 7-20a, we have

$$\Delta(\alpha'_{AB})^2 = [0.0264/R^{*3} + 0.0061/R^{*6} + 0.0043/R^{*6}] \times 10^{-30} \text{ cm}^4$$

$$= (C_1/R^{*3} + C_2/R^{*6} + C_3/R^{*6}) \quad . \tag{7-21a}$$

And from Eqs. 7-17b and 7-20b, we have

$$\Delta(\gamma'_{AB})^2 = [0.2743/R^{*3} + 0.0248/R^{*6} + 0.0569/R^{*6}] \times 10^{-30} \text{ cm}^4$$

$$= (C_1/R^{*3} + C_2/R^{*6} + C_3/R^{*6}) \quad . \tag{7-21b}$$

Substituting Eq. 7-21a into Eq. 7-18a and evaluating the integrals as described in Chap. VI, we get

$$\left\langle \Delta(\alpha'_{AB})^2 \right\rangle_R = 0.0031 \times 10^{-30} \text{ cm}^4 \quad .$$

From Eqs. 7-18b and 7-21b, we get

$$\left\langle \Delta(\gamma'_{AB})^2 \right\rangle_R = 0.0308 \times 10^{-30} \text{ cm}^4 \quad .$$

We calculated $\left\langle \Delta(\alpha'_{AB})^2 \right\rangle_R$, $\left\langle \Delta(\gamma'_{AB})^2 \right\rangle_R$ and N'_{12}/N_A for pairs of chlorine and benzene in several other orientations and for pairs of chlorine and carbon tetrachloride at two different orientations. The coefficients corresponding to Eqs. 7-21a and 7-21b are presented in Table XI. The calculated values of N'_{12}/N_A and the resulting intensity enhancement (ΔP) are shown in Table XII.

TABLE XI

COEFFICIENTS OF THE 1/R TERMS IN THE EXPRESSIONS FOR $\Delta(\alpha'_{AB})^2$ AND $\Delta(\gamma'_{AB})^2$ (EQS. 7-21a AND 7-21b) FOR SEVERAL DIFFERENT SOLUTE-SOLVENT (AB) ORIENTATIONS[a]

Case	Orientation of Solute-Solvent[b]		C_1[c]	C_2[c]	C_3[c]
(I)	o—o	A.[d]	0.0	0.0	0.0
	isolated A molecule	B.[d]	0.0	0.0	0.0
(II)	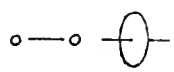	A.	0.0264	0.0061	0.0043
		B.	0.0740	0.0248	0.0570
(III)	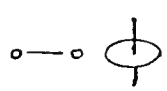	A.	0.0752	0.0111	0.0154
		B.	0.0740	0.0498	0.1425
(IV)	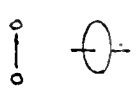	A.	- 0.0450	0.0036	0.0086
		B.	- 0.2190	0.0337	
(V)		A.	- 0.0132	0.0030	0.0037
		B.	- 0.1213	0.0131	0.1589

TABLE XI (continued)

(VI)	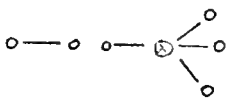	A.	0.0668	0.0292[e]
		B.	0.1910	0.2297[e]
(VII)	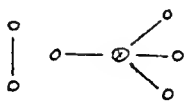	A.	- 0.0334	0.0111[e]
		B.	- 0.2308	0.1336[e]

---

a. The experimental values of the polarizability derivatives for chlorine [set (2) of Table VIII] in carbon tetrachloride have been used to obtain the coefficients.

b. See Table IX for a description of these symbols.

c. The units are 10^{-30} cm^4.

d. Lines A and B give the coefficients of $\Delta(\alpha'_{AB})^2$ and of $\Delta(\gamma'_{AB})^2$, respectively.

e. Both constants (C_2 and C_3) of $1/R^{*6}$ are combined into one term.

TABLE XII

THE CALCULATED VALUES[a] OF $\left\langle \Delta(\alpha'_{AB})^2 \right\rangle_R$[d], $\left\langle \Delta(\gamma'_{AB})^2 \right\rangle_R$[d], N'_{12}/N_A, AND THE ENHANCEMENT OF INTENSITY (ΔP)[b]

Case[c]	$\left\langle \Delta(\alpha'_{AB})^2 \right\rangle_R$[d]	$\left\langle \Delta(\gamma'_{AB})^2 \right\rangle_R$[d]	N'_{12}/N_A	ΔP[b]
(I)	0.0	0.0	--	0.0
(II)	0.003105	0.0308	35.9	1.34
(III)	0.00143	0.00634	31.0	0.356
(IV)	- 0.0008881	- 0.00415	31.2	- 0.225
(V)	- 0.00066	- 0.00262	33.9	- 0.158
(VI)	0.00276	0.00895	26.3	0.517
(VII)	- 0.00140	- 0.00885	26.9	- 0.353

a. As defined in the text in Eqs. 7-18a, 7-18b, and in Chap. VI (see text).
b. ΔP is defined in Eq. 7-22.
c. As defined in Table XI,
d. The units are 10^{-30} cm^4.

Here ΔP is the ratio of the calculated Raman intensity enhancement (averaged over R) for the AB pair compared to the Raman intensity of the isolated A (Cl_2) molecule; i.e.,

$$\Delta P = \frac{N'_{12}}{N_A} \cdot \frac{[45 \langle \Delta(\alpha'_{AB})^2 \rangle_R + \langle \Delta(\gamma'_{AB})^2 \rangle_R]}{[45 (\alpha'_A)^2 + 7 (\gamma'_A)^2]} \quad . \qquad (7\text{-}22)$$

Discussion

It is difficult to say just what the total Raman intensity enhancement will be when ΔP from Table XII is averaged over all possible orientations for chlorine in benzene (or in carbon tetrachloride). As Bernstein (81) points out, if we evaluate the unweighted average of the intensity enhancement over all possible orientations, it will be almost zero. On the other hand, if we expect that the chlorine-benzene pairs in an axial orientation are favored and form the predominant configuration, we predict a maximum enhancement of the Raman intensity of chlorine of 134% of the value for the isolated molecule. This value is still only a small enhancement, compared to our observation (Table V) that the intensification is by a factor of 4 (400%), based on total chlorine concentration.

We have also repeated this calculation, using the polarizability derivative for chlorine calculated from Lippincott's model [set (1) of Table VIII]. The predicted Raman intensity enhancement (ΔP values) is not much different from the values shown in Table XII. We have also calculated the intensity enhancement of the chlorine predicted from Eq. 7-19a and 7-19b for the case of axially oriented chlorine-benzene pairs at only one fixed value of R. At the van der Waals

distance ($R = 4.535$ Å), we predicted a 73% increase in intensity for a single one-to-one contact axial benzene-chlorine pair instead of the value of 134% predicted on averaging over all pairs with that orientation (see Table XII). However, we may have overestimated the number of pairs (N'_{12}/N_A) because the volume of the interacting sphere may possibly be too large, due to the choice of integration limits of the integral from $R^*_0 = 0.84$ to $R^*_a = 5.0$. Furthermore, it may not be true that there is simple additive contribution to the total Raman intensity enhancement for the chlorine molecule from all collision pairs (N'_{12}/N_A), since the electrostatic field of a benzene molecule far from the chlorine molecule could be shielded by an intervening benzene molecule. If this should happen to an important extent, we believe that predicted enhancement (Table XII) could be overestimated.

A similar dilemma occurs when we try to predict the magnitude of the intensity enhancement for chlorine from the gas phase to the solution in carbon tetrachloride, using the results in Table XII. Since there is no predominant orientation expected for chlorine in carbon tetrachloride solution, we may estimate an upper limit of 100% for the predicted enhancement of intensity. This value is obtained by noting that the enhancement predicted for the case VI oriented pair is greater than the decrease predicted for the case VII pair so that we estimate the total contribution to ΔP by multiplying the sum ($\Delta P_{VI} + \Delta P_{VII} \simeq 15\%$) by 2π (one half of the total solid angle). Unfortunately, there is no measured gas phase value for the absolute Raman intensity of chlorine for comparison with the

solution phase value (Table V) so that a definite conclusion about the ability of the Bernstein theory (81) to predict accurately the change in Raman intensity from gas phase to solution in an "inert" solvent is difficult to reach. However, this theory is similar to that for collision-induced infrared intensity (Chap. VI), and so it may be expected to predict this change for chlorine in carbon tetrachloride solution fairly well. It is quite clear from the comparison of results given above for the chlorine-benzene solutions that the observed intensification of the Cl_2 Raman shift in benzene solutions is much greater than can be explained by the Bernstein theory.

Theory of the Pre-resonance Raman Effect

It has been shown (for example see Ref. 83) that the total intensity of light with a frequency $\nu_\varepsilon = \nu_0 \pm \nu = \nu_0 + \nu_{mn}$, scattered on the average by one freely orientable molecule undergoing a transition from state m to state n (all in the electronic ground state for the vibrational Raman effect) can be expressed as

$$I_{mn} = (2^7 \pi^5/3^2 c^4)\, I_0 \nu_\varepsilon^4 \sum_{\rho,\sigma} |\alpha_{\rho\sigma,mn}|^2 \quad . \tag{7-23}$$

Here ν_0 is the frequency of the plane-polarized incident light, the vibrational frequency $\nu = |\nu_{mn}| > 0$, with $\nu_{mn} = -\nu_{nm} = (E_m - E_n)/hc$; c is the velocity of light and the sum goes over $\rho = x, y, z$ and $\sigma = x, y, z$ which independently refer to the molecule fixed coordinate system, and I_0 is the intensity of the incident light. According to the dispersion theory of Kramers and Heisenberg (85), the $\rho\sigma$th matrix element $\alpha_{\rho\sigma,mn}$ of the scattering tensor for the transition $m \rightarrow n$ is given by:

$$\alpha_{\rho\sigma,mn} = (1/h) \sum_{r} \left[\frac{(M_\rho)_{rn} (M_\sigma)_{mr}}{\nu_{rm} - \nu_0 + i\delta_r} + \frac{(M_\rho)_{mr} (M_\sigma)_{rn}}{\nu_{rn} + \nu_0 + i\delta_r} \right] . \quad (7\text{-}24)$$

Here h is Planck's constant and the sum goes over the intermediate states r of the molecule. Here $(M_\rho)_{rn}$, $(M_\sigma)_{mr}$, etc.,refer to the values of the corresponding transition moments. However, there are several ways (82-84) to estimate how $\alpha_{\rho\sigma,mn}$ and hence I_{mn} can best be approximated as the incident light frequency ν_0 approaches one of the vibronic transition frequencies ν_{rm}. (Note: ν_{rm} is an electronic transition frequency far removed from the vibrational frequency ν_{mn}.) The behavior observed as this happens, and before ν_0 actually becomes equal to ν_{rm} is called the pre-resonance Raman effect. The first attempt to estimate the vibration behavior of $\alpha_{\rho\sigma,mn}$ in this region was made by Shorygin and associates (see the review in Ref.82). The theory was reformulated later by Behringer with a quantum mechanical approach involving the Franck-Condon principle (82). There $\alpha_{\rho\sigma,mn}$ was approximated by considering that only the first excited vibronic state (with an allowed transition from the ground state) in the summation given in Eq. 7-24 is important. The result for the Raman scattering involving a fundamental vibrational transition ($v = 0 \rightarrow 1$) is given by:

$$\begin{aligned}(\alpha_{\rho\sigma})_{g,v_1=0;\ g,v_2=1} = {} & 1/h \{ [(2\nu_{eg})/(\nu_{eg}^2 - \nu_0^2)] \\ & \times [\partial |(M_\rho)_{eg} (M_\sigma)_{ge}| / \partial \xi_i]_0 \\ & - [2(\nu_{eg}^2 + \nu_0^2)/(\nu_{eg}^2 - \nu_0^2)] [|(M_\rho)_{eg} (M_\sigma)_{ge}| (\partial \nu_{eg} / \partial \xi_i)_0] \} \ \xi_0 .\end{aligned}$$

(7-25)

Here g and e designate the ground and the first (nondegenerate) electronic excited states, ξ_0 is what Behringer calls the zero-point amplitude and is just $\langle g_1 | \xi_i | g_0 \rangle$, and the "0" subscript indicates that the derivative is evaluated when the ith normal coordinate $\xi_i = 0$. In obtaining the above equation the states m and n are described by vibronic state quantum numbers; i.e., $m = gv_1$, $n = gv_2$, etc., with the first quantum number giving the electronic state, and the second the vibrational level in that state. The first term in Eq. 7-25 corresponds to the term appearing in Placzek's polarizability theory (86), while the second term accounts for the additional larger increase in $\alpha_{\rho\sigma,mn}$ associated with the pre-resonance Raman effect.

In the review of this effect by Koningstein (84), Albrecht's vibronic coupling model (83) has been cited as being a more flexible expression for $(\alpha_{\rho\sigma})_{g,v_1;g,v_2}$. In principle, the total wavefunction of the molecule (excluding the rotational part) can be written as

$$\Psi_{total} = \psi_g(\vec{r}, \xi_i)\, \psi_v(\xi_i) \quad . \tag{7-26}$$

Here $\psi_g(\vec{r},\xi_i)$ is the ground state electronic wavefunction, $\psi_v(\xi_i)$ is the vibrational wavefunction, r is the electronic coordinate and ξ_i is the ith normal coordinate. Retaining the first order term in the vibronic coupling model, $\psi_g(\vec{r}, \xi_i)$ can be expressed (85) as

$$\psi_g(\vec{r}, \xi_i) = \psi_g^0 + \sum_{t \neq g} h_{tg}^{\xi i} \cdot \xi_i \cdot \psi_t^0 \quad , \tag{7-27}$$

where

$$h_{tg}^{\xi i} = \frac{\langle \psi_t^0 \,|(\partial H/\partial \xi_i)_{\xi_1=0}|\, \psi_g^0 \rangle}{E_g^0 - E_t^0} \quad .$$

Here the superscript "0" denotes values at the point $\xi_i = 0$; e.g., $\psi_g^0 = \psi(\vec{r}, \xi_i = 0)$, H is the electronic Hamiltonian. With Eqs. 7-26 and 7-27, the $\rho\sigma mn$ element of the scattering tensor can now be written as:

$$(\alpha_{\rho\sigma})_{g,v_1;g,v_2} = (1/h) \sum_{r,v} \left[\frac{(M_\rho^0)_{rg} (M_\sigma^0)_{gr}}{\nu_{r,v;g,v_1} - \nu_0 + i\delta_{r,v}} \right.$$

$$\left. \times \left\langle \psi_{v_1}(\xi_i) \mid \psi_v(\xi_i) \right\rangle \left\langle \psi_v(\xi_i) \mid \psi_{v_2}(\xi_i) \right\rangle \right]$$

$$+ \sum_{\substack{r,t,v, \\ (t \neq r)}} h_{tr}^{\xi_i} \left[(M_\rho^0)_{rg} (M_\sigma^0)_{gt} \left\langle \psi_v(\xi_i) \mid \psi_{v_2}(\xi_i) \right\rangle \right.$$

$$\times \frac{\left\langle \psi_{v_1}(\xi_i) \mid \psi_v(\xi_i) \right\rangle}{\nu_{r,v;g,v_1} - \nu_0 + i\delta_{r,v}}$$

$$\left. + \frac{(M_\sigma^0)_{gr} (M_\rho^0)_{tg} \left\langle \psi_{v_1}(\xi_i) \mid \psi_v(\xi_i) \right\rangle \left\langle \psi_v(\xi_i) \mid \xi_i \mid \psi_{v_2}(\xi_i) \right\rangle}{\nu_{r,v;g,v_1} - \nu_0 + i\delta_{r,v}} \right]$$

$$+ \sum_{\substack{r,t,v, \\ (t \neq g)}} h_{tg}^{\xi_i} \left[(M_\sigma^0)_{tr} (M_\rho^0)_{rg} \left\langle \psi_{v_2}(\xi_i) \mid \psi_v(\xi_i) \right\rangle \right.$$

$$\times \frac{\left\langle \psi_v(\xi_i) \mid \xi_i \mid \psi_{v_1}(\xi_i) \right\rangle}{\nu_{r,v;g,v_1} - \nu_0 + i\delta_{r,v}}$$

$$\left. + \frac{(M_\rho^0)_{tr} (M_\sigma^0)_{rg} \left\langle \psi_{v_1}(\xi_i) \mid \psi_v(\xi_i) \right\rangle \left\langle \psi_v(\xi_i) \mid \xi_i \mid \psi_{v_2}(\xi_i) \right\rangle}{\nu_{r,v;g,v_1} - \nu_0 + i\delta_{r,v}} \right]$$

$$+ \text{terms containing } [\rho \leftrightarrow \sigma]/(\nu_{g,v_1;g,v_2} + \nu_0 + i\delta_{r,v}). \quad (7\text{-}28)$$

This expression was obtained under the assumption that all wavefunctions are real so that $(M_\rho^0)_{tr} = (M_\rho^0)_{rt}$ and also $h_{tr}^{*\xi_i} = h_{tr}^{*\xi_i}$ (see Ref. 84). Retaining only the zero-order terms in Eq. 7-28, we get

$$(\alpha_{\rho\sigma})_{g,v_1;g,v_2} = 1/h \sum_{r,v} \left[1/\left(\nu_{r,v_1;g,v_2} - \nu_0 + i\delta_{r,v}\right) + 1/\left(\nu_{r,v_1;g,v_2} + \nu_0 + i\delta_{r,v}\right) \right] \times \left[(M_\rho^0)_{rg} (M_\sigma^0)_{gr} \left\langle \psi_{v_1}(\xi_i) \mid \psi_v(\xi_i) \right\rangle \times \left\langle \psi_v(\xi_i) \mid \psi_{v_2}(\xi_i) \right\rangle \right] . \quad (7\text{-}29)$$

Eq. 7-29 is the starting point used by Behringer to obtain Eq. 7-25, under the conditions that $\nu_0 \to \nu_{r,g}$, $v_2 = v_1 + 1$; i.e., to predict the pre-resonance Raman effect for a fundamental vibrational transition. The second and third terms of Eq. 7-28 give the first order correction due to vibronic perturbation.

Application of the Pre-resonance Raman Effect Theory to the Interpretation of the Raman Intensity Data of Chlorine in Benzene Solutions

Since the visible and near ultraviolet absorption by chlorine in carbon tetrachloride solution is very weak, we assume that any strong pre-resonance Raman effect for that system must come from the first allowed electronic transition (around 60,000 cm^{-1}) (87). There is, however, a new strong absorption band (presumably the charge-transfer band) observed at about 36,000 cm^{-1} (or about 278 nm) when chlorine is dissolved in benzene solution (see Ref. 6 or

Chap. IV). In our studies, the experimental plane-polarized exciting incident light was from the Ne-He laser, so that the exciting frequency is about 16,000 cm^{-1} (632.8 nm). The frequency dependent factors were calculated for the terms in Eq. 7-25 corresponding to Placzek's normal Raman effect and corresponding to the pre-resonance Raman effect. The ratios of the squares of these two frequency dependent factors for chlorine in benzene to the squares of their values for chlorine in carbon tetrachloride solution were estimated to be 3.8 and 17.0 for $\nu_{eg}^2/(\nu_{eg}^2 - \nu_0^2)^2$ and for $(\nu_{eg}^2 + \nu_0^2)^2/(\nu_{eg}^2 - \nu_0^2)^4$, respectively.

One must be careful how the comparison is made between the theoretical predictions obtained above and the experimental Raman results given in Chap. IV. The observed change in the Raman intensity (in Table V) from that for a solution of chlorine in carbon tetrachloride to that for a solution of chlorine in benzene should be compared with the intensity calculated from Eq. 7-25, and not just with one of the ratios of the squared frequency factors given above. In order to make a direct comparison between theoretical and experimental values, we must know the absolute values of $[\partial|(M_\rho^0)_{eg}(M_\sigma^0)_{ge}|/\partial\xi_i]_0$ and of $|(M_\rho^0)_{eg}(M_\sigma^0)_{ge}|(\partial\nu_{eg}/\partial\xi_i)_0$ for both free and complexed chlorine. Unfortunately, these quantities are not easily obtainable. If we assume that both quantities have the same values for free chlorine and for complexed chlorine, and also assume that the second term is much more important than the first one in Eq. 7-25, then the observed intensification (by a factor of 20 -- see Chap. IV) of the chlorine Raman shift when the benzene is added is in good agree-

ment with that expected (a factor of 17.0, with these assumptions) from the pre-resonance Raman effect. The idea of a possible pre-resonance Raman effect due to the charge-transfer complex formation has also been suggested by Rosen, Shen and Stenman (32) for iodine in benzene solution. A pre-resonance Raman effect has been reported (88) in tetracyanoethylene charge-transfer complexes with benzene, but this observation is contrary to the conclusion reached in another study (89) of that system. Nevertheless, as Behringer has pointed out (82), better evidence that a pre-resonance Raman effect is responsible for intensity effects such as these would be the observation of some dependence of the Raman intensity on the frequency of the exciting light. We tried several experiments in the Chemistry Department at Old Dominion University, Norfolk, Va. (courtesy of Prof. A. Bandy) to observe the Raman spectrum of chlorine in benzene solutions using a tunable argon-ion laser with a Spex double monochromator (in a 1 ml liquid cell and with three different exciting lines at 514.5 nm, 488.0 nm and 457.9 nm). Unfortunately, the photochemical reaction occurred in the Raman cell so rapidly with these higher frequency exciting lines that we could not obtain any spectrum to test the possible frequency dependence.

If, indeed, the pre-resonance Raman effect is the main factor responsible for the large intensification of chlorine in benzene, an interesting feature appears from the theory (83, 84). The point group of an axial model for the chlorine-benzene complex state is C_{6v}. It is found to have this geometry in the solid [from a crystallographic study (90)], but the structure of the complex in solution is not known. However, from our statistical calculation (Chap. VI), the

axial structure is predicted to be dominant in the mixture because of the stabilization by quadrupole-induced dipole force (see also Ref. 31). The wavefunction for the ground state of the chlorine-benzene complex with C_{6v} symmetry belongs to the $^1A_1$ representation. According to the charge-transfer theory (37), there are two possible excited charge-transfer states: $^1A_1$ and $^1E_1$. If the excited charge-transfer state that is coupled vibronically to the ground state is $^1A_1$, then we will expect the intensity enhancement from pre-resonance Raman effect to appear as an increase in the value of α_{zz} for the complexed chlorine. If the excited charge-transfer state that couples vibronically is $^1E_1$, then we will expect the intensity enhancement to appear in α_{xx} and α_{yy} for the complexed chlorine. Thus, an accurate measurement of the depolarization ratio as a function of the percent of chlorine that is complexed might allow us to decide on the symmetry of vibronically coupled charge-transfer state. Since the charge-transfer state that couples vibronically is expected to be the one that also stabilized the ground state, we might hope to be able to decide the important question of which of these two states does indeed mix with the ground state. (See Ref. 37, sections 10.3, 11.2, 14.1, and elsewhere.) Unfortunately, the accuracy of our measurment for ρ (Chap. IV) that is possible with our spectrometer (PE LR-1; see Chap. IV) is not sufficient to determine this potentially interesting result.

One last point is worth mentioning. A further test of the question of whether pre-resonance Raman effect does really occur for the chlorine-benzene system can possibly be made by studying the

overtones of the complexed chlorine. The ratio of overtone intensity to fundamental intensity of a Raman band is usually less than 1% for vibrations when the spectra are observed outside the resonance region in liquids (see Ref. 60 and the references cited). However, in the resonance region, the ratio is expected to increase drastically (60, 91). The overtone of the chlorine vibration is expected near 1060 cm^{-1}, in a region which is overlapped by the Raman shift from benzene at 991.6 cm^{-1} and 1030 cm^{-1} (92). Possibly the improved characteristics of a good modern laser Raman spectrometer would allow observation of this overtone.

In summary, we have found in the first part of this chapter that the observed intensification of the chlorine Raman shift in benzene solution (compared to carbon tetrachloride) cannot be explained solely by Bernstein's theory of the electrostatic interaction effect. It is possible that a pre-resonance Raman effect acting in a benzene-chlorine complex as a result of the new, strong, and relatively low frequency charge transfer absorption band may explain the observed intensification of the Cl_2 Raman shift in benzene, without involving any vibronic charge-transfer effect. Attempts to verify such a pre-resonance Raman effect and attempts to obtain potentially important information about the symmetry of the charge-transfer state that is vibronically coupled to the ground state must await better instrumentation.

APPENDIX

THE ANGULARLY DEPENDENT PAIR CORRELATION FUNCTION $G(\vec{R}_{12},\omega_1,\omega_2)$

We will summarize below the pair correlation functions $G(\vec{R}_{12},\omega_1,\omega_2)$ for mixtures of chlorine in benzene and of chlorine in carbon tetrachloride, obtained from calculations based on the perturbation theory for the angular pair correlation function in molecular fluids developed by Gubbins and Gray (51) and on related methods (50, 52, 73, 93, 94).

Pair Correlation Function $G(\vec{R}_{12},\omega_1,\omega_2)$ for Chlorine-Benzene Pairs

From the perturbation theory (51) the pair correlation function $G(\vec{R}_{12},\omega_1,\omega_2)$ for the interaction of the axially symmetric chlorine molecule with the axially symmetric benzene molecule (about the six-fold symmetry axis) can be approximated by

$$G(\vec{R}_{12},\omega_1,\omega_2) = G^0_{12}(R_{12})\,[1 - u_a(\vec{R}_{12},\omega_1,\omega_2)/kT] \quad . \qquad \text{(A-1)}$$

Here $G^0_{12}(R_{12})$ is the Lennard-Jones radial distribution function at separation R_{12} for the chlorine-benzene pair; k is the Boltzmann constant; T is the temperature in °K; and $u_a(\vec{R}_{12},\omega_1,\omega_2)$ is the anisotropic intermolecular potential.

If we assume u_a arises from the quadrupole-quadrupole force, then (77)

$$\frac{u_a(\vec{R}_{12},\omega_1,\omega_2)}{kT} = \frac{3Q_1^*Q_2^*}{4r_1^{*5/2}r_2^{*5/2}T^*} F_{QQ}(\theta_1,\theta_2,\phi_{12}). \qquad \text{(A-2)}$$

Here $r_1^* = R_{12}/\sigma_1$, $r_2^* = R_{12}/\sigma_2$, $T^* = kT/\varepsilon_{12}$, $\varepsilon_{12} = (\varepsilon_1 \varepsilon_2)^{1/2}$,

$Q_1^* = Q_1/(\varepsilon_1 \sigma_1^5)^{1/2}$, $Q_2^* = Q_2/(\varepsilon_2 \sigma_2^5)^{1/2}$, and

$$F_{QQ} = 1 - 5\cos^2\theta_1 - 5\cos^2\theta_2 + 17\cos^2\theta_1\cos^2\theta_2 + 2\sin^2\theta_1\sin^2\theta_2\cos^2\phi_{12}$$

$$+ 16\sin\theta_1\sin\theta_2\cos\theta_1\cos\theta_2\cos\phi_{12} \quad .$$

The constants σ_1, ε_1 and σ_2, ε_2 are Lennard-Jones potential parameters for chlorine and benzene molecules, respectively, from gas phase studies; Q_1 and Q_2 are quadrupole moments of chlorine and benzene, respectively. The coordinate system is defined in Fig. 30. From values given in Table A-1, we estimated $u_a(\vec{R}_{12}, \omega_1, \omega_2)/kT$ for different chlorine-benzene pairs, with results shown in Table A-2.

$G_{12}^0(R_{12})$ of Eq. A-1 was obtained by assuming (52)

$$G_{12}^0(R_{12}/\sigma_{12};\ \rho,\ T,\ \varepsilon_{12}) = G^0(R_{12}/\sigma_{12};\ \rho\bar{\sigma}^3;\ kT/\varepsilon_{12}). \qquad \text{(A-3)}$$

Here $G^0(R_{12}/\sigma_{12};\ \rho\bar{\sigma}^3;\ kT/\varepsilon_{12})$ is the Lennard-Jones pair correlation function for pure benzene at $\rho^* = \rho\bar{\sigma}^3$, $T^* = kT/\varepsilon_{12}$, where $\bar{\sigma}^3$ is defined as

$$\bar{\sigma}^3 = \sum_\alpha \sum_\beta X_\alpha X_\beta \sigma_{\alpha\beta}^3 \quad . \qquad \text{(A-4)}$$

Here X_α and X_β are the mole fractions of chlorine and benzene, respectively; $\sigma_{\alpha\beta} = (\sigma_\alpha + \sigma_\beta)/2$. Since the concentration of chlorine is so low, $X_2 >> X_1$, so that

$$\bar{\sigma}^3 = X_1^2\sigma_1^3 + 2X_1X_2\sigma_{12}^3 + X_2^2\sigma_2^3 \simeq \sigma_2^3 \quad . \qquad \text{(A-5)}$$

Thus, we have finally

$$G^{0}_{12}(R_{12}/\sigma_{12}) \simeq G^{0}(R_{12}/\sigma_{12};\ \rho\sigma_{2}^{3};\ kT/\varepsilon_{12}) \quad . \qquad \text{(A-6)}$$

From Table A-1, we obtained $G^{0}_{12}(R_{12}/\sigma_{12})$ for chlorine-benzene pairs to be

$$G^{0}_{12}(R_{12}/\sigma_{12}) \simeq G^{0}(R_{12}/\sigma_{12};\ \rho^{*} = 0.9916;\ T^{*} = 0.886). \qquad \text{(A-7)}$$

The value of the right hand side of Eq. A-7 was taken from Table IV of Ref. 94, interpolating or extrapolating as needed to obtain the desired G^{0} values at each value of R_{12}/σ_{12}.

Pair Correlation Function $G(\vec{R}_{12},\omega_{1},\omega_{2})$ for Chlorine-Carbon Tetrachloride Pairs

By analogy with Eq. A-1, we obtained $G(\vec{R}_{12},\omega_{1},\omega_{2})$ for chlorine-carbon tetrachloride pairs in two different orientations. The potential u_{a} of a chlorine-carbon tetrachloride pair is assumed to be due only to the quadrupole-octapole force. The detailed procedures in obtaining the expression for u_{a} are shown elsewhere (80). Using the values from Table A-1 we obtained u_{a}/kT for the two different orientations. The results are shown in Table A-3. The value of $G^{0}_{12}(R_{12}/\sigma_{12})$ for chlorine-carbon tetrachloride pairs was estimated in the same way as that for chlorine-benzene pairs and was found to be

$$G^{0}_{12}(R_{12}/\sigma_{12}) = G^{0}(R_{12}/\sigma_{12};\ \rho^{*} = 0.75;\ T^{*} = 1.2365). \qquad \text{(A-8)}$$

TABLE A-1

PARAMETERS USED FOR THE CALCULATIONS OF THE PAIR-CORRELATION FUNCTIONS OF CHLORINE-BENZENE AND CHLORINE-CARBON TETRACHLORIDE PAIRS

Parameter	Chlorine	Benzene	Carbon Tetrachloride
σ (Å)	4.40[a]	5.27[a]	4.93[b]
ε/k (^{0}K)	257[a]	440[a]	226[b]
Q ($\times 10^{26}$ esu cm^{2})	6.14[a]	- 15.6[c]	--
Ω ($\times 10^{34}$ esu cm^{3})	--	--	26.1[b]

a. From Ref. 74.

b. From Ref. 93.

c. From Ref. 30.

TABLE A-2

THE POTENTIAL FUNCTION $u_a(\vec{R}_{12}, \omega_1, \omega_2)/kT$ FOR CHLORINE-BENZENE PAIRS AS A FUNCTION OF RELATIVE ORIENTATION (AT T = 298 ^{0}K)

Configuration[a] Chlorine-Benzene	θ_1[b]	θ_2[b]	ϕ_{12}[b]	F_{QQ}	u_a/kT[c]
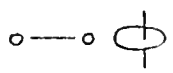	0	$\pi/2$	0	- 4	$2.65/(R^*)^5$
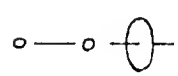	0	0	0	8	$- 5.30/(R^*)^5$
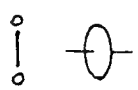	$\pi/2$	0	0	- 4	$2.65/(R^*)^5$
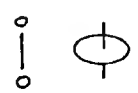	$\pi/2$	$\pi/2$	0	3	$- 1.99/(R^*)^5$
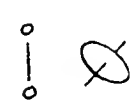	$\pi/2$	$\pi/2$	$\pi/2$	1	$- 0.661/(R^*)^5$

a. "O" is a chlorine atom; see Table VIII for definition of symbols.

b. See Fig. 30

c. R^* is defined as R_{12}/σ_{12}, $\sigma_{12} = (\sigma_1 + \sigma_2)/2$; see text.

TABLE A-3

THE POTENTIAL FUNCTION $u_a(\vec{R}_{12}, \omega_1, \omega_2)/kT$
FOR CHLORINE-CARBON TETRACHLORIDE PAIRS ($T = 298^0 K$)

Configuration[a]	u_a/kT [b]
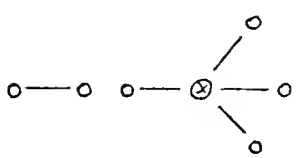	$0.879/(R^*)^6$ [b]
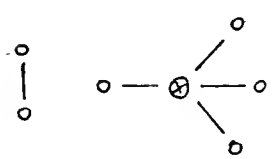	$-0.176/(R^*)^6$ [b]

a. Symbols were defined in Fig. 31.

b. R^* is defined as $R^* = R_{12}/\sigma_{12}$, $\sigma_{12} = (\sigma_1 + \sigma_2)/2$.

REFERENCES

1. H.A. Benesi and J.H. Hildebrand, J. Am. Chem. Soc., 70, 2382 (1948).

2. H.A. Benesi and J.H. Hildebrand, J. Am. Chem. Soc., 71, 2703 (1949).

3. T.M. Cromwell and R.L. Scott, J. Am. Chem. Soc., 72, 3825 (1950).

4. R.M. Keefer and L.J. Andrews, J. Am. Chem. Soc., 72, 4677 (1950).

5. R.S. Mulliken, J. Am. Chem. Soc., 72, 600 (1950).

6. L.J. Andrews and R.M. Keefer, J. Am. Chem. Soc., 73, 462 (1951).

7. L.J. Andrews and R.M. Keefer, J. Am. Chem. Soc., 74, 4500 (1952).

8. M. Tamres, D.R. Virzi and S. Searles, J. Am. Chem. Soc., 75, 4358 (1953).

9. J.A.A. Ketelaar. J. Phys. Radium, Paris 15, 197 (1954).

10. R.M. Keefer and L.J. Andrews, J. Am. Chem. Soc., 77, 2164 (1955).

11. R.S. Mulliken, J. Am. Chem. Soc., 74, 811 (1952).

12. R.S. Mulliken, J. Chem. Phys., 23, 397 (1955).

13. a. J. Collin and L. D'Or, J. Chem. Phys., 23, 397 (1955).
    b. L. D'Or and J. Collin, Rec. Trav. Chim., 75, 862 (1956).

14. R.L. Scott, Rec. Trav. Chim., 75, 787 (1956).

15. O. Hassel and K.O. Strømme, Acta Chem. Scand., 12, 1146 (1958).

16. O. Hassel and K.O. Strømme, Acta Chem. Scand., 13, 1781 (1959).

17. E.K. Plyler and R.S. Mulliken, J. Am. Chem. Soc., 81, 823 (1959).

18. W.B. Person; R.E. Humphrey and A.I. Popov, J. Am. Chem. Soc., 81, 273 (1959).

19. O. Hassel, Molec. Phys., 1, 241 (1958).

20. G. Kortum and H. Walz, Z. Electrochem., 57, 73 (1953).

21. W.B. Person, R.E. Erickson and R.E. Buckles, J. Am. Chem. Soc., 82, 29 (1960).

22. H. Stammreich, R. Forneris, and Y. Tavares, Spectrochim. Acta, 17, 1173 (1961).

23. H.O. Hooper, J. Chem. Phys., 41, 599 (1964).

24. A. Fratiello, J. Chem. Phys., 41, 2204 (1964).

25. F.T. Long and R.L. Strong, J. Am. Chem. Soc., 87, 2345 (1965).

26. H.B. Friedrich and W.B. Person, J. Chem. Phys., 44, 2161 (1966).

27. P. Klaeboe, J. Am. Chem. Soc., 89, 3667 (1967).

28. W.B. Person, C.F. Cook and H.B. Friedrich, J. Chem. Phys., 46, 2521 (1967).

29. Y.R. Shen, H. Rosen and F. Stenman, Chem. Phys. Lett., 1, 671 (1968).

30. M.W. Hanna, J. Am. Chem. Soc., 90, 285 (1968).

31. M.W. Hanna and D.E. Williams, J. Am. Chem. Soc., 90, 5358 (1968).

32. H. Rosen, Y.R. Shen and F. Stenman, Molec. Phys., 22, 33 (1971).

33. J.P. Kettle and A.H. Price, J.C.S. Faraday II, 8, 1306 (1972).

34. L.E. Orgel and R.S. Mulliken, J. Am. Chem. Soc., 79, 4839 (1957).

35. G. Briegleb, Electron Donator-Acceptor Komplexe (Springer-Verlag, Berlin, 1961).

36. L.J. Andrews and R.M. Keefer, Molecular Complexes in Organic Chemistry (Holden-Day, San Francisco, 1964).

37. R.S. Mulliken and W.B. Person, Molecular Complexes (Interscience, New York, 1969).

38. J. Rose, Molecular Complexes (Pergamon Press, New York, 1967).

39. R. Foster, Organic Charge-Transfer Complexes (Academic Press, London, 1969).

40. M. Tamres, "Charge-Transfer Complexes in the Vapor Phase" (to be published).

41. W.B. Person, Chapter I in The Spectroscopy and Structure of Molecular Complexes (J. Yarwood, ed.) (Plenum, London, 1973).

42. E.R. Lippincott and G. Nagarajan, Bull. Soc. Chim. Belges, 74, 551 (1965).

43. a. J. Van Kranendonk, Ph.D. dissertation, University of Amsterdam, 1952.
b. J. Van Kranendonk, Physica, 23, 825 (1957).
c. J. Van Kranendonk, Physica, 24, 347 (1958).

44. J. Fahrenfort, Ph.D. dissertation, University of Amsterdam, 1955.

45. V.N. Filimonov, Soviet Physics Uspekhi, 2, 894 (1960).

46. G.W.F. Pardoe, Trans. Faraday Soc., 66, 2699 (1970).

47. M.J. Mantione, Theor. Chim. Acta, 15, 141 (1969).

48. C.G. Gray, J. Phys. B: Atom. Molec. Phys., 4, 1661 (1971) and the references cited.

49. L. Marabella and G.E. Ewing, J. Chem. Phys., 56, 5445 (1972).

50. S.K. Garg, J.E. Bertie, H. Kilp and C.P. Smyth, J. Chem. Phys., 49, 2551 (1968).

51. K.E. Gubbins and C.G. Gray, Molec. Phys., 23, 187 (1972).

52. G.A. Mansouri and T.W. Leland, Trans. Faraday Soc., 68, 320 (1972).

53. W.B. Person, J. Am. Chem. Soc., 87, 167 (1965).

54. a. D.A. Deranleau, J. Am. Chem. Soc., 91, 4044 (1969);
b. ibid., 4050 (1969).

55. Gmelins Handbuch der Anorganischen Chimie, 8th edition, System-number 6, Supplementary Volume, Part A, "Chlorine," p. 374 (Verlag Chemie, Gmbh, Weinheim/Bergstr., 1968).

56. Methoden der Organischen Chemie, 4th edition (E. Müller, ed.), Vol. 5, Part 3, "Halogen Compounds," p. 522 (Georg Thieme Verlag, Stuttgart, 1962).

57. E.H. Land, S.D. Christian and J.D. Childs, "Spectral and Solubility Studies of Molecular Complex Equilibria. Concentration Scale Dependence and Activity Coefficient Effects." (To be published in J. Am. Chem. Soc.)

58. D.A. Bahnick and W.B. Person, J. Chem. Phys., 48, 1251 (1968).

59. H. Kayser, Handbuch der Spectroscopie, Vol. 6, p. 160 (Verlag von S. Hirzel, Leipzig, 1912).

60. Instruction Book for LR-1 Laser-Excited Raman Spectrometer (Perkin-Elmer, Norwalk, Connecticut, 1965).

61. M. Tamres, J. Phys. Chem., 65, 654 (1961).

62. H.J. Bernstein and G. Allen, J. Opt. Soc., Am., 45, 237 (1955).

63. D.A. Long, R.B. Gravenor and D.C. Milner, Trans. Faraday Soc., 59, 46 (1963).

64. R.E. Hester, Raman Spectroscopy (H.A. Szymanski, ed.), p. 133 (Plenum Press, New York, 1967).

65. W. Holzer, W.F. Murphy and H.J. Bernstein, J. Chem. Phys., 52, 399 (1970).

66. D.A. Ramsay, J. Am. Chem. Soc., 74, 72 (1952).

67. W.S. Benedict, R. Herman, G.E. Moore and S. Silverman, Can. J. Phys., 34, 830 (1956).

68. R.N. Jones, K.V. Seshadsi, N.B.W. Jonathan and J.W. Hopkins, Can. J. Chem., 41, 750 (1963).

69. A.S. Wexler, App. Spec. Rev., 1, 29 (1967).

70. R.P. Young and R.N. Jones, Chem. Rev., 71, 219 (1971).

71. M.J.D. Powell, "Minimum of Function of Several Variables," QCPE # 60, Department of Chemistry, University of Indiana.

72. a. R.G. Gordon, J. Chem. Phys., 43, 1307 (1965).
b. J.P. Perchard, W.F. Murphy and H.J. Bernstein, Molec. Phys., 23, 499, 519, 535 (1972).

73. T.M. Reed and K.E. Gubbins, Applied Statistical Mechanics (McGraw-Hill Book Co., New York, 1973).

74. J.O. Hirschfelder, C.F. Curtis and R.B. Bird, Molecular Theory of Gases and Liquids (John Wiley and Son., Inc., New York, 1954).

75. E.B. Wilson, J.C. Decius and P.C. Cross, Molecular Vibrations (McGraw-Hill Book, Co., New York, 1955).

76. J. Overend, Infrared Spectroscopy and Molecular Structure, p. 353 (M. Davies, ed.) (Elsevier Publishing Co., New York, 1963).

77. A.D. Buckingham, Quart. Rev., 13, 183 (1959).

78. T.-C. Jao, Special Report on "Angularly Dependent Pair Correlation Functions for Linear and Tetrahedral Molecules," Molecular Spectroscopy Laboratory, University of Florida (1973).

79. T.-C. Jao., N. Beebe, W.B. Person and J.R. Sabin (to be published in Chem. Phys. Lett.).

80. Landolt-Börnstein, Zahlenwerte und Functionen, Vol. I, p. 510 (Springer-Verlag, Berlin, 1951).

81. H.J. Bernstein (private communication).

82. J. Behringer, Chapter 6 in Raman Spectroscopy, Vol. 1 (H.A. Szymanski, ed.) (Plenum Press, New York, 1967).

83. A.C. Albrecht, J. Chem. Phys., 34, 1476 (1961).

84. J.A. Koningstein, Introduction to the Theory of the Raman Effect (D. Reidel Publishing Co., Dordrecht, Holland, 1972).

85. H.A. Kramers and W. Heisenberg, Z. Physik., 31, 681 (1925).

86. G. Placzek, Handbuch der Radiologie, Vol. 6 (Academische Verlagsgesell-schaft, Leipzig, 1934).

87. G. Herzberg, Spectra of Diatomic Molecules, p. 519 (D. Van Nostrand Company, Inc., New York, 1950).

88. L.M. Fraas, J.E. Moore and R.E. Bruns, Chem. Lett. 21, 357 (1973).

89. E.M. Voigt (to be published in Chem. Phys. Lett.).

90. O. Hassel and C. Rømming, Quart. Rev., 16, 1 (1962).

91. W. Holzer, W.F. Murphy and H.J. Bernstein, J. Mol. Spectry., 32, 13 (1968).

92. G. Herzberg, Infrared and Raman Spectra, p. 364 (D. Van Nostrand Company, Inc., Princeton, 1966).

93. K.E. Gubbins, C.G. Gray, P.A. Eglstoff and M.S. Ananth (to be published).

94. L. Verlet, Phys. Rev., 165, 20 (1968).

BIOGRAPHICAL SKETCH

Tze Chi Jao was born in Taitung, Taiwan on April 3, 1940. He attended high school there and obtained his B.S. degree in entomology in 1963 from the National Chung-Hsing University. In 1967 he obtained his M.S. degree in chemistry from the University of Puerto Rico at Mayagüez. He has been an instructor in physical chemistry at the University of Puerto Rico since 1967. He entered the Graduate School at the University of Florida in 1970 with a special financial assistantship provided by a grant from the University of Puerto Rico at Mayagüez.

I certify that I have read this study and that in my opinion it conforms to acceptable standards of scholarly presentation and is fully adequate, in scope and quality, as a dissertation for the degree of Doctor of Philosophy.

Willis B. Person, Chairman
Professor of Chemistry

I certify that I have read this study and that in my opinion it conforms to acceptable standards of scholarly presentation and is fully adequate, in scope and quality, as a dissertation for the degree of Doctor of Philosophy.

Yngve N. Öhrn
Professor of Chemistry

I certify that I have read this study and that in my opinion it conforms to acceptable standards of scholarly presentation and is fully adequate, in scope and quality, as a dissertation for the degree of Doctor of Philosophy.

James D. Winefordner
Professor of Chemistry

I certify that I have read this study and that in my opinion it conforms to acceptable standards of scholarly presentation and is fully adequate, in scope and quality, as a dissertation for the degree of Doctor of Philosophy.

R. Carl Stoufer
Associate Professor of Chemistry

I certify that I have read this study and that in my opinion it conforms to acceptable standards of scholarly presentation and is fully adequate, in scope and quality, as a dissertation for the degree of Doctor of Philosophy.

Thomas M. Reed III
Associate Professor of
Chemical Engineering

This disserration was submitted to the Graduate Faculty of the Department of Chemistry in the College of Arts and Sciences and to the Graduate Council, and was accepted as partial fulfillment of the requirements for the degree of Doctor of Philosophy.

March, 1974

Dean, Graduate School